Unfolding and Refolding of Monomeric and Heptameric α-Hemolysin

A Masters Thesis by

Marsiyana M. Henricus



Submitted to the University of Oxford

for the *Degree of Master of Science by Research in Chemical Biology*

Hertford College

Trinity 2010

Unfolding and Refolding of Monomeric and Heptameric α-Hemolysin

Marsiyana M. Henricus
Hertford College

M.Sc. by Research in Chemical Biology
Trinity 2010

Alpha-hemolysin (αHL) is a membrane protein derived from *Staphylococcus aureus*. The structural stability of the monomeric and heptameric protein was investigated under high pH conditions (8.0–13.0) and in various concentrations of urea (0–8.0 M). The dimensions of the αHL heptameric pore are ideal for the translocation of single-stranded polynucleotides such as DNA or RNA. Therefore, it could potentially be used as a DNA sequencing device. Exploring the pore's ability to withstand harsh conditions would help determine whether it could be used in the translocation of double stranded DNA (dsDNA), which dissociates into single-stranded DNA (ssDNA) at high pH or ssDNA that loses its secondary structure in the presence of urea. Studying the behavior of monomeric αHL under various denaturing and renaturing conditions will aid in improving the conditions used to purify and refold mutated forms of αHL.

The pH and urea studies revealed that the heptamer is more resistant to structural change than the monomer. The heptamer remained stable up to pH 12.0, which is ideal since dsDNA dissociates into ssDNA at pH 11.7. The majority of the heptamer's structure was lost at pH conditions above 12.5. Structural studies on the heptamer at various urea concentrations revealed that a fraction of the heptamer was still intact even at 8.0 M urea whereas the monomer seems to unfold completely at high urea concentrations. However, upon refolding via dilution, the monomer seems to regain its structure and function. Urea was determined as an ideal denaturant even after incubating the monomer in guanidinium chloride (GdnCl) or organic acids.

The structural stability of the αHL monomer and heptamer was elucidated using techniques such as circular dichroism, intrinsic tryptophan emission spectroscopy, SDS-PAGE, light scattering hemolytic assays and single-channel recording experiments.

Declaration

The work described in this thesis was completed in the Chemistry Research Laboratory at the University of Oxford, UK from October 2008 to June 2010 in Professor Hagan Bayley's laboratory. All of the work written is entirely my own work, unless acknowledged and stated otherwise in the text. This work has not been submitted previously for any other degree within the University of Oxford or elsewhere.

Marsiyana M. Henricus

June 2010

Dedication

I would like to dedicate this body of work to the people that have believed in me throughout my academic career. To my Mother and Father for their undying love, encouraging actions, constant prayers and for their own sacrifices; I am nothing without them. To my undergraduate mentors and advisors: Dr. Ipsita Banerjee, Dr. Donna Heald, Mark Massa, S.J., Ms. Maria Noonan, Dr. John Kezel and Dr. Brennan O'Donnell.

Acknowledgements

I would like to take this opportunity to sincerely thank those individuals who have supported me and believed in me throughout my time at the University of Oxford. Firstly, I would like to thank Prof. Hagan Bayley for giving me the opportunity to work in his laboratory. I greatly appreciate his advice and guidance while tackling my project throughout my time at Oxford. I would like to thank The Merage Foundation for their financial support and their belief in my dreams. I would like to thank Dr. Giovanni Maglia for his constant guidance, advice and moral support. Thank you to Ms. Qiuhong Li for teaching me various techniques in the lab. I am forever indebted to her for her friendship, expertise and guidance. Thank you to Dr. Deanpen Japrung, who was a D.Phil. student at the time, for her experimental guidance, friendship and scientific discussion.

I am incredibly grateful for every member in the HB lab that I have come to respect and appreciate as scientists and friends. Big thanks to my good friends Lai Song Choi, Ruhma Syeda, Sarah Rogers and Leon Harrington for their help and advice in areas of molecular biology and electrophysiology. I am grateful for the welcoming environment at Hertford College and for its financial support. Thank you to my examiners, Dr. Paula Booth and Dr. Christina Redfield for their time, discussion and advice.

My accomplishments are as much accredited to the love and support of my family, especially my Mother and Father, and those individuals that have believed in me. I am indebted to members of Fordham University that nurtured my passion for science. Thank you to Dr. Ipsita Banerjee for allowing me to work in her lab for two years. Next to my parents, she is and remains my strongest support system. Thank you to Mark Massa, S.J., Dr. Donna Heald, Ms. Maria Noonan, Dr. John Kezel and Dr. Brennan O'Donnell for their guidance and support during my undergraduate education. Last but not least, Thank you to God for all the blessings that have been bestowed upon me.

Table of Contents

Chapter I: General Introduction

1.1. Background of α-Hemolysin (αHL) 1

1.2. DNA sequencing 7

1.3. Unfolding of Proteins 9

1.3.1. Unfolding of Proteins with pH 11

1.3.2. Unfolding of Proteins with Urea 12

1.4. Refolding of Proteins 15

1.5. Circular Dichroism (CD) 18

1.6. Intrinsic Tryptophan Fluorescence Emission (ITFE) Spectroscopy 25

1.7. Light Scattering Hemolytic Assay 28

1.8. Single-Channel Recording 28

1.9. Thesis Overview 31

1.10. References 32

Chapter II: Unfolding Studies of Monomeric and Heptameric αHL at Alkaline pH

2.1. Introduction 41

2.2. Results 42

2.2.1. CD Studies of Monomeric αHL 42

2.2.2. ITFE Studies of Monomeric αHL 44

2.2.3. CD Studies of Heptameric αHL 44

2.2.4. ITFE Studies of Heptameric αHL 46

2.2.5. SDS-PAGE Studies of Heptameric αHL 48

2.3. Discussion 49

2.4. Conclusions 53

2.5. Materials and Methods 54

2.5.1. Protein Preparation 54

2.5.2. CD 54

2.5.3. ITFE 55

2.5.4. SDS-PAGE 55

2.6. References 57

Chapter III: Unfolding Studies of Heptameric αHL in Urea

3.1. Introduction 59

3.2. Results 60
3.2.1. CD Studies of Heptameric αHL 60
3.2.2. ITFE Studies of Heptameric αHL 62
3.2.3. SDS-PAGE Studies of Heptameric αHL 63
3.3. Discussion 63
3.4. Conclusions 67
3.5. Materials and Methods 68
3.5.1. Protein Preparation 68
3.5.2. CD 68
3.5.3. ITFE 69
3.5.4. SDS-PAGE 69
3.6. References 70
Chapter IV: Unfolding and Refolding Studies of Monomeric αHL in Urea
4.1. Introduction 72
4.2. Results 73
4.2.1. Structural Studies of Unfolded Monomeric αHL 73
4.2.2. Structural Studies of Refolded Monomeric αHL 76
4.2.3. Activity Studies of Monomeric αHL 80
4.2.4. Single-Channel Recording Studies 87
4.3. Discussion 92
4.4. Conclusion 98
4.5. Materials and Methods 99
4.5.1 Protein Preparation. 99
4.5.2. CD 100
4.5.3. ITFE 101
4.5.4. Light Scattering Hemolytic Assays 101
4.5.5. Proteolysis Studies 103
4.5.6. Single-Recording Studies 104
4.6. References 105
Chapter V: Appendix
5.1. Materials and Methods Supplementary 108
5.1.1. Protein Preparation: αHL Heptamer 108

5.1.2. Protein Preparation: αHL Monomer 110
5.1.3. Rabbit Red Blood Cell Preparation 112
5.1.4. Hemolytic Assays: Urea Buffer Controls 112
5.1.5. Curve Fitting 113

Chapter I: General Introduction

1.1 Background of α-Hemolysin

α-Hemolysin (αHL) is a heptameric membrane protein that has been implemented as a sensing device for various analytes in the field of bio-nanotechnology due to its structural characteristics. αHL is secreted in water-soluble monomeric form by the gram positive bacterium, *Staphylococcus aureus* [1]. Seven monomers assemble on the membrane of cells such as erythrocytes to form a heptameric pore disturbing the cell's semi-permeability and osmotic pressure [1]. αHL and other β-barrel forming toxins provide a model for studying protein-membrane interactions. The solution of the crystal structure in 1996 by Song *et al.* to 1.9 Å resolution has allowed researchers to understand and explore the structure as a nanodevice [2].

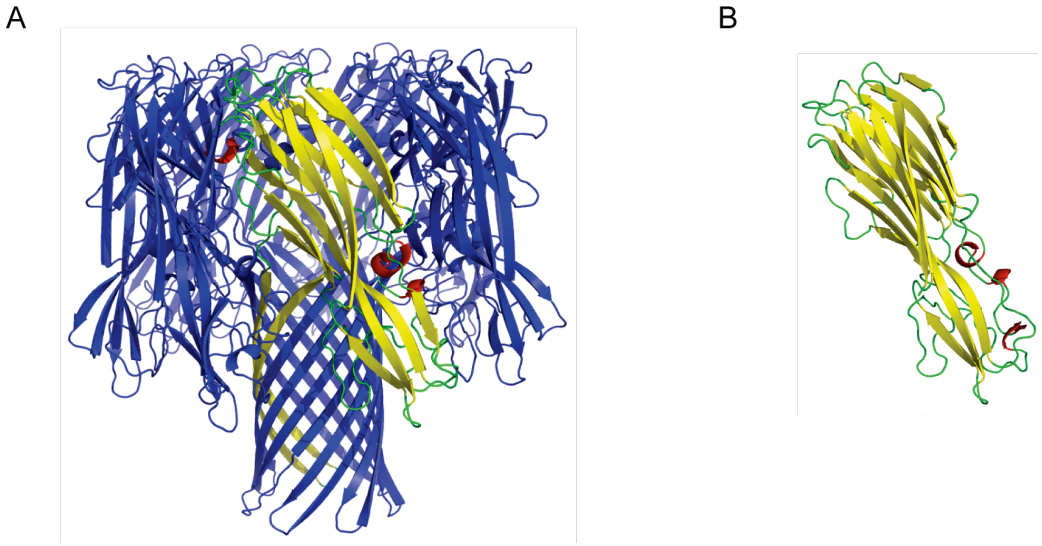


Fig. 1. Ribbon representation of the α-hemolysin (αHL) heptamer and monomer. *Six subunits are in blue, while the residues in the β-sheets, α-helices and random coil in one protomer are highlighted in yellow, red and green, respectively. (B) Ribbon representation of αHL homologue, leukocidin F. Residues in β-sheets are in yellow, α-helices are in red and random coil are in green.*

The αHL monomer has not been crystallized; however, its structure is likely to be similar to that of leukocidin F (LukF), a toxin also secreted by *Staphylococcus aureus* (Fig. 1.). LukF possesses a sequence identity of approximately 30% with αHL [3] and its core tertiary structure is similar to the protomers, in the αHL heptamer. Each monomeric subunit (33.2 kDa) of the αHL pore contains 293 amino acid residues with 16 β strands, which comprise 52.9% of the secondary structure. There are also 4 short stretches of either α- or 3_{10}-helix (4.3%), a region of random coil from Asp183 to Lys205 (7.9%) and non-α, non-β elements (34.9%). Inspection of the primary structure of the monomer reveals that, cysteine residues are absent in the amino acid sequence. Therefore, disulfide bonds do not stabilize the structure. Hydrophobic and non-charged polar residues comprise 19.1% and 16.7% of the structure, respectively. The tertiary structure of the protomer is composed of regions that make the cap domain (strands 1, 2, 3, 13, 6, 9, 10, 5, 14, 15 and 16 shown in blue in Fig. 2.), containing the β-sandwich, the rim domain (strands 4, 5, 11, 12, 14 and 15 shown in red in Fig. 2.) and the stem domain (strands 7 and 8) of the heptamer. The cap domain is composed of 2 six-stranded anti-parallel β-sheets. The rim domain extends underneath the cap domain and helps in binding the protein to the membrane phospholipid bilayer [3]. The stem domain is composed of a two-stranded anti-parallel β-sheet that composes the 14-stranded β barrel of the heptamer, containing a high quantity of glycine residues. It is linked to the β-sandwich by hydrophobic interactions.

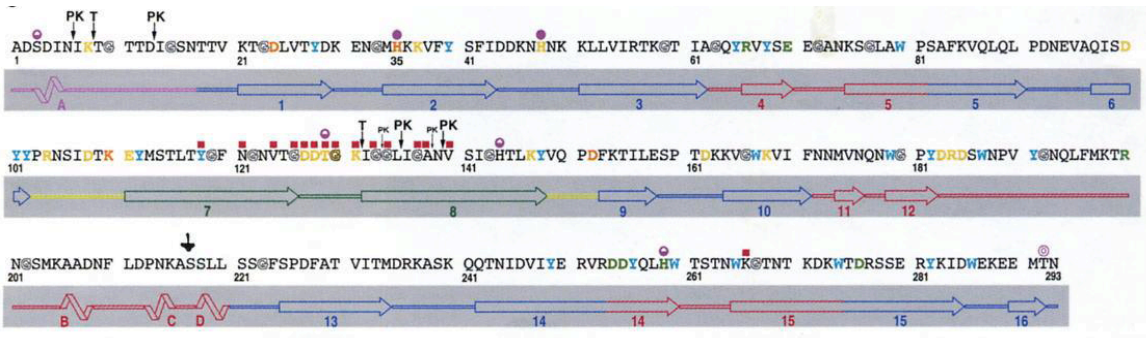


Fig. 2. Map of the primary sequence and secondary sequence of the αHL protomer. *The strands seen in blue, red and green represent the regions that form the cap, stem and rim domains of the heptamer, respectively. Image taken from Song et al. 1996* [2].

The αHL protomer has a large percentage of β-sheet secondary structure, while its other parts are non-α and non-β (Fig. 1A). The protomer measures 70 Å long, 45 Å wide and 20 Å thick [2]. The β-sandwich, which creates the cap domain, protrudes out of the membrane into the extracellular environment due to its hydrophilicity [2]. It consists of 5 + 6 β-sandwiches. The stem domain (Lys110–Tyr148) is composed of 2 antiparallel β-strands per protomer that composes the β barrel, which spans the length of the lipid membrane and contains 8 glycine residues similar to LukF. Both ends of the stem contain polar and charged residues. The rim domain forms a three-stranded β-sheet and is directly linked to the cap domain. The amino latch (Ala1–Val20) has been thought to be important for heptamer formation and cell lysis since it interacts with the inner β-sheets of adjacent protomers [4]. The protomer's amino latch and the stem domain are orientated differently to LukF monomer. The amino latch in LukF possesses a β-conformation while the protomer consists of non-α and non-β structure with one 3_{10}-helix [3]. The spatial disposition of the amino latch and the stem domain is different between the two structures. The triangle region links the stem domain to the core of the protomer. Two short sections of

polypeptides (Pro103–Thr109 and Val149–Asp152) form two sides of the triangle and interact between protomers and in the conformational rearrangements that occur during channel formation [2].

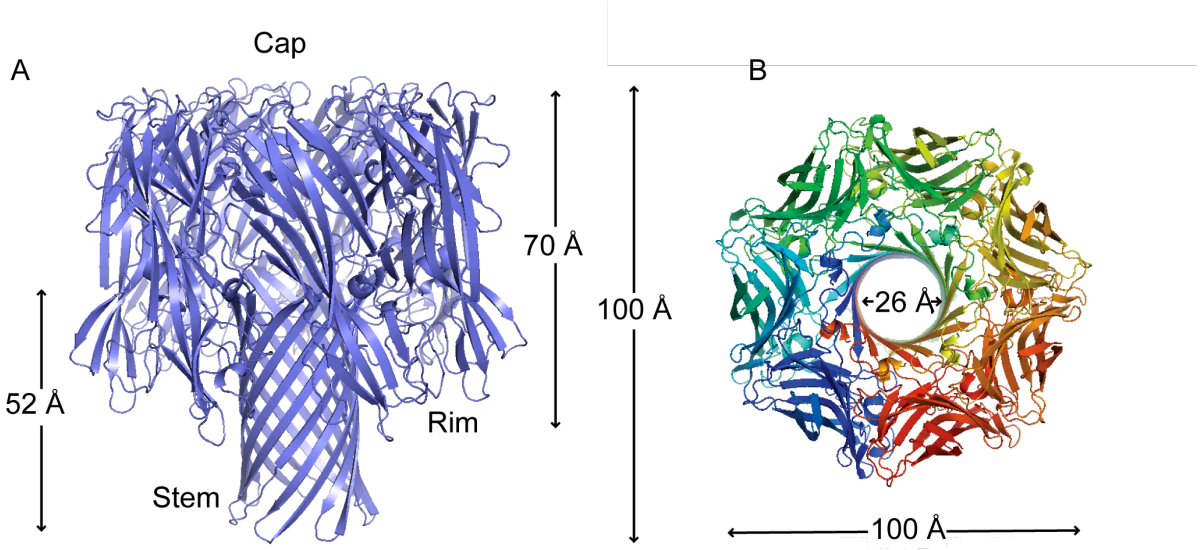


Fig. 3. Ribbon representation of α-hemolysin (αHL) heptamer. *(A) View perpendicular to the seven-fold axis. All seven subunits are colored in blue. (B) View from the top, parallel to the seven - fold axis. Each subunit is in a different color. (Figure modified from Song et al. 1996 [3]).*

The structure of the heptamer (232.4 kDa) is commonly divided into the cap, rim, stem domains and the amino latch (Fig. 3). The rim domain is mainly hydrophilic and is linked to the cap domain; therefore it orientates itself externally from the membrane while the stem is embedded within the lipid bilayer. The protein pore measures 100 Å long and 100 Å wide. The vestibule region, which is the interior of the cap domain, ranges from 14 Å to 46 Å. The cap domain forms the majority of the heptamer's mass (approximately 80%) and is composed of 7 β-sandwiches and of 7 amino latches that are each contributed by one of the seven protomers. Side chain-side chain hydrophobic and hydrophilic interactions between protomers help maintain the structure of the cap domain. The entrance

of the cap domain contains amino latches and has a diameter of 28 Å. The rim domain has a less compact secondary structure with the presence of large loops at its base. The rim domain is essential in membrane binding due to the neutral and nonpolar residues present in this region and its proximity to the stem domain [5]. Solvent-exposed aromatic residues are present on the surface of the rim that can interact with the membrane. The stem domain represents less than 10% of the total mass of the heptamer and measures 52 Å in height and 26 Å in diameter (measured from α-carbon positions). Therefore, the stem's structure allows it to span the phospholipid bilayer of target cells. This transmembrane region is composed of 14 anti-parallel β-strands, 2 contributed by each protomer. The protomer-protomer interactions are largely main chain-main chain interactions. The stem has hydrophobic residues on its exterior that create a belt that is 28 Å thick, which is ideally suited for insertion in the cell membrane (measuring 28 Å to 30 Å). Aromatic residues on the top (Tyr118 and Phe120) and Gly126 on the bottom, interact with nonpolar portions of the lipid bilayer. The charged amino acid residues accommodate the charged head groups of the phospholipids that form the membrane. Aromatic residues have dipole-dipole interactions with the carbonyl groups of the lipids while the hydrophobic belt interacts with their hydrocarbon chains [3]. There are hydrophobic bands composed of 7 methionines (position 113) and 7 leucines (position 135) that are solvent exposed on the interior of the pore [2]. The interior of the pore is mostly hydrophilic and is weakly selective towards anions. The diameter of the pore changes from the cap domain (the extracellular *cis* side) to the end of the stem domain (the cytosolic *trans* side). The diameter of the pore at the beginning of the cap domain is 28 Å. Proceeding downwards, the channel widens at the vestibule region, which is encased by the inner sheets of the β-sandwich of the cap domain. Pro103 is the start of the triangle region of the channel where the diameter is 46 Å. At the

junction between the triangle region and the stem domain, the channel shrinks to 14 Å. This constriction site is formed by the side chains of the residues Glu111, Lys147 and Met113 [2]. This narrowing explains the size limit of the transport of macromolecules through the pore.

Heptamer formation is a three-step process [3]. The bacteria first release the water-soluble monomers, which bind to the target membrane, either mediated by specific receptors or spontaneous assembly. Second, the membrane-bound monomers assemble to form an inactive nontoxic pre-pore. Third, a conformational change occurs to form the heptameric pore. This final step is irreversible and rate-limiting [3]. It is a cooperative process that may occur in a series of sub-states that comprises some amino acids in the glycine-rich region moving from a hydrophilic to a hydrophobic environment after oligomerization of the monomers on the membrane [2, 6]. The amino terminus has a role in pore opening while the carboxyl terminus is involved in initial oligomerization [6]. The structure of the αHL pore and its ability to withstand harsh conditions such as SDS denaturation and high temperatures [2] as well as mutations, has made it an ideal device for sensing various analytes and genomic material made possible by their passage through or interaction with the pore. The αHL heptamer can be used as a biosensor because it allows the passage of ions after applying a potential, detected through single channel recording experiments [7, 8]. When an analyte enters the pore, it obstructs the flow of ions, which is detected by the decrease in conductivity. αHL can be modified by site-directed mutagenesis allowing for covalent or noncovalent attachment of an analyte. It has been used to detect and discriminate divalent metal cations such as Zn (II), Co (II), Ni (II), and Cu (II) when polyhistidine sequences are introduced [7]. The Glu111 residues present at the constriction of the pore favorably bind to di- and trivalent cations [2]. With the help of

adaptors such as β-cyclodextrin it can also detect and bind to organic molecules [9]. In this body of work we have focused on αHL's potential ability to act as a DNA sequencing device.

1.2 DNA Sequencing

The dimensions of the αHL protein pore are ideal for the translocation of polynucleotides such as DNA and RNA in single-stranded form, which occurs at a speed of 1–5 μs per base [10]. The constriction site (diameter of 14–15 Å) of αHL prevents the translocation of polynucleotides that have secondary structure or are double stranded. Single-base recognition has been conducted with a modified form of αHL and with the help of immobilized ssDNA or an enzyme to convert double stranded (dsDNA) to ssDNA [11, 12]. However, certain problems must be solved in creating a novel DNA sequencing device, which include: obtaining ssDNA from double-stranded DNA (dsDNA), eliminating secondary structure of ssDNA/RNA and finding a method to slow their movement through the constriction site. Implementing nanopores as DNA sequencing devices would not require the amplification or modification of DNA, ultimately reducing costs and potentially allowing long reads. αHL is a convenient pore to use since it is stable at various conditions and has been used in numerous applications. The studies described in this thesis investigate the protein's behavior at high pH and high urea concentrations that cause nucleic acids to dissociate from their dsDNA form to ssDNA and lose their secondary structure [10-15]. The conditions investigated will potentially allow ssDNA as well as other macromolecules such as proteins that are normally too large to pass through the αHL pore in unfolded form.

Since the structure of DNA was defined by Maurice Wilkins, Rosalind Franklin, Francis Crick and James Watson in 1953 [16, 17], the field of genetics has expanded to decode entire human genomes. Techniques such as restriction fragment length polymorphism (RFLP), which was employed to map the human genome, or polymerase

chain reaction (PCR), a common method used in laboratories allowing for the rapid replication of a small amount of DNA, [18] were developed in the 1970s and 1980s. With the evolution of research and technology, the idea of sequencing the human genome was becoming more of a reality with the implementation of semi-automated DNA sequencing devices and rapid DNA sequencing using fluorescent chain-terminating deoxynucleotides by companies. Later the Human Genome Project (HGP), started in 1990 by the US Department of Energy (DOE) and US National Institutes of Health (NIH), aimed to create genetic maps, physical maps and ultimately the complete nucleotide sequence map of human chromosomes. The first sequence of a free-living organism *Haemophilus influenzaeli* [19, 20] was completed in 1995. In 1999 human chromosome 22 was sequenced and in 2004, the genetically active parts of the genome that lead to the transcription of the DNA into mRNA of the human genome were sequenced [21].

With the culmination of the human genome project, the next step was to develop an efficient and cheap method to sequence DNA that could revolutionize the processing and the use of genetic information in the medical field. In 2004, the NIH presented a challenge to researchers to sequence a whole individual human genome by 2010 for $100,000 or by 2015 for $1000. The most inexpensive and ultra rapid methods have been the use of single-molecule recording devices since they do not require the amplification of DNA. Keller in 1991 proposed the used of the enzyme exonuclease to cut fluorescent labeled bases for fluorescent detection [23, 24] allowing for the sequencing of 100 to 1000 bases per second. Another technique, which is the basis of our studies, involves translocating DNA molecules through a natural or synthetic nanopore. The change in ionic current when the DNA passes through the pore will give different information depending on the base sequence. Kasianowicz *et al.* [10] proved that ssDNA polymers can be pulled through αHL with the

help of an electric field. αHL can now participate in single-base recognition of an immobilized strand of DNA [13]. Synthetic solid-state nanopores made with Si_3N_4 and SiO_2 have also been constructed for this purpose [25]. Nanopores will speed sequencing to a speed of one base per millisecond. Using denaturing conditions such as alkaline pH and urea, we intended to find a condition that would allow DNA to be at an ideal conformation for translocation in an appropriate time without the aid of an additional protein. Therefore studying the structural stability of the αHL under denaturing conditions was essential.

1.3 Unfolding of Proteins

Determining whether and at what point the αHL pore would unfold was crucial for studies that would facilitate DNA translocation through the pore. The studies conducted on the αHL monomer were intended to broaden the understanding of the protein's ability to unfold and refold. The conditions used could potentially be applied in protein purification methods.

Understanding the significance of a protein's sequence in encoding its biological activity and functional state is a key aspect of structural biology. Purification protocols have allowed proteins found in nature to be obtained in bulk in their unfolded form. The final crucial steps of purification involve folding the protein into its native active conformation. *In vivo,* proteins are denatured to certain conformations that allow for their translocation across the cell's lipid bilayer [26-28]. Therefore proteins must be partially folded or denatured either spontaneously or with the help of enzymes [29-31]. Studies have been conducted on monomeric forms that assemble into channels such as diphtheria, coicin, aerolysin and anthrax toxins [32-34], whose behavior in denaturants such as urea and guanidinium chloride (GdnCl) has been studied in depth using fluorescence and circular dichroism spectroscopy, optical rotatory dispersion, nuclear magnetic resonance, and

various hydrodynamic techniques. The thermodynamic hypothesis of soluble protein folding, states that a protein's Gibbs free energy is at its minimum in its native conformation [35]. The free energy of unfolding of monomeric αHL has been explored by Bortoleo *et al.* [36] at mildly acidic conditions between pH 5.0 and 7.5 during urea denaturation. It was revealed that as the pH decreases the calculated free energy of unfolding also decreases.

The unfolding of multimeric membrane proteins is not as predictable as soluble proteins; thus, the exploration of their unfolding and refolding has been scarce because it is hard to distinguish whether each subunit of the protein unfolds simultaneously or separately. Spectroscopic techniques are most commonly used to assess the state of proteins upon unfolding. However these techniques show the average of what is occurring in bulk solution. In order to determine the mechanism of denaturation, the interactions between each subunit of the protein as well as their interaction with the denaturant must be considered. Most membrane proteins need a surfactant or detergent to solubilize the protein in solution, which must also be considered in determining the unfolding mechanism. Determining an appropriate denaturing condition is crucial for both soluble and membrane proteins. An ideal denaturant would easily allow the renaturation of the protein along its denaturation curve. In both soluble and membrane protein studies, an ideal denaturation curve is often sigmoidal in which the unfolding of the protein is described as being cooperative. The extremes of a sigmoidal curve represent the native and denatured states. A common perception with regards to unfolding soluble proteins is that these two states are present with no intermediates states. The steeply sloped region between these two extremes represents the phase at which the population of folded protein present decreases and unfolded protein increases as the concentration of denaturant increases. Therefore, the

midpoint of the sigmoidal curve represents the point at which 50% of the protein is either folded or unfolded. According to Dill and Shortle [26], there are a few states that can be observed in the denaturing of proteins. The fixed two-state-model represents free energy behaviors in which there is a two state transition from native to denatured state. The variable two-state model represents a free energy barrier separating the two states but the denatured state depends on the concentration of denaturant. The higher-order transition model states that there is no energy barrier between the native and denatured states; therefore, during the transition there are significant amounts of intermediate states observed. In the classical three-state model there are three stable states: the native, denatured and intermediate states with two free energy barriers [37-40]. In this work we investigated the behavior of monomeric and heptameric αHL using two denaturing agents: pH and urea.

1.3.1 Unfolding Proteins with pH

Changing the pH conditions in conjunction with other denaturants such as urea or temperature has been useful in unfolding proteins. Acidic pH conditions have commonly been used to promote the unfolded states of proteins rather than basic pH conditions, which we explore in this work. Proteins contain basic and acidic residues that possess a charge, which increases as the solution becomes more acidic or more basic relative to the isoelectric pH. Acidic and alkaline induced unfolding of proteins is due to the protonation and deprotonation of amino acid residues, respectively. The formation of strong electrostatic repulsions between residues results in a conformation of the protein that is different from its native state or the denaturation of the protein itself.

Studies observing the unfolding of proteins under the influence of acidic pH, concluded that denatured states of proteins such as cytochrome c are only partially unfolded

with each state retaining a significant water-inaccessible core [41-43]. The fraction of the buried surface that is exposed upon denaturation is increased by electrostatic repulsion when the polypeptide is charged, a result of decreasing the pH. The electrostatic free energy of a charged protein is reduced upon denaturation because charge repulsion is reduced as charges are distributed over the larger volume of the denatured molecule. Thermal unfolding under acidic conditions of proteins such as ribonuclease, lysozyme and chymotrypsinogen show that the low-pH thermal denaturation process does not fully unfold the protein [43, 44]. Other studies conducted on carbonic anhydrase, beta-lactamase, apomyoglobin and others confirmed these findings and revealed that unfolding under acidic conditions often leads to a compact denatured state which is referred to as a "molten-globule" state [45, 46]. This seems to represent two stable populations of the denatured state at low pH, which are separated by a free energy barrier [47]. Low pH denaturation can lead to both an open unfolded state and a compact denatured state, which are a result of various forces such as charge repulsion that drives expansion or hydrophobic interactions that drive contraction of the protein [26].

In our studies we investigated the unfolding of the αHL heptamer and monomer at alkaline conditions from a pH of 8.0 to 13.0. The purpose of these studies was to determine whether the pore was stable at pH conditions that would facilitate the dissociation of dsDNA to ssDNA and allow its translocation.

1.3.2 Unfolding Proteins with Urea

Urea is a small hydrophilic molecule that is commonly used to reversibly denature soluble proteins, transmembrane β barrels and helical proteins; however, it is not universally effective in doing so [35-48]. In the case of membrane proteins, one of the major issues when determining whether urea is an effective denaturant is its ability to solubilize a

membrane protein in the absence of detergent micelles. Studies conducted on OmpA reveal that it is highly soluble in 8 M urea in the absence of lipid vesicles, stays denatured when vesicles are added and then refolds after dilution of the urea in the presence of lipid vesicles [35, 49-52]. The structural difference between α-helical and β-sheet proteins must be considered when deciding which denaturants to use. Predominately α-helical proteins contain continuous stretches of hydrophobic amino acids, whereas β barrel proteins contain alternating hydrophobic and hydrophilic residues. Therefore, β barrel proteins tend to be soluble in chemical denaturants even in the absence of lipid vesicles or detergent micelles [48].

Urea's interaction with proteins is not completely understood. Direct and indirect mechanisms have been developed to describe a protein's unfolding pathway in the presence of urea. The direct mechanism implies that there is an interaction between urea and the polypeptide whereas the indirect mechanism implies that urea incorporates into water's hydrogen bond network and that there is no segregation of urea from water [53-56]. Molecular dynamics (MD) simulations have been employed to determine the exact interaction between urea and proteins during the unfolding process. Simulations conducted on the 20 amino acids by Stumpe and Grubmueller [57] suggest that urea interacts with the hydrophobic side chains of amino acid residues and contributes to the destabilization of proteins. Urea was preferred over water by nonpolar and aromatic amino acid residues (phenylalanine, tryptophan and tyrosine) as well as the protein backbone while polar residues with large partial charges interact with water. The hydrogen bonds formed between the urea and the protein, prevent the protein from forming new interactions that could result in protein aggregation. Simulations conducted on 22 glycine-capped tri-peptides, show that urea is favored over water with increasing side chain hydrophobicity,

which is explained by van der Waals forces. A study of the interaction of 7.0 M urea with a chain of purely hydrophobic groups by Zangi *et al.* [58] also supports the direct mechanism, which seems to be a result of the weakening of hydrophobic interactions between polymer groups [58-61].

Simulations by Hua *et al.* [56] suggested a two-step direct mechanism in urea's impact on lysozyme. The first stage involves the solvation of the protein's globular state by urea driven by van der Waals forces. These "dry globules" of the protein are short-lived intermediates, in which the protein core is largely undisrupted. The native structure of the protein is lost once urea intrudes into the tertiary structure expelling water molecules. There are direct interactions formed by urea between the protein backbone and side chains, which are stronger than their interactions with water. There is hydrogen bond formation between urea's carbonyl and the backbone amides of the protein. The behavior of urea with lysozyme is similar to that of a surfactant that solubilizes the side chains in aqueous solution and prevents the aggregation of hydrophobic groups. Urea does not seem to disrupt the structure of water or its hydrogen bond network since it has more attractive forces towards hydrophobic residues than hydrophilic ones.

MD simulation studies conducted by Bennion *et al.* [55] support both the direct and indirect mechanism of urea's interaction with chymotrypsin. Urea disturbs the structure of water by diminishing the hydrogen bond strength and encouraging the solvation of hydrophobic groups. In 4.0 M urea, 76% of water is in contact with at least one urea molecule, leading to the inference that urea does perturb water [55, 61]. It also seems that urea interacts directly with polar residues as well as the peptide backbones, stabilizing nonnative conformations. Residues Ile20, Leu49 and Ile57, found in the hydrophobic core of the protein, are first solvated by water and then by urea. The solvent-accessible surface areas of

these key residues increased in 8.0 M urea. There is an increase in hydrogen-bonding between urea and water and a drop in the number of strong water-water hydrogen bonds, resulting in the weakening of water structure.

In our studies, we utilized urea's ability to unfold proteins and applied it to both the heptameric and monomeric forms of αHL. Studies conducted in 0–8.0 M urea with the heptamer were important in ascertaining the protein's stability for ssDNA/RNA translocation. Urea was investigated as an unfolding reagent for the monomeric form of the protein.

1.4 Refolding of Proteins

The unfolding and refolding of proteins have aided the understanding of the structure and function of newly synthesized polypeptide chains, membrane proteins and their assembly into biological membranes. Experiments conducted by Anfinsen, demonstrated that a denatured protein can refold *in vitro* to its native conformation in the absence of energy input [35]. The refolding of the proteins during purification is the final and most essential step. A protein's primary sequence, and the environment in which it is placed, is of major significance since it is one of the crucial factors in determining whether it will refold to its original conformation. In most cases, denaturation is reversible and the folded form lies at the thermodynamic free energy minimum. Refolding is believed to occur via intermediates that contain locally folded structures that will initiate the folding process. Many refolding studies have focused on water soluble proteins while a few studies have been conducted on the refolding of membrane proteins. One of the first examples was bacteriorhodopsin, a protein present in the membrane of the halophilic bacteria that catalyzes light-driven proton translocation across the membrane using retinal as a cofactor [62]. Huang *et al.* were able to show the successful denaturation with organic acids such as

trifluoroacetic acid (TFA) and renaturation with cholic acid or deoxycholate acid of bacteriorhodopsin, which was fully active in light-driven proton translocation. Other refolding studies conducted on integral membrane proteins have been limited to lipophilin, Ca^{2+}-ATPase for sacroplasmic reticulum, cytochrome b5 and glycophorin, all of whose hydrophobic portions are resistant to complete unfolding [63]. Techniques such as dialysis and evaporation and lyophilization have facilitated refolding. Refolding via dilution has been possible with the enzyme rhodanase with the aid of detergents such as dodecyl-beta-D-maltoside after incubation in GdnCl as well as hexameric glutamate dehydrogenases from bovine liver, *Clostridium symbosium* [64].

The unfolding and refolding efficiency of a protein is a function of both kinetics and thermodynamics. Both can appear negative or incomplete because the kinetics is too slow for it to occur or finish on the experimental time scale or because the folding free energy is unfavorable or small. The hydrophobic environment in which a protein is placed, affects the folding reaction of a membrane protein. The lipids used with membrane proteins also affect the folding efficiency, activation energy to folding and the final membrane protein stability [35]. Barriers such as misfolding into kinetic traps, aggregation of the unfolded state upon dilution of the denaturant and unproductive partitioning into vesicles in the case of membrane proteins can affect refolding [65, 66]. These competing reactions increase the folding barrier, reduce the folding rate constant and decrease the folding efficiency. Changes occurring to amino acids can raise the free energy of the folded state without affecting the free energy of the unfolded state, contributing to protein misfolding.

In the unfolding and refolding of monomeric αHL protein in urea, we attempt to understand the folding behavior of the protein *in vivo*. The conditions used in these studies are important for purification techniques and chemical synthesis of modified αHL. This

will allow us to sense other analytes and further develop the area of single-molecule chemistry. Manipulation of protein structure to determine its function is often done by site-directed mutagenesis (SDM). However this technique has been limited to only the naturally occurring amino acids. Using chemical synthesis to produce proteins, allows the incorporation of unnatural amino acids and peptide backbone modification enabling us to generate precise modification of the structural properties of αHL. Determining the unfolding and refolding conditions will be useful for techniques such as native chemical ligation (NCL) and expressed protein ligation (EPL), which use synthetic and semi-synthetic ways to create proteins [67-70].

In NCL a peptide with an N-terminal cysteine reacts with a peptide with a C-terminal thioester to link the two peptides with a native peptide bound at the ligation site. These methods have been explored in the formation of modified membrane proteins such as potassium channel KcsA and the porin OmpF. However, the recombinant expression of protein fragments is difficult due to the over-production of long hydrophobic polypeptides that are difficult to solubilize and purify. The most crucial and difficult step to pass is the final step that involves protein folding from unstructured polypeptides.

The purpose of using chemical ligation to synthesize KcsA, which conducts potassium ions across membranes, was to introduce unnatural amino acids and peptide backbone modifications, which will help in the further understanding of the protein's structure and function in ion selectivity. Valiyaveetil *et al.* [67] used EPL to semi-synthesize a truncated version of KcsA. The semi-synthetic method was employed where KcsA (1–125) was formed from 2 component peptides by one ligation reaction. The method called for the formation of an N-terminal recombinant peptide alpha-thioester (residues 1–73) and synthetic C-terminal peptides (74–125). The buffers used to carry out the

ligation reactions are critical because of the solubility properties of the fragment being constructed. Denaturants such as GdnCl, SDS and urea were added to solubilize the protein while TFE, TFA and SDS were used in its refolding, confirmed by $AgTx_2$ binding. A modular semi-synthetic technique using two NCL reactions was employed for the construction of a full-length subunit of KcsA by Komarov *et al.* [71] where three segments were constructed: a central peptide obtained by SPPS and N- and C-terminals that were obtained by recombinant means. NCL was also used by Retiz *et al.* [72] in implementing synthetic modulators into the β barrel of OmpF, a trimeric porin from *Escherichia coli*. Protein semi-synthesis with azide/alkyne click chemistry in which the N-terminal fragment thiol ester and the C-terminal fragment bearing an N-terminal cysteine residue were prepared. The ligation of the thiol ester and the N-terminal cysteine to the OmpF hybrid was conducted under denaturing conditions and the fragments were refolded by insertion into mixed uni-lamellar vesicles.

Furthermore, I attempt to explore the unfolding and refolding of the αHL monomer to screen different conditions for NCL or EPL. The implementation of these methods on the synthesis of mutated forms of αHL pores, would make them applicable for sensing or for single-molecule chemistry.

1.5 Circular Dichroism (CD)

Circular dichroism (CD) has been a key technique used to decipher protein secondary structure and monitor unfolding and refolding of proteins. In this particular work it is used to determine changes in secondary structure of the αHL monomer and heptamer after incubation at alkaline pH or with denaturants such as urea.

CD is the differential absorption of plane-polarized light, which is composed of two circularly polarized light, rotating clockwise (right-handed, R) and counter-clockwise (left-handed, L) (Fig. 4) [73].

A B

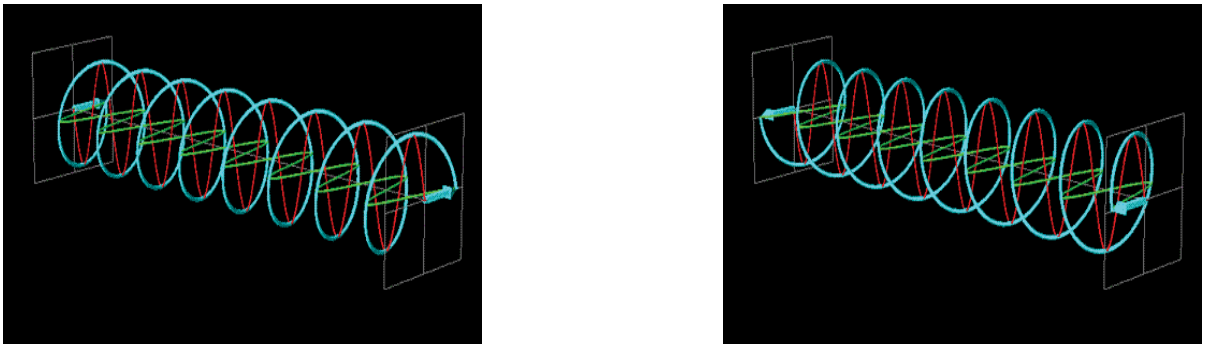


Fig. 4. Circularly Polarized Light. *(A) Representation of left circularly polarized light and (B) right circularly polarized light. Vertically polarized light is represented in red, horizontally polarized light is represented in green and circular polarized light is represented in blue. (Taken from Applied Photophysics).*

When the two components of light are not in phase because they do not have the same amplitude or they are not ninety degrees out of phase, the electric vector traces out an ellipse. This is defined as elliptical polarization and the difference in absorption of the two light components is described as the ellipticity, θ. This is measured when the incident radiation is continuously switched between the two components of circularly polarized light. The two components of light pass through a modulator consisting of a piezoelectric quartz crystal and thin plate of isotropic material tightly coupled to the crystal. The alternating electric field that results, forces the quartz crystal to change structure resulting in the plate transmitting circular polarized light at the extremes of the field that are detected by the photomultiplier. The Chirascan Circular Dichroism Spectrometer used in my

measurements contains a dual polarizing quartz prism monochromator, with a large prism and mirror optical surfaces allowing a large amount of light to be collected and passed through the monochromator. A linearly polarized monochromatic beam that emerges from the exit slit of the monochromator is refocused down through the photo-elastic modulator, which modulates the beam into alternately left and right circularly polarized states.

Once the light passes through an optically active sample, the L and R are absorbed differently depending on the sample being tested, the light passes to the photomultiplier CD detector. The CD signal is observed when a sample is chiral or it is placed in an asymmetric environment. CD instruments are designed to measure the difference in absorbance between left (A_L) and right (A_R) circularly polarized light:

$$\Delta A = A_L - A_R$$

The CD data is commonly reported as the ellipticity, θ, where the numerical relationship between absorbance and ellipticity is $\theta = 3298.2 \times \Delta A$. The data can be normalized by accounting for the concentration of the protein and the number of amino acid residues. The mean residue weight (MRW) for the peptide bond is

$$MRW = M/ (N-1)$$

Where M is the molecular mass of the polypeptide chain in units of Daltons and N is the number of amino acids in the chain, and N-1 is the number of peptide bonds. Therefore the mean residue molar ellipticity at a particular wavelength, $[\theta]_{mrw, \lambda}$ whose units are deg x cm^2 x $dmol^{-1}$, is represented by:

$$[\theta]_{MRW, \lambda} = (MRW \cdot \theta_\lambda)/ (10 \cdot d \cdot c)$$

θ_λ is the observed ellipticity, d is the path length in centimeters and c is the concentration in grams per milliliters. If the molar concentration is known, the molar ellipticity of a sample can be given by:

$$[\theta]_{\text{Molar},\lambda} = (100 \cdot \theta_\lambda)/ (M \cdot d)$$

Various aspects of the CD data such as the shape of the spectra, the wavelength shift and the absorbance/ellipticity can be used to analyze a protein sample. Most commonly, CD is used in elucidating the secondary structure of proteins, which usually fall under categories such as: α-helix (prominent peaks present at 208 nm and 222 nm), β-sheet (prominent peak at 215 nm or 218 nm), anti-parallel β-pleated sheet, β-turn and random conformations (Fig. 5).

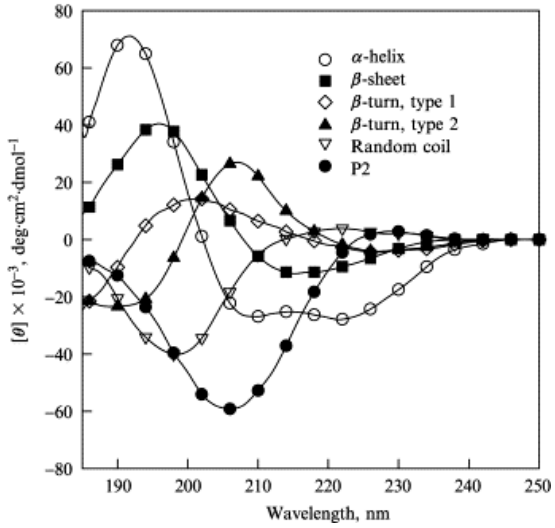


Fig. 5. Common secondary structures identified in circular dichroism. *Image taken from Greenfield N Methods of Enzymology 2004: The spectra of the α-helix, β-sheet, β-turns, and random coil were drawn from Brahms and Brahms 1980 J. Mol. Biol and B. Brodsky (Robert Wood Johnson Medical School, Piscataway, NJ)*[73].

Before NMR or crystallography techniques were used, the spectra of unknown peptides were fit by a combination of spectra of polypeptides with known conformations. Once

conformations of proteins were known; many proteins were characterized using algorithms such as SELCON, VARSLC, CDSSTR, K2d and CONTIN, which give an estimation of the secondary structural composition of the protein. Programs may have their drawbacks. Most of these reference databases have been used to determine the structural components of soluble proteins but the results are not as satisfactory when applied to membrane proteins. Wallace *et al.* [74] claimed that altered wavelength shifts due to dielectric constants of the surrounding hydrophobic environments of the membrane protein and that of the water surrounding the protein, result in these differences [75-77]. Additional hydrogen bonding to the aqueous solvent can change the electronic distribution in the amides that can be evident on the CD spectra. Accurate calculations of the composition are difficult to obtain if data are not collected in the far UV region from 170 nm and below. Using a CD instrument with a Xe arc light source makes measurements below 180 nm difficult because the intensity of the radiation falls off in this region.

Significant information regarding the tertiary structure can be determined by analyzing the far UV regions of the spectra. Chromophores of interest include the peptide bond, which absorbs below 240 nm. There is a weak but broad $n \rightarrow \pi^*$ transition appearing at 220 nm, while there is a more intense $\pi \rightarrow \pi^*$ transition appearing at 190 nm. Aromatic amino acid side chains absorb at 260–320 nm while disulfide bonds absorb at 260 nm [78]. Tryptophan residues show a peak between 290 and 305 nm, tyrosine peaks are present between 275 and 282 nm and phenylalanine peaks are between 255 and 270 nm. There has also been evidence of the affect of aromatic molecules on the far UV region below 250 nm. The shape of the spectrum in the near UV area depends on the number and the types of amino acids present in addition to other characteristics such as their mobility in their environment and the effect of adjacent amino acids. Non-protein cofactors such as flavins,

heme groups, chlorophyll moieties, or ligands that are chiral can also be detected over a wide spectral range.

Conducting CD studies meticulously is crucial in order to ascertain secondary structural changes, particularly when slight changes occur in structures that are only evident through knowing experimental conditions such as concentration of the protein and the effects of the buffer used. When testing a sample, it is important to be aware of insoluble protein aggregates and artefacts that can result in differential light scattering, an effect of the plane polarized light falling on chiral objects that are floating in solution [79-81]. Absorption flattening is a result of high concentrations of protein that leads to protein aggregates that distort the shape and magnitude of the spectra. These can be eliminated by centrifuging or filtering the samples; however, the loss of protein sample is a disadvantage. It is essential to consider the effects of the buffer being used, which in itself can cause a change in the spectrum that may include a detergent, surfactant or lipid. Detergents such as Triton X-100; for example, can be difficult to remove from proteins but they lead to high absorbance around 280 nm. The effects of this are particularly prominent at low wavelengths in the UV region. Using a cuvette of very short path length can minimize the absorbance. Difficulties can arise when testing samples in buffers that are used in pH studies between 4 and 6 since these buffers contain carboxylic acid groups that absorb strongly below 200 nm. Buffers containing a large amount of salt having chloride ions or those that are based on zwitterionic sulphonic acids of heterocyclic nitrogen bases (HEPES, MOPS, MES or PIPES) also absorb at 200 nm. Imidazole, which is often used to elute His-tagged proteins from Ni-NTA columns, absorbs strongly in the far UV region. Denaturants such as urea or GdnCl absorb strongly at or below 210 nm. It is important to observe the

high tension voltage value, which should be below 700 V, in some cases, at the wavelength at which the protein absorbs since it can distort the spectra.

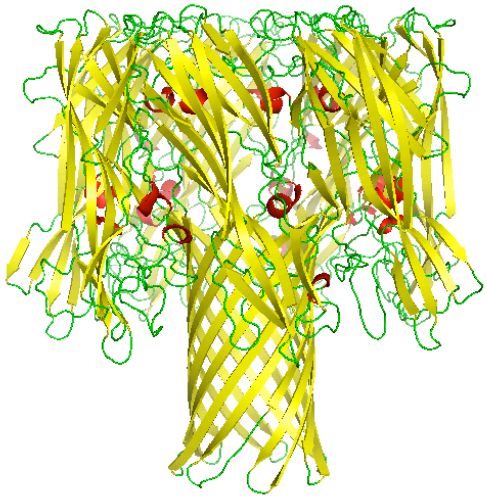


Fig. 6. Ribbon representation of αHL heptamer's secondary structure. *The β-sheets are shown in yellow, the α-helices are shown in red and the random coils are shown in green.*

In this particular work, CD was used to determine the changes in secondary structure of the αHL monomer and heptamer. This method is an ideal spectroscopic way to detect changes that occur once the protein is incubated in the conditions tested at alkaline pH and at various urea concentrations. The monomeric form of the protein is composed of 52.6% of β-sheet with 16 β-strands, which is found in the cap domain. Due to the majority of the mass and β-sheet content found in the cap domain, changes that occur in the CD spectra are most likely reflective of changes in the cap domain (Fig. 6). Therefore, changes in the CD data particularly in wavelengths between 220 nm and 210 nm for the monomer and heptamer at varying pH (8.0–13.0) or urea concentrations (0–8.0 M) were expected.

1.6 Intrinsic Tryptophan Fluorescence Emission (ITFE) Spectroscopy

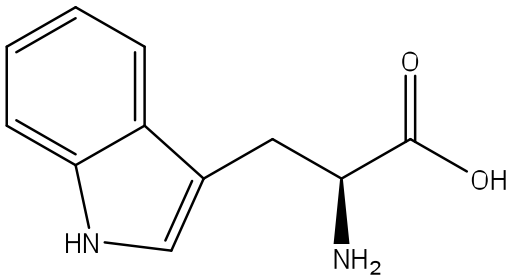


Fig. 7. Tryptophan Residue. *The L-stereoisomer of tryptophan is commonly used for proteins.*

Fluorescence spectroscopy is a useful technique for monitoring changes in chromophores found in solution or those that are attached to proteins such as aromatic amino acids residues: tryptophan (Trp), tyrosine (Tyr) or phenylalanine (Phe) [82-84]. Of the three aromatic amino acids, tryptophan is the most commonly detected since it is sensitive to the polarity of its environment. The two excited electronic states of Trp, ^1L_a and ^1L_b are the result of a two-photon excitation. Studies on Trp fluorescence have supported the idea that ^1L_a is the state that fluoresces in all proteins. Quantum mechanics show that the electron density is shifted from the pyrrole ring to the benzene ring upon excitation to the ^1L_a state [88]. Therefore, positive charges near the benzene ring or negative charges near the pyrrole end of the Trp will shift the wavelength maxima to longer wavelengths that results in a red shift while the opposite mechanism results in a blue shift (Fig. 7).

Changes in fluorescence intensity, wavelength maximum, band shape, anisotropy, fluorescence lifetimes and energy transfer are observed in order to decipher changes in protein structure and function. In Intrinsic Tryptophan Fluorescence Emission (ITFE) Spectroscopy Trp's emission peak (λ_{max}^{em}) can range from 308−355 nm depending on its solvent exposure and polarity [85, 86]. In hydrophobic environments the λ_{max}^{em} is blue-shifted while red-shifted in polar environments. If the fluorescence λ_{max}^{em} is less than 330 nm the

Trp residue is buried in a non-polar environment and if it is larger, it is in a polar solvent environment. However, the relative orientation of the solvent molecule's dipole to the ring determines a shift. The unfolding of proteins results in a red shift in the λ_{max}^{em} in the range of 345–355 nm as buried tryptophans become more exposed to the solvent [89].

Studies conducted by Vivian *et al.* [82] determined the extent to which the fluorescence wavelength is mediated by solvents and protein residues. Simulation results show that this may be a result of the orientation and polarization of the charged and polar protein residues and the electronic polarization of the Trp ring by an electric field formed by water and the protein. The solvent contributes to a red shift that results in the ^1L_a excited state, when there is more electron transfer from the pyrrole to the benzene ring. The protein contributes to spectral shift with the presence of charged side chains, polar side chains and a Trp backbone. Charged residues can have a large impact because of the long range nature of the Coulomb interaction of a point monopole and a point dipole. Polar side chains and backbones contribute shifts of 5–10 nm primarily by a dipole-dipole mechanism by a short range van der Waals contact. Charged amino acid residues such a lysine and arginine contribute largely to spectral shifts. The orientation of the charge to the Trp ultimately determines whether there will be a red shift, a blue shift or no shift.

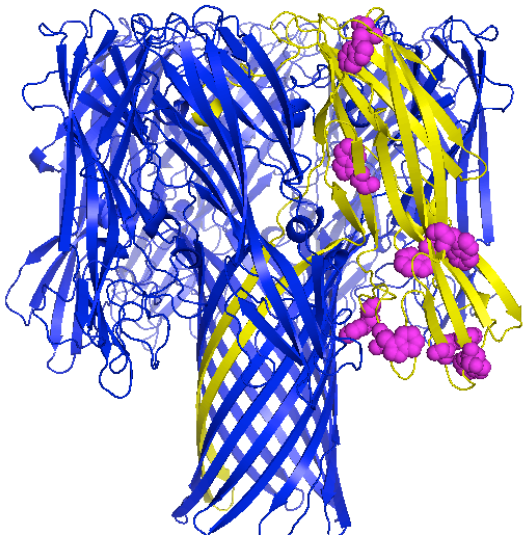


Fig. 8. Ribbon representation of αHL heptamer exposing the Trp residues. *Six subunits are in blue, with one protomer highlighted in yellow and the 8 Trp residues shown as pink spheres.*

Fluorescence spectroscopy is a key element in tertiary structural analysis; however, its results can be ambiguous particularly with membrane proteins making some data hard to interpret. For instance, the partitioning of Trp side chains into lipid bilayers places residues in a less polar environment than water, which can shift the emission maxima to shorter wavelengths, mimics the burial of the residues in the interior of proteins [35]. The denaturant can also change the fluorescence properties of tryptophan [35, 86]. ITFE was implemented in our studies since the αHL monomer contains eight tryptophan residues situated in the β-sandwich: Trp80, Trp167, Trp265, Trp286, Trp179, Trp187, Trp260 and Trp274. The residues are all buried in a hydrophobic environment. Therefore, the heptameric form of the protein contains 56 Trp residues that rearrange slightly after oligomerization (Fig. 8). Four residues on each protomer are almost entirely buried within the hydrophobic core of the protein (Trp80, Trp167, Trp265 and Trp286), while the remaining four are at least partly solvent exposed (Trp179, Trp187, Trp260 and Trp274). If the tertiary structure of the

protein was to change and the protein was to unfold, the buried tryptophan residues are expected to become more solvent exposed and display red-shifted λ_{max}^{em} values.

1.7 Light Scattering Hemolytic Assay

The toxic activity of the αHL involves the monomer assembling onto the phospholipid bilayer of target cells such as human platelets, erythrocytes, monocytes, lymphocytes and endothelial cells [1]. The protein is assembled as a result of a receptor triggering the binding of the monomer or the spontaneous oligomerization. Cell lysis is due to the disruption of the semi-permeability and osmotic activity of the cell, which allows the entrance of ions, water and low molecular weight molecules [1]. Human erythrocytes have been cited to require 1 μM of αHL for lysis [87]. Light scattering hemolytic assays assess the activity of the monomer on rabbit red blood cells (rRBCs) as well as its proper folding. It provides a way of quantifying the activity of the monomer. The method is based on the concept that objects can scatter light. Cells that are not lysed can deviate incoming light from its linear trajectory. If a detector is placed after the sample, the amount of absorption reflects the amount of light that is scattered, which will be proportional to the concentration of cells. The more cells that are present in solution, the more light is scattered. When cells are lysed the light scattering is reduced. By probing the absorption of samples, the activity of the αHL monomer can be quantified as a function of both time and monomer concentration. In this particular body of work, the light scattering hemolytic assays have been used to probe the monomer's ability to regain activity after being unfolded in various denaturants such as urea, GdnCl, trifluoroacetic acid, formic acid and formic acid: ethanol.

1.8 Single-Channel Recording

Electrophysiology recordings of single-channel currents have helped to obtain kinetic information revealing the behavior of ion channels. The technique used in this work utilizes

planar lipid bilayers to mimic the activity of αHL in its cellular environment. Single channel currents are meant to appear as step-like changes in current as the channel opens and closes. The use of the αHL heptamer as a biosensor has its foundations in the Coulter Principle [7], which describes the movement of particles through a pore. When two electrolyte solutions are separated by an aperture with one side containing particles and a potential is applied causing an ionic current to flow, a particle is able to travel through the aperture. The ionic current is initially reduced due to the size of the particle, since its blocking of the pore will allow fewer ions to flow through. By measuring the decrease in current, the volume of the particles can be identified and quantified since each current drop corresponds to a translocation of one particle. When an analyte enters the αHL pore, it obstructs the flow of ions, which is detected by the decrease in conductivity. The pore can be modified according to the analyte by direct mutagenesis to specific sites on the inside of the pore allowing for covalent or non-covalent attachment of the analyte. Identifying the analyte and the amount passing through the pore is determined by the duration and amplitude of the binding event. The use of the protein pore allows for single-molecule sensing and leads to high sensitivity and ultra-rapid response times.

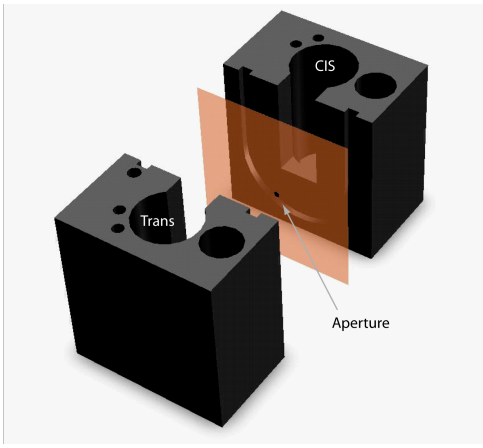


Fig. 9. Image of the electrophysiology chamber. *The cis and trans side of the chamber are separated by Teflon film, containing an aperture where the lipid bilayer is formed at the interface. Image courtesy of the HB group.*

This work employs the use of a chamber with an aperture separating the *cis* and *trans* side (Fig. 9). The volume of both sides of the chamber can occupy 500 μL to 1 mL of buffer. Each side of the chamber also contains areas that accommodate an Ag/AgCl electrode, which allows a potential to be applied to the solution. The aperture is constructed from 25 μm thick Teflon film containing a 100 μm diameter hole, which is created by an electric arc. The *cis* and *trans* side are electrically isolated by forming a bilayer at the interface. In order to do this, the orifice of the chamber is first pre-treated with a 10% solution of hexadecane in pentane (v/v) on both sides. A buffer solution is added to both sides of the chamber and then a 1% solution of diphytanoyl phosphatidylcholine (DPhPC) in hexadecane (w/v) is added. The composition of the lipids that forms the membrane is important in the formation of the αHL pore. Liposomes created by other lipids: phosphatidylethanolamine, phosphatidylserine, phosphatidylglycerol or phosphatidylinositol do not provide the ideal environment for αHL pore formation [88, 89]. However, those composed of phosphatidylcholine or sphingomyelin and cholesterol are a suitable environment for insertion [3]. Pipetting the solution from either the *cis* or *trans* side up and down, creates the planar lipid bilayer. The size and quality of the membrane formed can be verified by observing the capacitance, which is obtained by applying a triangular wave potential whose corresponding reading is a square current wave function. This phenomenon is evident by the formula:

$$I = C\,(dV/dt)$$

I is the current, C is the capacitance, V is the voltage and t is the time. An aperture with a 100 μm diameter hole shows a capacitance of 60–100 pF, which corresponds to 60–100 pA since the system is calibrated with a Bilayer Model Cell that has a capacitance of 100 pF.

Once a stable bilayer, can withstand an applied voltage, protein is added to the *cis* side of the chamber, which is grounded. Observing the rectification pattern of the protein [90], once inserted into the bilayer will help determine whether the protein is folded properly and inserted in the correct orientation. Studies have shown that channel conductance depends linearly on the buffer conductivity [90]. αHL channels have shown anion-selectivity, which increases at low pH due to the protonation of acidic residues such as E111 in the barrel [90]. As stated, the αHL has been modified to detect various analytes via single-channel recording. Single-channel recording has been implemented in this work to detect whether attempts at refolding αHL monomer after incubation in urea were successful and compared favorably to heptamer and native monomer.

1.9 Thesis Overview

The goal of this body of work was to study the unfolding and refolding behavior of the αHL monomer and heptamer, under conditions that include high pH and high concentrations of urea as a denaturant. These studies were conducted on the heptamer in order to determine whether these conditions would facilitate DNA/RNA translocation and aid in DNA sequencing. Unfolding and refolding studies conducted on the monomeric form of αHL were conducted in order to investigate conditions that would aid in the refolding of αHL after chemical ligation studies. The main techniques used to investigate the behavior of the monomeric and heptameric αHL include circular dichroism, intrinsic tryptophan fluorescence spectroscopy, light scattering hemolytic assays and single-channel recording.

1.10 References

1. Bhakdi, S. and Tranum-Jensen J., *Alpha-toxin of Staphylococcus aureus.* Microbiological Reviews, 1991. **55**: 733–751.
2. Song, S., et al. *Structure of Staphylococcal α-hemolysin, a heptameric transmembrane pore*. Science, 1996. **274**: 1859–1866.
3. Montoya, M., et al. *β-Barrel membrane protein folding and structure viewed through the lens of α-hemolysin*. Biochimica et Biophysica Acta, 2003. **1609:** 19–27.
4. Walker, B., et al. *Assembly of the oligomeric membrane pore formed by Staphylococcal Alpha-hemolysin examined by truncation mutagenesis*. J Biol Chem, 1992. **267**: 21782 – 6.
5. Walker, B., and Bayley, H., *Key residues for membrane binding, oligomerization, and pore forming activity of Staphylococcal α-Hemolysin identified by cysteine scanning mutagenesis and targeted chemical modification.* J Biol Chem, 1995. **270**: 23065–71.
6. Sangha, N., et al. *Importance of the carboxyl terminus in the folding and function of α-hemolysin of Staphylococcus aureus.* J Biol Chem, 1999. **274**: 9193–9.
7. Bayley, H., et al. *Resistive-pulse sensing-from microbes to molecules*. Chem Rev, 2000. **100:** 2575–94.
8. Bayley, H. *Sequencing single molecules of DNA*. Current Opinion in Chemical Biology, 2006. **10**: 628–37.
9. Gu, L., et al. *Stochastic sensing of organic analytes by a pore-forming protein containing a molecular adapter.* Nature, 1999. **398**: 686–90.
10. Kasianowicz, J., et al. *Characterization of individual polynucleotide molecules using a membrane channel*. Proc Natl Acad Sci U S A, 1996. **93**: 13770–3.

11. Ashkenasy, N., et al. *Recognizing a single base in an individual DNA strand: a step toward DNA sequencing in nanopores*. Angew Chem International Edition, 2005. **44**: 1401–4.

12. Astier, Y., et al. *Toward single molecule DNA sequencing: direct identification of ribonucleoside and deoxyribonucleoside 50-monophosphates by using an engineered protein nanopore equipped with a molecular adapter*. J Am Chem Soc, 2006. **128**: 1705– 10.

13. Zimmer, C. *Alkaline denaturation of DNA's from various sources*. Biochim Biophys. Acta, 1968. **161**: 584–586.

14. Ageno, M., et al. *Alkaline denaturation of DNA*. Biophys J, 1969. **9**:1281–1311.

15. Chapman, R., et al. *Volume changes accompanying thermal denaturation of deoxyribonucleic acid. II. Denaturation at alkaline pH.* Biopolymers, **9**:445–447.

16. Watson J. and Crick F., *Genetical Implications of the structure of deoxyribonucleic acid*. Nature, 1953. **171**: 964–967.

17. Watson J. and Crick F., *A structure for deoxyribose nucleic acid*. Nature, 1953. **171**: 737–738.

18. Saiki, R., et al. *Enzymatic amplification of beta-globin genomic sequences and restriction site analysis for diagnosis of sickle cell anemia*. Science, 1985. **230**: 1350 – 54.

19. Fleischmann, R., et al. *Whole-genome random sequencing and assembly of Haemophilus influenzae*. Science, 1995. **269** :496–512.

20. Blattner, F., et al. *The complete genome sequence of Escherichia coli K-12.* Science, 1997. **277**: 1453 – 62.

21. The International Human Genome Mapping Consortium, *Finishing the euchromatic*

sequence of the human genome. Nature, 2004. **431**: 931–945.

22. Stephan, J. et al. *Towards a general procedure for sequencing single DNA molecules*. Journal of Biotechnology, 2001. **86**: 255–67.
23. Davis, L., et al. *Rapid DNA sequencing based upon single molecule detection*. Genetic Analysis: Biomolecular Engineering, 1991. **8**: 1 – 7.
24. Stoddart, D., et al. *Single-nucleotide discrimination in immobilized DNA oligonucleotides with a biological nanopore.* Proc Natl Acad Sci U S A, 2009. **106**: 7702–7.
25. Storm, A.J., et al. *Fabrication of solid-state nanopores with single-nanometer precision.* Nat Mater, 2003. **2**: 537–40.
26. Dill, K. and Shortle, D., *Denatured states of proteins.* Annu Rev Biochem, 1991. **60**: 795– 825.
27. Tanford, C., *Protein Denaturation*. Adv Protein Chem, 1968. **23**: 121 – 282.
28. Tanford, C., *Protein Denaturation: Part C, Theoretical models for the mechanism of denaturation.* Adv Protein Chem, 1970. **24**: 1–95.
29. Rothman, J. and Kornberg, R., *An unfolding story of protein translocation*. Nature, 1986. **322**: 209–210.
30. Verner, K. and Schatz, G., *Import of an incompletely folded precursor protein into isolated mitochondria requires an energized inner membrane, but no added ATP*. EMBO J, 1987. **6**: 2449–56.
31. Deshaies, R., et al. *The role of stress proteins in membrane biogenesis.* Trends Biochem Sci, 1988. **13**: 384–88.
32. Pastoriza-Gallego, M., et al. *Urea denaturation of a-hemolysin pore inserted in planar*

lipid bilayer detected by single nanopore recording: loss of structural asymmetry. FEBS Letters, 2007. **581**: 3371–6.

33. Parker, M., et al. *Pore forming protein toxins: from structure to function*. Prog Biophys Mol Biol, 2005. **88:** 91–142.

34. Tilley, S., and Saibil, H., *The mechanism of pore formation by bacterial toxins*. Curr Opin Struct Biol, 2006. **16**: 230–6.

35. Stanley, A. and Fleming, K., *The process of folding protein into membranes challenges and progress*. Archives of Biochemistry and Biophysics, 2008. **469**: 46–66.

36. Bortoleto, R. and Ward, R., *A Stability transition at mildly acidic pH in the alpha-hemolysin (alpha-toxin) from Staphylococcus aureus*. FEBS Letters, 1999. **459**: 438–42.

37. Pace, C., *Determination and analysis of urea and guanidine hydrochloride denaturation curves.* Methods Enzymol, 1986. **131**: 266–80.

38. Santoro, M., and Bolen, D., *Unfolding free energy changes determined by the linear extrapolation method. 1. Unfolding of phenylmethanesulfonyl .alpha.- chymotrypsin using different denaturants.* Biochemistry, 1988. **27**: 8063–8.

39. Santoro, M., and Bolen, D., *A test of the linear extrapolation of unfolding free energy changes over an extended denaturant concentration range*. Biochemistry, 1992. **31**: 4901–7.

40. Hong, H. and Tamm, L., *Elastic coupling of integral membrane protein stability to lipid bilayer forces*. Proc Natl Acad Sci U S A, 2004. **101**: 4065–70.

41. Lau, F. and Bowie, J., *A method for assessing the stability of a membrane protein*. Biochemistry, 1997. **36:** 5884–92.

42. Chalikan, T., et al. *Spectroscopic and volumetric investigation of cytochrome c unfolding at alkaline pH: characterization of the base-induced unfolded state at 25°C.* The FASEB Journal, 1996. **10**: 164–70.

43. Lee, B. *isoenthalpic and isoentropic temperatures and the thermodynamics of protein denaturation.* Proc Natl Acad Sci U S A, 1991. **88**: 5154–58.

44. Richards, F., Folded and unfolded proteins: an introduction in protein folding (Creighton, TE ed) 1-58, WH freeman & Co., New York.

45. Aune, K., et al. *Evidence for residual structure in acid- and heat-denatured proteins*. J Biol Chem, 1967. **242**: 4486–9.

46. Dolgikh, D., et al. *α-Lactalbumin: compact state with fluctuating tertiary structure*. FEBS Lett, 1981. **136**: 311–5.

47. Goto, Y., and Fink, A., *Phase diagram for acidic conformational states of apomyoglobin.* J Mol Biol, 1990. **214**: 803–5.

48. Ptitsyn, O., J. *Protein folding: hypotheses and experiments*. Prot Chem, 1987. **6**: 273–93.

49. Stigter, D., et al. *Protein stability: electrostatics and compact denatured states*. Prot Natl Acad Sci, 1991. **88**: 4176–80.

50. Buchanan, S., *β-Barrel proteins from bacterial outer membranes: structure, function and refolding.* Curr Opin Struct Biol, 1999. **9**: 455–61.

51. Pocanschi, C. et al. *Curvature elasticity and refolding of OmpA in large unilameller vesicles.* Biophys J, 2006. **91**: L75–77.

52. Pocanschi, C. et al. *The major outer membrane protein of Fusobacterium nucleatum (FomA) folds and inserts into lipid bilayers via parallel folding pathways*. J Mol Biol, 2006. **355**: 548–61.

53. Rossky, P., *Protein denaturation by urea: slash and bond*. Proc Natl Acad Sci U S A, 2008. **105**: 16825–6.

54. Soper, A., et al. *A Impact of urea on water structure: a clue to its properties as a Denaturant.* Biophys Chem, 2003. **105**: 649–66.

55. Bennion, B., and Daggett, V. *The molecular basis for the chemical denaturation of proteins by urea.* Prot Natl Acad Sci U S A, 2003. **100**: 5142–7.

56. Hua, L., et al. *Urea denaturation by stringer dispersion interactions with proteins than water implies a 2-stage unfolding.* Prot Natl Acad Sci U S A, 2008. **105**: 16928 – 33.

57. Stumpe, M., and Grubmueller, H., *Interaction of urea with amino acids: implications for urea-induced protein denaturation.* J Am Chem Soc, 2007. **129**: 16126–131.

58. Zangi, R., et al. *Urea's action on Hydrophobic interactions*. J Am Chem Soc, 2009. **131**: 1535–41.

59. Wallqvist, A., and Covell, D., *Hydrophobic interactions in aqueous urea solutions with implications for the mechanism of protein denaturation*. J Am Chem Soc, 1998. **120**: 427– 428.

60. O'Brien, E., et al. *Interactions between hydrophobic and ionic solutes in aqueous guanidinium chloride and urea solutions : lessons for protein denaturation mechanism.* J Am Chem Soc, 2007. **129**: 7346–53.

61. Mountain, R. and Thirumalai, D., *Molecular dynamics simulations of end-to-end contact formation in hydrocarbon chains in water and aqueous urea solution.* J Am Chem Soc, 2003. **125**: 1950–7.

62. Huang, K., et al. *Refolding of an integral membrane protein*. J Biol Chem, 1981. **256**: 3802–3809.

63. Cramer, J., et al. *Reversible trifluoroacetic acid-induced conformational change in*

glycoporin A as detected by proton nuclear magnetic resonance spectroscopy. Biochim Biophys Acta, 1980. **595**: 235–43.

64. West, S., and Price, N., *The unfolding and refolding of glutamate dehydrogenases from bovine liver, baker's yeast and Clostridium symbosium.* Biochem J, 1988. **251**: 135–9.
65. Mogensen, J., et. al. *Barriers to folding of the transmembrane domain of the Escherichia coli autotransporter adhesion involved in diffuse adherence.* Biochemistry, 2005. **44**: 4533–45.
66. Mi, D., et al. *Irreversible misfolding of diacylglycerol kinase is independent of aggregation and occurs prior to trimerization and membrane association*. Biochemistry, 2006. **45**:10072–10084.
67. Valiyaveetil, F., et al. *Semisynthesis and folding of the potassium channel KcsA*. J Am Chem Soc, 2002. **124**: 9113–120.
68. Muir, T., et al. *Expressed protein ligation: A general method for protein engineering.* Prot Natl Acad Sci U S A, 1998. **95**: 6705–10.
69. Severinov, K. and Muir, T., *Expressed protein ligation, a novel method for studying protein-protein interactions in transcription*. J Biol Chem, 1998. **273**: 1605–209.
70. Kent, S., *Total chemical synthesis of proteins.* Chem Soc Rev, 2009. **38**: 338–51.
71. Komarov, A., et al. *A modulator strategy for the semi-synthesis of a K+ channel: investigating interactions of the pore helix*. ACS Chem Biol, 2008. **4**: 1029 – 38.
72. Reitz, S., et al. *On the Function and structure of synthetically modified porins*. Angew Chem Int Ed, 2009. **48**: 4853–7.
73. Greenfield, N., *Analysis of Circular Dichroism Data*. Methods in Enzymology, 2004. **383**: 282–317.
74. Wallace, B., et al. *Analyses of circular dichroism spectra of membrane proteins*.

Protein Science, 2003. **12**: 875–84.

75. Cascio, M., and Wallace, B., *A red and blue shifting in the circular dichroism spectra of polypeptides due to dipole effects.* Protein Pept Lett 1, 1994. **1**: 136–40.
76. Cascio, M., and Wallace, B., *Effects of local environment in the circular dichroism spectra of polypeptides.* Anal Biochem, 1995. **227**: 90–100.
77. Chen, Y., and Wallace, B., *Secondary solvent effects on the circular dichroism spectra of polypeptides: Influence of polarization effects on the far ultraviolet spectra of alamethicin.* Biophys Chem, 1997. **65**: 65–74.
78. Kelly, S., et al. *How to study proteins by circular dichroism.* Biochimica et Biophysica Acta, 2005. **1751**: 119–39.
79. Wallace, B. and Mao, D. *Circular dichroism analyses of membrane proteins: An examination of light scattering and absorption flattening in large membrane vesicles and membrane sheets.* Anal Biochem, 1984. **142**: 317–28.
80. Wallace, B., and Teeters, C. *Differential absorption flattening optical effects are significant in the circular dichroism spectra of large membrane fragments.* Biochemistry, 1987. **26**: 65–70.
81. Teeters, C., et al. *A theoretical analysis of the effects of sonication on differential absorption flattening in suspensions of membrane sheets.* Biophys J, 1987. **51**: 527–32.
82. Vivian, J., and Callis, P., *Mechanisms of tryptophan fluorescence shifts in proteins.* Biophysical Journal, 2001. **80**: 2093–109.
83. Callis, P., *^1L_a and ^1L_b transitions of tryptophan: applications of theory and experimental observations to fluorescence of proteins*. Methods in Enzymology, 1997. **278**: 113–51.

84. Chen, Y., and Barkley, M., *Toward understanding tryptophan fluorescence in proteins*. Biochemistry, 1998. **37**: 9976 – 82.

85. Callis, P., et al. *Ab initio calculations of vibronic spectra for indole.* Chem Phys Letters, 1995. **244**: 53–8.

86. Eftink, M.,. *Fluorescence techniques for studying protein structure*. Methods Biochem Anal, 1991. **35**: 127–205.

87. Hildebrand, A., et al. *Staphylococcus aureus alpha-toxin. Dual mechanism of binding to target cells.* J Biol Chem, 1991. **266**: 17195–200.

88. Watanabe, M., et al. *Membrane-damaging action of staphylococcal alpha-toxin on phospholipid-cholesterol liposomes*. Biochim Biophys Acta, 1987. **898**: 257 – 65.

89. Tomita, T., et al. *Influence of membrane fluidity on the assembly of Staphylococcus aureus alpha-toxin, a channel-forming protein, in liposome membrane.* Biol Chem, 1992. **267**: 13391 – 7.

90. Menestrina, G., *Ionic channels formed by Staphylococcus aureus alpha-toxin: Voltage-dependent inhibition by divalent and trivalent cations*. J Membrane Biology, 1986. **90**: 177–90.

Chapter II: Unfolding Studies of Monomeric and Heptameric αHL at Alkaline pH

2.1 Introduction

The αHL heptameric pore has been under intense investigation as a nanopore sensing device due to its dimensions. It has been most recently implemented as a translocator of DNA with the aid of an electrical potential [1]. Therefore, it can be used as a rapid, cheap and efficient system of sequencing DNA. One of the setbacks to achieving this goal is to find conditions that would convert double-stranded DNA (dsDNA) to single stranded DNA (ssDNA) or to prevent ssDNA from forming secondary structures. Previous studies have shown that dsDNA is converted to ssDNA by increasing the pH > 11.5 due to the ionization of nucleotide bases that cause repulsion between the two complementary strands of DNA [2-4]. Therefore, the stability of the αHL heptameric pore in alkaline pH conditions from pH 8.0–13.0 was studied. The behavior of proteins in various pH conditions, particularly acidic conditions in conjunction with various temperatures and urea concentrations, has been studied in the past to aid in the understanding of protein structure and function; especially in determining the importance of charged residues [5]. The effect of alkaline pH on the structure of monomeric and heptameric αHL in solution was investigated using circular dichroism (CD), intrinsic tryptophan fluorescence emission (ITFE) spectroscopy and SDS-PAGE studies. The results obtained for the heptamer were compared to single-channel recording studies conducted on lipid bilayers, which monitored the translocation of DNA conducted by Giovanni Maglia [6].

2.2 Results

2.2.1 CD Studies of Monomeric αHL

CD studies were conducted on the monomer to compare its structural changes with those of the heptamer at pH 8.0–13.0 (10 mM Na phosphate, 10 mM Tris-HCl, 10 mM CAPS, 150 mM NaCl). The time at which the monomer was at equilibrium was determined before conducting the experiments. A prominent peak between 210 and 220 nm was observed for the monomer at pH 8.0 at 215 nm, which is characteristic of a β-sheet. Therefore, the mean residue molar ellipticity at 215 nm was used to decipher whether there were changes occurring in the monomer over the course of increasing pH. The $[\theta]_{RMME\ 215\ nm}$ is −6042.2 at pH 8.0, which is consistent with previous studies [7]. Once the pH is increased, the monomer loses the majority of its secondary structure at pH 11.5 as portrayed by the change in the CD signal (Fig. 1A). A sigmoidal change is observed with a midpoint at pH 10.1 ± 0.1, signifying the pH at which 50% of the monomer is denatured (Fig. 1B).

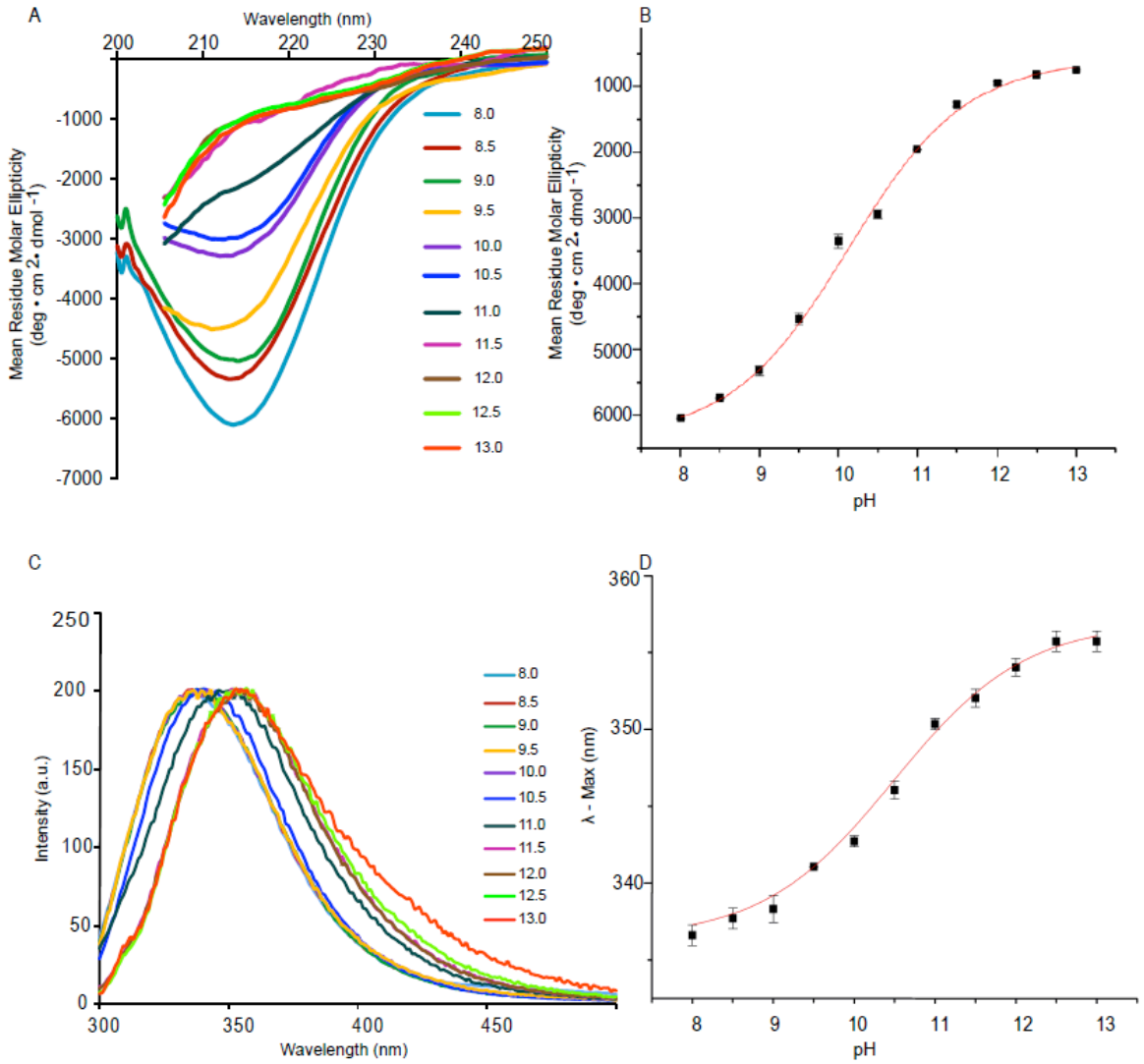


Fig. 1. Effect of alkaline pH on the structure of αHL monomers. *(A) Effect of high pH on the shape of the CD spectra measured from 200 to 250 nm. (B) Changes in the mean residue molar ellipticity at 215 nm ($[\theta]_{RMME\ 215\ nm}$) as a function of pH. The midpoint to the sigmoidal fit is at pH 10.1 ± 0.1. (C) Effect of high pH on the emission spectra of αHL monomers (λ_{max}^{em}, excitation at 280 nm). All of the fluorescence emission spectra have been scaled to the same intensity. (D) Changes in the λ_{max}^{em} of αHL monomers with increasing pH. The midpoint to the sigmoidal fit is at pH 10.5 $\pm$ 0.1. The αHL monomers (50 ug mL^{-1}) were incubated for the appropriate time to reach equilibrium at each pH 8.0–13.0 in 10 mM Na phosphate, 10 mM Tris-HCl, 10 mM CAPS, 150 mM NaCl.*

2.2.2 ITFE Studies of Monomeric αHL

ITFE studies were conducted to monitor tertiary structural changes, due to the sensitivity of tryptophan (Trp) residues depending on their solvent environment. ITFE is often used to detect changes in structure of proteins with excitation of the Trp that can range from 280 to 295 nm and an emission peak, λ_{max}^{em} that can range from 308 to 355 nm depending on solvent polarity [6, 8]. The λ_{max}^{em} is relatively blue-shifted in nonpolar environments and relatively red-shifted in polar environments. Therefore the unfolding of proteins generally leads to a red shift in the λ_{max}^{em} value as buried Trp become more exposed to the solvent [9, 10]. ITFE was employed to determine the relative position of the 8 Trp residues on the αHL monomer. A sigmoidal change of the emission maxima (λ_{max}^{em}, with an excitation at 280 nm) is observed from 335 nm at pH 8.0 to 355 nm at pH 13.0 (Fig. 1B). The midpoint at pH 10.5 $\pm$ 0.1 is close in value to that of the CD experiments, indicating that the loss of secondary and tertiary structure is concomitant. By pH 12.0, the Trp residues seem fully exposed to the solvent environment indicating that the monomer is most likely unfolded.

2.2.3 CD Studies of Heptameric αHL

CD was used to monitor the secondary structural changes of the αHL heptamer. Since the majority of the heptamer's mass and β-sheet content is concentrated in the cap domain, any changes detected with increasing pH most probably reflect changes in this region as opposed to the stem domain. Wild-type (WT) αHL at pH 8.0 seen in Fig. 3A (10 mM Tri-HCl, 10 mM CAPS, 10 mM Na phosphate, 150 mM NaCl, 0.3% (w/v) SDS) has a prominent peak at 215 nm [7, 11, 12]. The incubation time at each pH condition (8.0–13.0) was first determined by a time course conducted over a period of 24 h after which 6 h was determined as an appropriate incubation time; as shown for pH 13.0 in Fig. 2.

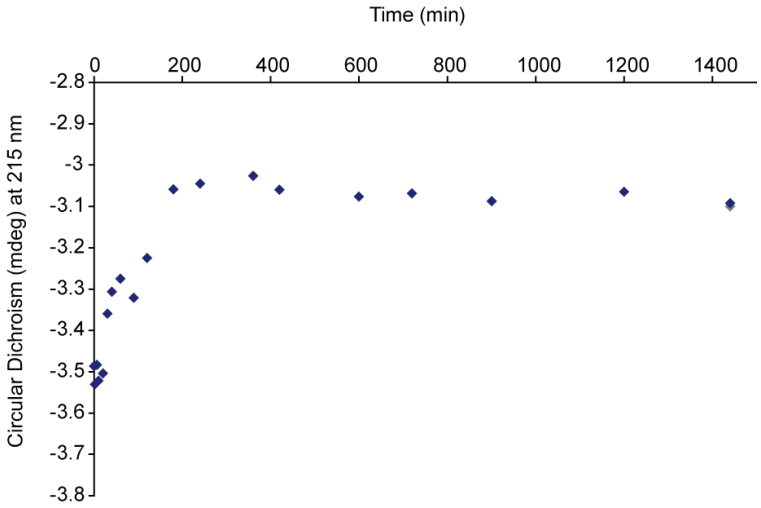


Fig. 2. Time dependence of the behavior of the αHL heptamer at pH 13.0 monitored by CD. *Heptamers (100 μg mL^{-1}) were incubated in pH 13.0 for 24 h and their behavior was monitored by measuring the change in the CD signal portrayed in mdeg at 215 nm. This experiment was completed at pH 8.0 –13.0 made in 10 mM Na phosphate, 10 mM Tris-HCl, 10 mM CAPS, 10 mM Na phosphate, 150 mM NaCl, 0.3% (w/v) SDS.*

The effects of incubating αHL heptamer (100 μg mL^{-1}) in pH 8.0–13.0 reveal that its secondary structure remains almost unchanged until pH 11.5 with the peak at 215 nm still prominent (Fig. 3A). Between pH 12.0 and pH 13.0, the secondary structure begins to change and the β-sheet content is lost. The $[\theta]_{\text{RMME 215 nm}}$ changes from –6042 at pH 8.0 to –3122 at pH 13.0. The change in signal at 215 nm from pH 8.0–13.0 was fitted to a sigmoidal curve with a midpoint of pH 12.0 ± 0.1 (Fig. 3B).

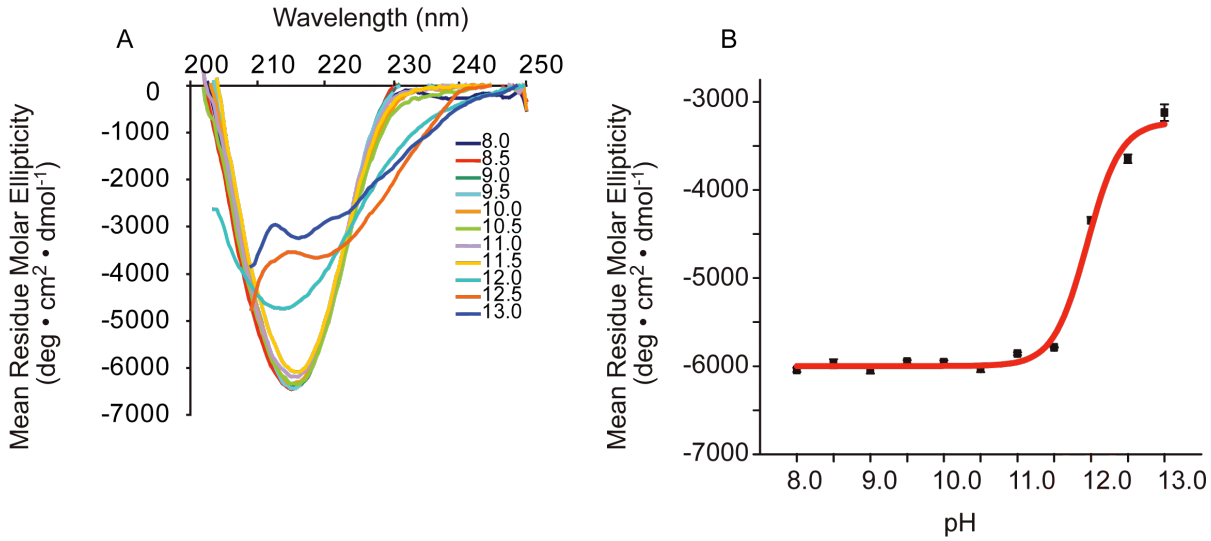


Fig. 3. Effect of alkaline pH on the structure of αHL heptamers. *(A) Effect of high pH on the shape of the CD spectra measured from 200 to 250 nm. (B) Changes in the* $[\theta]_{RMME\ 215\ nm}$ *as a function of pH. The midpoint of the sigmoidal fit is a pH of 12.0 ± 0.1. The αHL heptamers (100 ug* mL^{-1}*) were incubated for 6 h in 10 mM Na phosphate, 10 mM Tris-HCl, 10 mM CAPS, 150 mM NaCl, 0.3% (w/v) SDS at pH 8.0–13.0.*

2.2.4 ITFE Studies of Heptameric αHL

ITFE Spectroscopy was employed to detect structural changes in the heptamer by observing the average changes occurring to its 56 tryptophan residues.

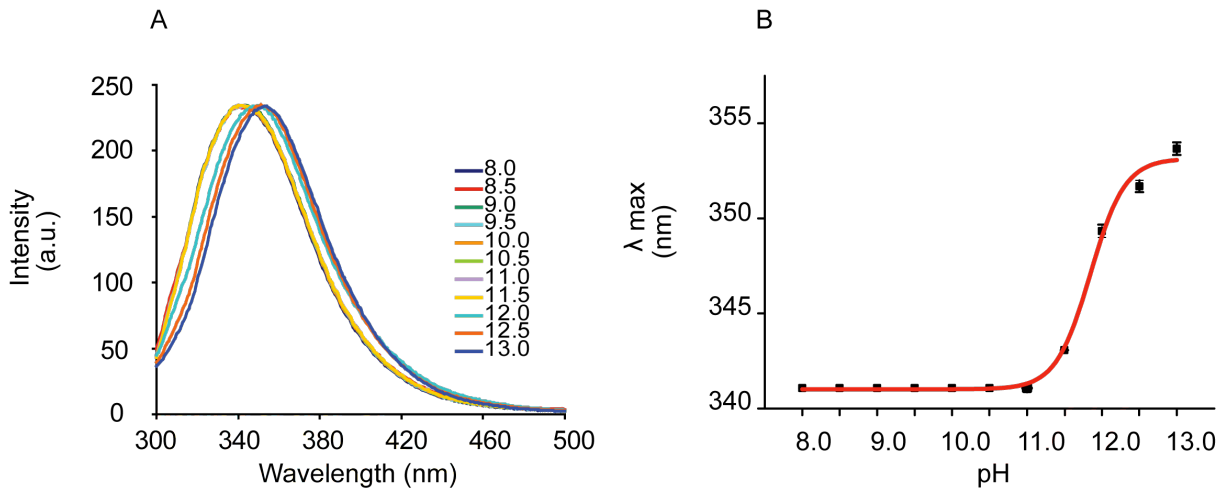


Fig. 4. Effect of alkaline pH on the structure of αHL heptamers. *(A) Effect of high pH on the emission spectra of αHL heptamers (λ_{max}^{em}, excitation at 280 nm). All of the fluorescence emission spectra have been scaled to the same intensity. (B) Changes in λ_{max}^{em} of αHL heptamers with increasing pH condition. The midpoint of the sigmoidal fit is at pH 11.9 ± 0.1. The αHL heptamers (100 ug mL^{-1}) were incubated for 6 h in 10 mM Na phosphate, 10 mM Tris-HCl, 10 mM CAPS, 150 mM NaCl, 0.3% (w/v) SDS at pH 8.0–13.0*

As seen in Fig. 4A, at pH 8.0 (10 mM Na phosphate, 10 mM Tris-HCl, 10 mM CAPS, 150 mM NaCl, 0.3% (w/v) SDS), the heptamer (100 µg mL^{-1}) has a λ_{max}^{em} of 341 nm that is retained until pH 11.5 (Fig. 4B). These results represent the average emission of the buried and solvent exposed Trp residues. A dramatic red shift to 350 nm at pH 12.0 and then to 356 nm at pH 13.0 is observed (Fig. 4B). The λ_{max}^{em} at pH 13.0 is similar to that of N-acetyltryptophanamide in solution (λ_{max}^{em} = 358 nm) [13]. This is evidence of completely exposed Trp residues unless the buried tryptophan residues are completely quenched by nearby residues. The pH dependence of λ_{max}^{em} on αHL heptamers is fitted to a sigmoidal curve with a midpoint at pH 11.9 ± 0.1.

2.2.5 SDS-PAGE Studies of Heptameric αHL

Gel electrophoresis is a method employed to separate biopolymers such as DNA, RNA or proteins according to their charge and mass, a result of an electrophoretic force applied by a potential. We utilize SDS-PAGE in our studies to elucidate the effect of pH on the disassembly of the αHL heptamer. These studies provide a visual understanding of what may be happening in bulk solution, which cannot be depicted in the spectroscopy techniques.

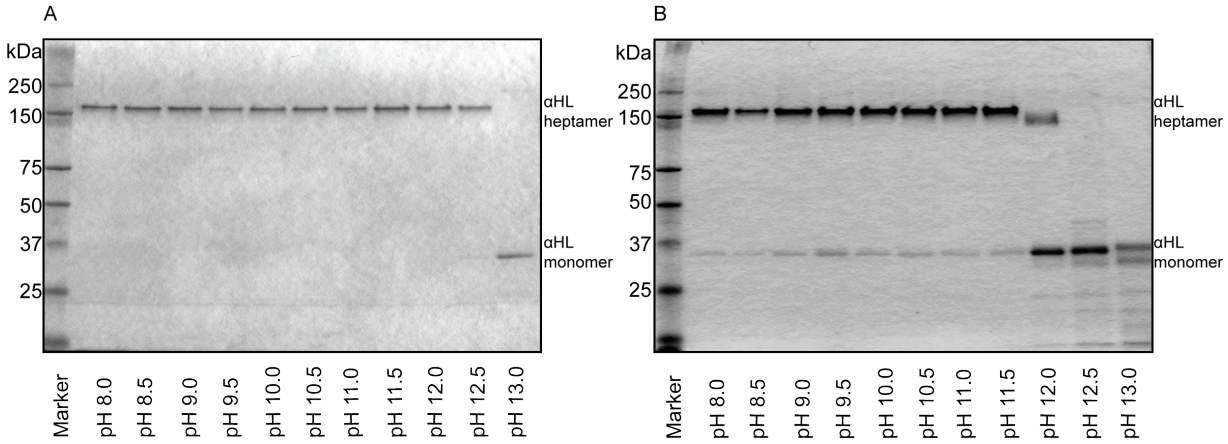


Fig. 5. The effect of alkaline pH on the structure of αHL heptamer. *SDS-PAGE was conducted on a 10% Bis-Tris gel of (A) αHL heptamers (50μg mL^{-1}) incubated for 8 h and (B) αHL heptamers (100 μg mL^{-1}) incubated for 1 wk from pH 8.0–13.0. All pH buffers were made in 10 mM Tris-HCl, 10 mM CAPS, 10 mM Na phosphate, 150 mM NaCl, containing 0.3% (w/v) SDS .*

The behavior of the heptamer (100 μg mL^{-1}) in 10 mM Na Phosphate, 10 mM Tris-HCl, 10 mM Caps, 150 mM NaCl, 0.3% (w/v) SDS in pH 8.0–13.0 was studied via SDS-PAGE after 8 h of incubation (Fig. 5A). The quaternary structure of the heptamer appears to be stable up to pH 12.5. Upon incubation at pH 13.0, the αHL heptamer seems to degrade in SDS-PAGE into monomers. Even after a week of incubation, the heptamer is stable at pH 8.0–11.5 and only a small percentage breaks down to monomer (Fig. 5B).

2.3 Discussion

The purpose of these studies was to determine the stability of the αHL monomer (33.2 kDa) and heptamer (234 kDa) at high pH conditions and to determine optimal conditions for DNA sequencing, since the conditions tested are suitable for the dissociation of dsDNA to ssDNA. Previous studies conducted on dsDNA have shown that alkaline pH results in the ionization of nucleotide bases G and T. Charge repulsion ultimately results in the separation of dsDNA to ssDNA [2-4].

Studies on the denaturation of proteins as a function of pH have been conducted mostly on soluble proteins and at acidic pH in conjunction with other unfolding agents. Increasing the pH results in the deprotonation of amino acid side chains, eventually causing charge repulsion. Charged residues such as the 27 Lysine (Lys) and 10 arginine (Arg) residues (Fig. 6) may contribute largely to the repulsion that results in the monomer and heptamer's denaturation at high pH conditions. The pKas of Lys and Arg are 10.53 and 12.48, respectively, pH values at which the majority of the protein's structure is affected [14].

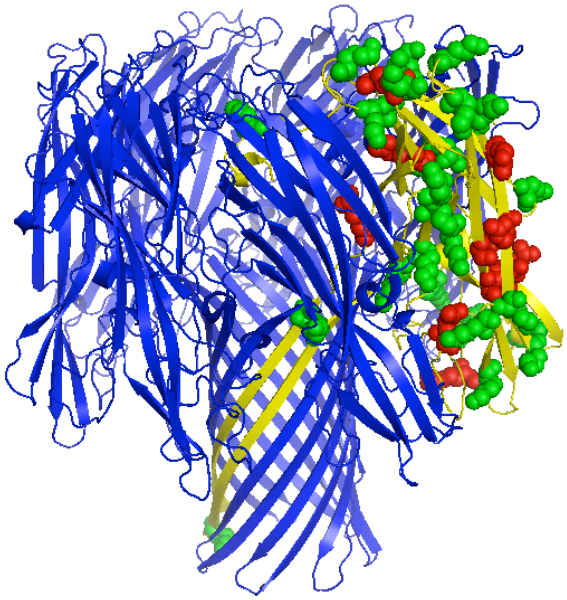


Fig. 6. Ribbon representation of αHL heptamer exposing the Lys and Arg residues. *Six subunits are in blue, with one protomer highlighted in yellow and the Lys and Arg residues shown as green and red spheres.*

Experiments conducted in this work show that the αHL monomer unfolds gradually as the pH is increased from 8.0–13.0. The denaturation is fitted to a sigmoidal curve for both the CD and ITFE studies with a midpoint at pH 10.1 ± 0.1 and 10.5 ± 0.1 M, respectively. The similarity in midpoint values suggests that the monomer unfolds cooperatively as the pH is increased. The monomer is less stable than the heptamer since it seems to unfold completely by pH 12.0, whereas the heptamer starts to loose its structure at this point. The αHL heptamer is stable at alkaline conditions up to a pH of 11.5 and starts degrading at pH conditions ≥ 12.0. The ITFE studies depict the change in behavior of 56 Trp residues present on the heptamer as the pH is increased. Each of the seven subunits on the heptameric pore contain 8 Trp residues; 4 of which are buried in a hydrophobic environment (Trp80, Trp167, Trp265 and Trp286) while the other 4 are at least partially exposed to the solvent (Trp179, Trp187, Trp260 and Trp274). The heptamer has a λ_{max}^{em} of

341 nm, which is not indicative of completely buried Trp residues, which is observed in the αHL monomer at 334 nm. When the pH is increased from 8.0–13.0, a red-shift is observed to 356 nm displaying the transfer of Trp residues to a more polar environment, representing completely exposed Trp residues similar to results observed for the monomer. It seems that at pH ≥ 12.5, the protein's cap domain is completely unfolded. The change in the λ_{max}^{em} of the heptamer as a function of alkaline pH was fitted to a sigmoidal curve with a midpoint at pH 11.9 ± 0.1, which is in agreement with that of the CD results having a midpoint at pH 12.0 ± 0.1. Since the majority of the β-sheet content of the heptamer is in the cap domain, it seems the cap domain of the heptamer is most probably denaturing cooperatively, when all subunits are unfolding simultaneously. A significant amount of the heptamer's unfolding occurs over a short range of pH values, between pH 11.5 and 13.0. The SDS-PAGE studies confirm what is observed in the spectroscopy studies. The heptamer is stable until pH 11.5 and starts degrading by pH 12.0 into monomer. It seems that between pH conditions 12.0 and 13.0 the amino acid side chains of Arg residues most likely become deprotonated, forcing intramolecular repulsion that results in the protein unfolding. Additionally, the heptamer is able to withstand alkaline conditions between pH 8.0–11.5 even after a week of incubation.

Structural changes that were observed on the heptamer in bulk solution were compared to single-channel recording studies of the heptamer, where the translocation of dsDNA was investigated by Giovanni Maglia [6]. Studies conducted at pH 8.0 on the WT-αHL pore at positive potential revealed that single-stranded DNA (ssDNA) causes blockades of low and mid-amplitude that reflect translocation and vestibule events, respectively [15, 16]. The translocation of 92-nt ssDNA is pH dependent with translocation ceasing at pH values above 10.7 in 1.0 M KCl and +120 mV, which is probably due to the

deprotonation of Lys residues that normally would aid DNA translocation at physiological pH. The deprotonation of Lys at high pH results in the pore becoming less positive and reducing the positive electrostatic interactions between the pore and the negatively charged DNA and reducing the capture rate. Therefore to force the translocation of DNA at high pH, site-directed mutagenesis was employed to introduce an Arg residue at the constriction site that would remain protonated at high pH. Testing the addition of ssDNA with the mutated αHL pore, M113R at pH 11.7, produced frequent current blockades depicting translocation events that were similar to those observed for WT-αHL at pH 8.0. The occurrence of vestibule events (mid-amplitude events) is significant since they show that the cap domain is still intact at pH 11.7.

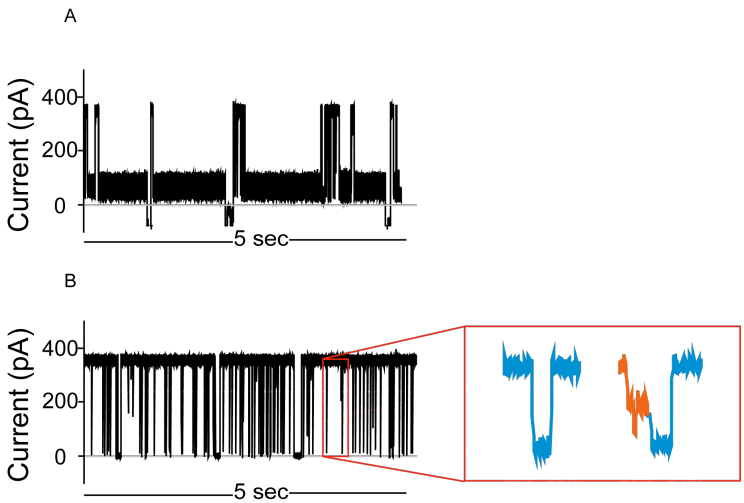


Fig. 7. Single-channel recording depicting the interaction of dsDNA with αHL. *(A) dsDNA does not translocate through WT-αHL pores at pH 8.0. (B) Increasing the pH to 11.7, dsDNA denatures to ssDNA and translocates through M113R pores. The inset displays a closer view of translocation events seen in blue and vestibule events seen in orange. Figure modified from Maglia et al. 2009* [6].

After conducting studies with ssDNA the same conditions were investigated with dsDNA. Using a 60-mer dsDNA at pH 8.0 in 3.0 M KCl at +150 mV on the WT-αHL pore resulted

in very long and short blockades (Fig. 7A). Testing these conditions at pH 11.7 with the M113R αHL pore, long and mid-amplitude events were observed (Fig. 7B), which is similar to the results seen with the WT pore and ssDNA at pH 8.0. This suggests that dsDNA is denatured at 11.7 and is translocated through the pore as ssDNA.

2.4 Conclusions

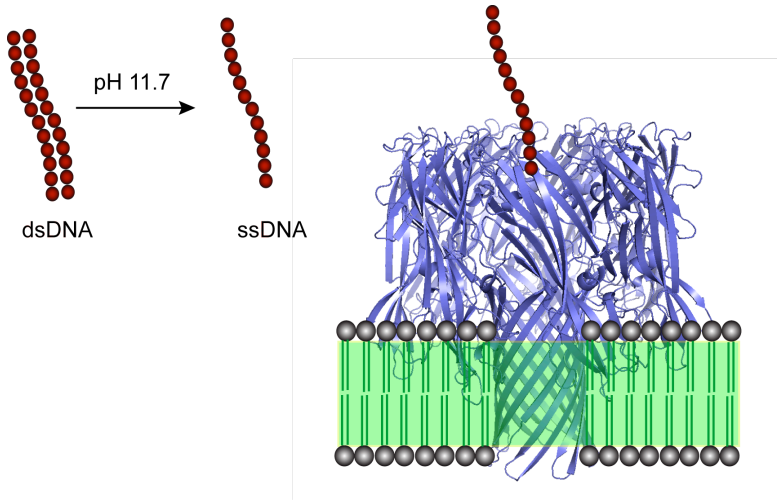


Fig. 8. Diagram showing the dissociation of dsDNA to ssDNA and its translocation through αHL pores.

Investigating the effects of high pH on the αHL monomer and heptamer is essential in understanding protein structure and function in addition to probing methods to facilitate DNA translocation through the pore. The protein's structural stability in bulk solution at a pH range of 8.0–13.0 was studied in order to monitor its behavior. The denaturation of the monomeric protein is less cooperative than the heptamer. Experiments conducted in planar lipid bilayers, facilitated in determining the appropriate conditions at which the pore was stable enough to translocate ssDNA, which was dissociated from dsDNA. The heptameric protein pore is a suitable device to study polynucleotides under harsh conditions that may be applied to DNA sequencing. Other conditions and methods may also be developed to

slow down the speed at which DNA or RNA is translocated. Additionally, these conditions can potentially be used to study the translocation of other macromolecules and analytes.

2.5 Materials and Methods

2.5.1 Protein Preparation

The WT-αHL monomer and heptamer preparation was obtained from Wood 46 strain of *Staphylococcus aureus* by Qiuhong Li as previously reported (See Chapter V: Appendix) [6]. Before the CD and ITFE experiments were conducted, the buffer of the extracted monomer and pre-oligomerized heptamer (1 mg mL^{-1}) was exchanged with 10 mM Na phosphate, 10 mM Tris-HCl, 10 mM CAPS, 150 mM NaCl from pH 8.0–13.0 by using P6 microcentrifuge columns (732-6221, Bio-Rad) that were spun at 2000 Xg (Eppendorf, 5417R). The same buffer was used for the heptamer with the addition of 0.3% SDS. Stock solutions of the pH buffers were adjusted using 1.0 M NaOH. The protein was diluted to 100 μg mL^{-1} in each of the pH conditions and the pH was confirmed using the Orion Ross pH electrode from Thermo (Fisher Scientific UK Ltd) before conducting the CD and ITFE studies.

2.5.2 CD

CD data were collected for both the monomer and heptamer at high pH. A time course was conducted for the heptamer over a period of 24 h for the pH studies. After the steady state was ascertained, experiments were conducted to study the behavior of the heptamer under high pH conditions and were replicated three times. The samples were placed in a 0.1 cm path length CD cuvette (Hellma UK, Essex, UK) and the signal was measured between 200 and 250 nm (Chirascan, Applied Photophysics Limited, Leatherhead, UK). The signals were collected at 0.5 nm intervals for 1 s per point at 25 °C. At least 10 spectra were collected for each sample at each pH value (8.0 to 13.0). The pH

measurements began with the protein in solution that had been incubated at pH 8.0 and ended with the solution at pH 13.0. The spectra were averaged and smoothed with the Chirascan Pro Data Viewer. The signal in millidegrees was converted to mean residue molar ellipticity [θ] with the same software. The signal at 215 nm, corresponding to the minimum in the β-sheet signal, was plotted versus the values for pH. The average of the three experiments conducted were taken, and the standard deviation was derived in order to ascertain the error. The OriginPro 8 program was used to add the error bars.

2.5.3 ITFE Spectroscopy

ITFE studies were conducted for the monomer and heptamer after incubation at alkaline pH. The heptamer was placed in a fluorescence cuvette of 1.0 cm path length (Hellma UK) and the fluorescence emission was measured every 0.2 nm from 300 to 500 nm with excitation at 280 nm and 5 nm slit width with a Cary Eclipse fluorescence spectrophotometer (Varian Inc, Palo Alto, CA, USA) at 25 °C. At least 10 spectra were collected, averaged and smoothed before determining the λ_{max}^{em} value. Three separate experiments were repeated in this manner for each pH condition for the heptamer. The average of the three experiments conducted were taken, and the standard deviation was derived in order to ascertain the error. The OriginPro 8 program was used to add the error bars. All of the fluorescence emission spectra were sacled to the same intensity. The same procedure was followed for the monomer studies.

2.5.4 SDS-PAGE

SDS-PAGE studies were conducted for the heptamer at alkaline pH. A gel analyzing the effect of pH 8.0 to 13.0 in 10 mM Na phosphate, 10 mM Tris-HCl, 10 mM CAPS, 150 mM NaCl containing 0.3% (w/v) SDS on the structure of the heptamer, was run after 8 h (having a concentration of 50 μg mL^{-1}) and again after a week (having a concentration of

100 μg mL^{-1}). For all of the studies the heptamer was diluted 1:2 at room temperature with loading buffer (XT sample buffer, Bio-Rad Laboratories Ltd, Hertfordshire, UK) and loaded onto a Criterion XT Bis-Tris 10% gel (Bio-Rad Laboratories). The Precision Plus Protein Marker (161-0374, Bio-Rad) was used to determine the position of the heptamer after electrophoresis. The SDS-PAGE was run at 200 V for 55 min with 1X MOPS as running buffer. The gels were then stained with Instant Blue buffer (no. ISB01L, Expedeon Protein Solutions) overnight and then washed thoroughly with water.

2.6 References

1. Kasianowicz, J., et al. *Characterization of individual polynucleotide molecules using a membrane channel.* PNAS, 1996. **93**: 13770–3.
2. Zimmer, C. *Alkaline denaturation of DNA's from various sources.* Biochim Biophys Acta, 1968. **161**: 584–6.
3. Ageno, M., et al. *Alkaline denaturation of DNA.* Biophys J, 1969. **9**: 1281–311.
4. Chapman, R., et al. *Volume changes accompanying thermal denaturation of deoxyribonucleic acid. II. Denaturation at alkaline pH.* Biopolymers, **9**: 445–7.
5. Dill, K. and Shortle, D., *Denatured states of proteins.* Annu Rev Biochem, 1991. **60**: 795–825.
6. Maglia, G., et al. *DNA strands from denatured duplexes are translocated through engineered protein nanopores at alkaline pH.* Nano Lett, 2009. **9**: 3831-6.
7. Tobkes, N., et al. *Secondary structure and assembly mechanism of an oligomeric channel protein.* Biochemistry, 1985. **24**: 1915 –20.
8. Vivian, J., and Callis, P., *Mechanisms of tryptophan fluorescence shifts in proteins.* Biophysical Journal, 2001. **80**: 2093–109.
9. Eftink, M., Fluorescence *techniques for studying protein structure.* Methods Biochem Anal, 1991. **35**: 127– 205.
10. Swaminathan, R., et al. *Similarity of fluorescence lifetime distributions for single tryptophan proteins in the random coil state*. N Biophys J, 1994. **67**: 2013– 23.
11. Kelly, S., et al. *How to study proteins by circular dichroism*. Biochimica et Biophysica Acta, 2005. **1751**: 119–39.
12. Greenfield, N., *Analysis of circular dichroism data*. Methods in Enzymology, 2004. **383**: 282–317.

13. Lotte, K., et al. *Static and time-resolved fluorescence investigations of tryptophan analogues – a solvent study.* Photochem Photobiol Sci, 2004. **3**: 348-59.

14. pka Data: CRC handbook of Chemistry, v. 1988-1989. CRC Press, Inc., Boca. Florida.

15. Butler, T., et al. *Ionic current blockades from DNA and RNA molecules in the alpha-hemolysin nanopore.* M Biophys J, 2007. **93**: 3229– 40.

16. Maglia, G., et al. *Enhanced translocation of single DNA molecules through alpha-hemolysin nanopores by manipulation of internal charge.* Proc Natl Acad Sci USA, 2008. **105**: 19720–5.

Chapter III: Unfolding Studies of Heptameric αHL in Urea

3.1 Introduction

The distinctive shape and structure of the αHL heptameric pore makes it suitable as a nanodevice in the detection of certain analytes, particularly polynucleotides. In order to mould the αHL heptamer into a device that could potentially be used for DNA sequencing, it must allow the passage of single stranded DNA (ssDNA) and ssRNA, which can be detected by single-channel recording as they are electrically driven through the pore from the *cis* entrance through the *trans* exit. Once DNA/RNA passes through the pore, it blocks the flow of ions, which can vary according to the composition of the polynucleotide sequence [1-4]. The formation of secondary structures by ssDNA has been shown to inhibit the recognition of bases and long reads [5-8]. Additionally, the αHL heptamer has a constriction site having a diameter of 14–15 Å, which makes it selective in the macromolecules it can translocate. Studies in this work focus on conditions needed to facilitate the translocation of ssDNA, which may contain secondary structure, through the pore.

In this chapter, I investigated the structural stability of the αHL heptameric pore in various concentrations of urea at which the secondary structure of ssDNA/RNA is known to unfold from previous studies [9-11]. The effect of urea on the structure of the αHL pore in solution was investigated using circular dichroism (CD), intrinsic tryptophan fluorescence emission (ITFE) spectroscopy and SDS-PAGE. The results obtained were correlated to single-channel recording studies on the heptamer focusing on the translocation of ssDNA and ssRNA through the pore conducted by Deanpen Japrung [12].

3.2 Results

3.2.1 CD Studies of Heptameric αHL

Secondary structural changes in the αHL heptamer upon incubation in various concentrations of urea were detected by circular dichroism (CD). Wild-type (WT) αHL in 0 M urea seen in Fig. 2A (20 mM Na phosphate, 150 mM NaCl, 0.3% (w/v) SDS at pH 8.0) has a prominent β-sheet peak at 218 nm, which is in agreement with previous studies [13]. The incubation time at each urea concentration was determined by a time course conducted over a period of 24 h in which 6 h was determined as an appropriate incubation time for the heptamer in each urea concentration (Fig. 1). The effects of incubating the αHL heptamer (100 μg mL^{-1}) in 0 M–8.0 M urea reveal a change in the CD signal as the urea concentration increases with the peak at 218 nm still prominent (Fig. 2A). Since urea has a tendency to absorb in the far-UV regions of the CD spectra [13], data in the region between 200–210 nm in 1.0–8.0 M urea has been excluded. The mean residue molar ellipticity at 218 nm ($[\theta]_{RMME\ 218\ nm}$) changes from –6025 at 0 M urea to –4359 at 8.0 M urea. The change in signal at 218 nm from 0–8.0 M urea was fitted to a sigmoidal curve with a midpoint of 4.3 $\pm$ 0.2 M urea (Fig. 2B). As the urea concentration increases, the peak at 218 nm persists with 73% of the $[\theta]_{RMME\ 218\ nm}$ retained at 8.0 M urea.

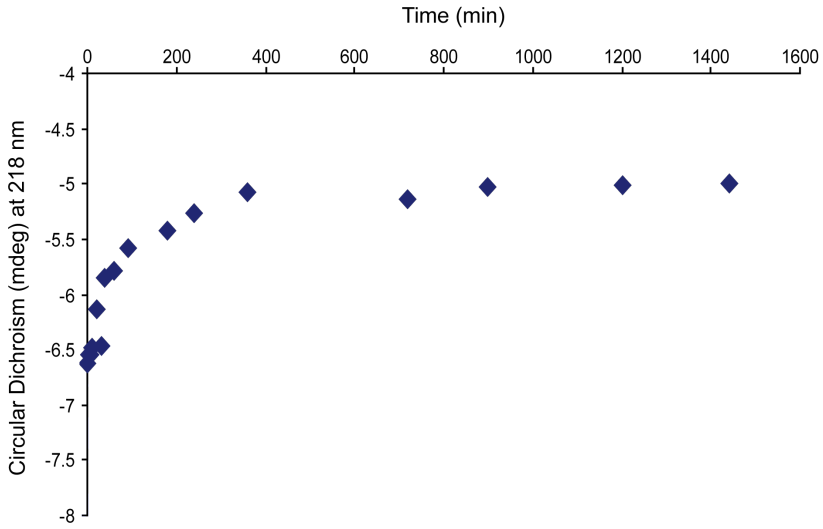


Fig. 1. Time dependence of the behavior of the αHL heptamer in 8.0 M urea monitored by CD. *Heptamers (100 μg mL^{-1}) were incubated in 8.0 M urea for 24 h and their behavior was monitored by CD in mdeg at 218 nm. After 400 min the CD signal was constant, indicating that the protein had reached equilibrium. This experiment was completed with urea buffers made in 20 mM Na phosphate, 150 mM NaCl, 0.3% (w/v) SDS at pH 8.0.*

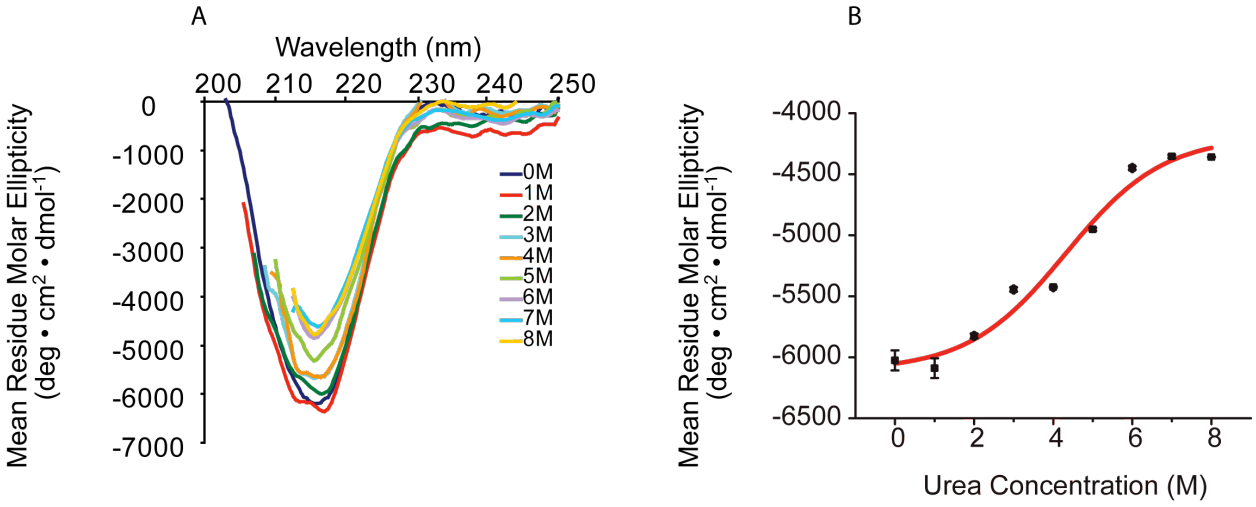


Fig. 2. Effect of urea on the structure of αHL heptamers. *(A) Effect of urea on the shape of the CD spectra measured from 200 to 250 nm. (B) Changes in the Mean Residue Molar Ellipticity at a wavelength of 218 nm ($[\theta]_{RMME\ 218\ nm}$) as a function of urea. The midpoint of the sigmoidal fit is 4.3*

± 0.2 M urea. The αHL heptamers (100 ug mL^{-1}) were incubated for 6 h in 20 mM Na phosphate, 150 mM NaCl, 0.3% (w/v) SDS at pH 8.0 in urea concentrations that varied from 0 to 8.0 M.

3.2.2 ITFE Studies of Heptameric αHL

The effect of urea on the structure of the heptamer was also investigated by intrinsic tryptophan fluorescence (ITFE) spectroscopy, which detects the changes in fluorescence emissions of the 56 tryptophan residues present on the αHL heptamer. The ITFE spectrum of αHL (100 μg mL^{-1}) at 0 M urea (in 20 mM Na phosphate, 150 mM NaCl, 0.3 % SDS at pH 8.0) has a maximum emission wavelength, λ_{max}^{em} (excitation of 280 nm) of 340 nm representing the average emission of the partially exposed and buried Trp residues. As the urea concentration is increased from 0–8.0 M, a red shift is observed from 340 nm at 0 M to 350 nm at 8.0 M urea. The λ_{max}^{em} across the various concentrations of urea were fitted to a sigmoidal curve with a midpoint at 3.3 ± 0.1 M urea (Fig. 3).

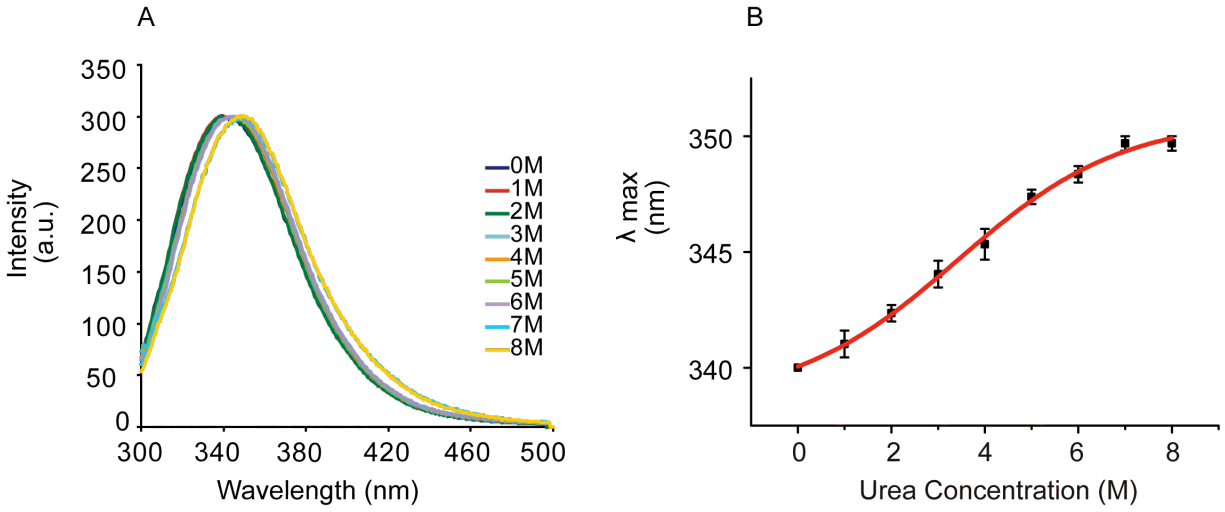


Fig. 3. Effect of urea on the structure of αHL heptamers. *(A) Effect of urea on the emission spectra of αHL heptamers (λ_{max}^{em}, excitation at 280 nm).). All of the fluorescence emission spectra*

have been scaled to the same intensity. (B) Changes in λ_{max}^{em} of αHL heptamers with increasing urea concentration. The midpoint of the sigmoidal fit is at 3.3 ± 0.1 M urea. The αHL heptamers (100 ug mL^{-1}) were incubated for 6 h in 20 mM Na phosphate, 150 mM NaCl, 0.3% (w/v) SDS at pH 8.0 in urea concentrations that varied from 0 to 8.0 M.

3.2.3 SDS-PAGE Studies Heptameric αHL

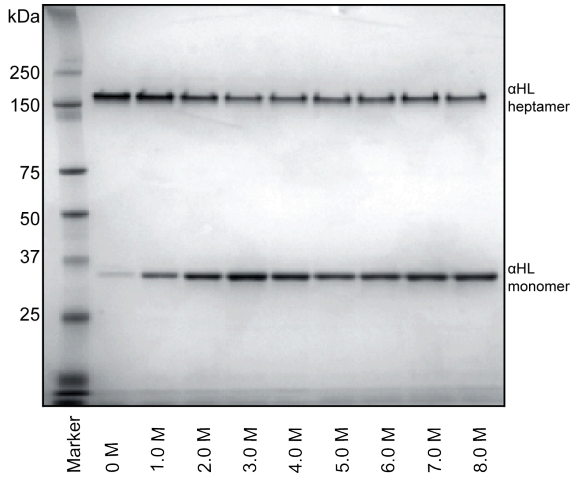


Fig. 4. The effect of increasing urea concentration on the structure of αHL heptamer. *SDS-PAGE 10%, Bis-Tris of αHL heptamers (100 μg mL^{-1}) incubated for 10 h in 20 mM Na phosphate, 150 mM NaCl, 0.3% (w/v) SDS at pH 8.0 in 0–8.0 M urea.*

The behavior of the heptamer (100 μg mL^{-1}) after 10 h of incubation in 20 mM Na phosphate, 150 mM NaCl, 0.3% (w/v) SDS at pH 8 in 0–8.0 M urea was studied via SDS-PAGE. A heptamer band was present at 234 kDa from 0–8.0 M urea as well as a monomer band at 33 kDa (Fig. 4). The density of the monomer band increases from 0 to 8.0 M urea as the density of the heptamer band decreases. The percentages of monomer in 0 M and 8.0 M urea were 13% and 62%, respectively.

3.3 Discussion

The purpose of these studies was to investigate the behavior of αHL heptamer (234 kDa) after incubation in 0–8.0 M urea. The majority of the work conducted on the

denaturation of proteins using urea has been done on soluble proteins while few studies have focused on membrane proteins. It is difficult to determine how and if a membrane protein unfolds in denaturing conditions using spectroscopy techniques, since they present an average of what is occurring in solution. Additionally, inspecting a series of spectra can give very little insight as to whether the unfolding of a multimeric protein is cooperative, in which all subunits of the protein unfold simultaneously, or whether each subunit unfolds at a different time.

Our studies show that the αHL heptamer is stable even at high concentrations of urea. The ITFE studies reflect the change in behavior of the 56 Trp residues present on the heptamer as the urea concentration is increased. Each of the seven protomers on the heptamer contains 8 Trp residues of which four are buried (Trp80, Trp167, Trp265 and Trp286) and four are partially exposed to the solvent environment (Trp179, Trp187, Trp260 and Trp274). WT-αHL heptamer in 0 M urea has a λ_{max}^{em} of 340 nm, suggesting that the Trp of the heptamer are more solvent exposed than in the monomer which has a λ_{max}^{em} of 334 nm (Chapter II and IV). When the concentration of urea is increased from 0 to 8.0 M urea, a red shift is observed to 350 nm, which shows the transfer of Trp residues to a more polar environment but probably not completely solvent exposed Trp [14]. This could be a fraction of the heptamers degrading into monomer and then unfolding or it could be a result of the heptamers loosening its tertiary structure without completely unfolding, as suggested by the SDS-PAGE studies. A fraction of heptamers retains their quaternary structure. The change in the λ_{max}^{em} of the heptamer as a function of urea was fitted to a sigmoidal curve with a midpoint of 3.3 $\pm$ 0.1 M urea, which is not in agreement with the sigmoidal curve fitted to the change in the $[\theta]_{RMME\ 218\ nm}$ seen in the CD data, 4.3 $\pm$ 0.2 M urea. The differences in midpoint values suggest that the heptamer does not denature cooperatively

since the secondary and tertiary structure do not seem to unfold in the same manner. The unfolding of the heptamer may also be a step-wise process in which intermediates may be present. Therefore the sigmoidal fit may represent multiple intermediates that are hard to distinguish because they merge together displaying only one transition. Observing the changes in ellipticity of the heptamer as the urea concentration increases, show that a population of αHL heptamers maintains their β-sheet structure even at 8.0 M urea. Since the 80% of the αHL heptamer is composed of β-sheet, the majority of which is in the cap domain (69%), the changes observed in the spectra are most likely changes that are occurring in the cap domain of the protein and not the stem domain. Therefore, the results suggest that the concentration of stable heptamer is decreased with increasing urea concentration with a percentage of stable heptamer still giving a strong signal at 218 nm at 8.0 M urea.

The SDS-PAGE studies provide a visual representation of what may be happening in bulk solution. The results support the idea that a percentage of stable heptamer is decreasing as unstable heptamer dissociates into monomer with increasing urea concentration. The monomers must then denature at high concentrations of urea (confirmed in Chapter IV). Approximately 30–45% of the heptamers are unstable in 1.0–2.0 M urea while the rest remain in their heptameric conformation even at 8.0 M urea. The shift that would be seen in the monomer at high urea concentrations may be masked by the signal present for the heptamer resulting in one broad peak as opposed to two sharp peaks in the spectroscopy data. The interaction between SDS and urea may also contribute to the inconsistencies seen between the unfolding of secondary and tertiary structures.

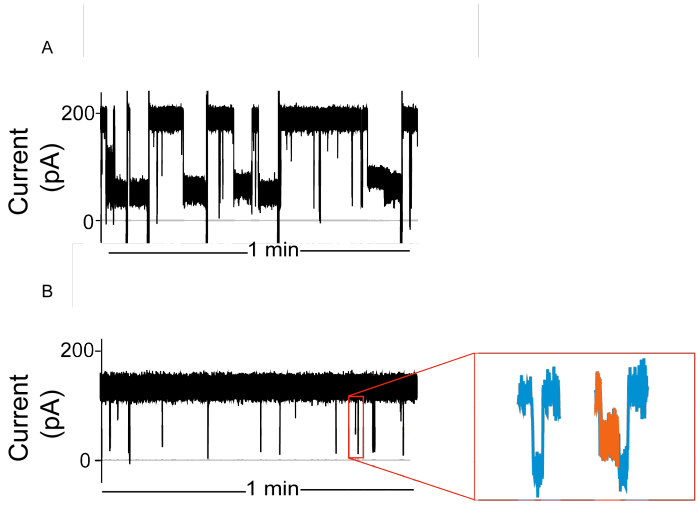


Fig. 5. Single-channel recording depicting the translocation of ssDNA through αHL. *(A) ssDNA containing secondary structure is unable to translocate through the WT-αHL pores in 0 M urea. (B) In 4.0 M urea, ssDNA loses its secondary structure and translocates through the pore. The inset in B shows vestibule events seen in orange and translocation events shown in blue. Figure modified from Japrung et al. 2010* [12].

The structural changes of the heptamer in bulk solution were compared to single-channel recording studies conducted by Deanpen Japrung [12], which represent the interaction of the heptamer and ssDNA/RNA in 4.0 M urea. A 100-nt strand of DNA ($A_{30}C_{70}$) was added from the *cis* entrance. The most abundant ionic current blockades observed were low amplitude events with 75–90% block representing DNA translocation events and mid-amplitude events with 45–75% block representing vestibule events. The number of translocation events observed when the urea concentration was raised from 0 M to 4.0 M increased. At 0 M urea, 45% of the events were vestibule events while 55% were translocation events (Fig. 5A). In contrast 20% vestibule events and 80% translocation events were observed at 4.0 M urea (Fig. 5B). The translocation of the secondary structure

containing 95-nt ssDNA and 95-nt ssRNA at +180 mV in 1 M KCl, 5 mM HEPES, pH 7.5 in the absence of urea resulted in very long or permanent blockades of 70%, indicating that they did not translocate through the pore. The same conditions were applied under 4.0 M urea, translocation events were observed with 75–95% current blockades and translocation times similar to those observed with ssDNA of similar size, having no secondary structure. Therefore the results are indicative of the unfolding of ssDNA secondary structures. The results also prove that the heptamer's cap domain is intact due to the presence of vestibule events.

Furthermore, studies conducted in bulk solution in 0–8.0 M urea show that the majority of the cap domain is still intact and does not unfold at high urea concentrations. Single-channel recording studies confirm that urea has the ability to unfold the secondary structure and allow for increased translocation events of ssDNA/RNA. Additionally, the concentration of urea used to carry out these experiments (4.0 M urea) is a condition that maintains the structure of the heptamer.

3.4 Conclusions

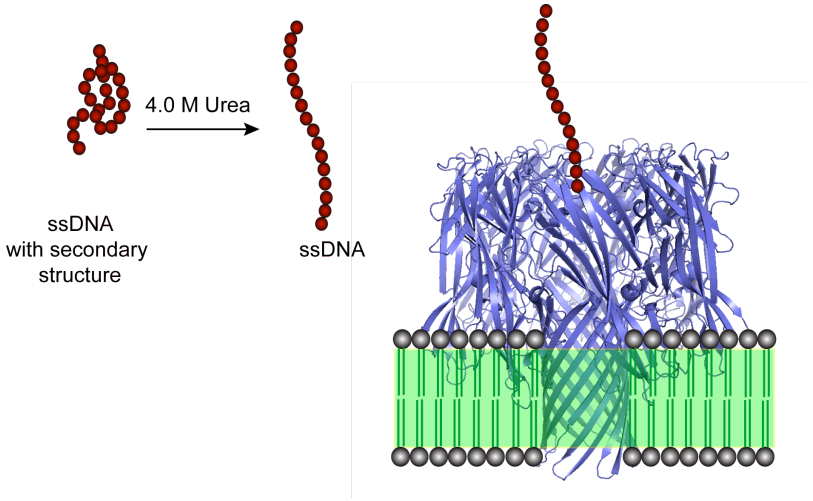


Fig. 6. Diagram showing the unfolding of ssDNA with secondary structure and its translocation through αHL pores.

The heptameric αHL pore is able to withstand harsh conditions subjected by denaturants such as urea. Using various biochemical and biophysical techniques, it seems that the majority of the heptameric structure is intact. The cap domain is intact at high concentration of urea, revealed by the spectroscopy data as well as single-channel recording. Therefore these conditions can be applied in the field of bio-nanotechnology in order to further develop the use of the αHL nanopore for DNA sequencing. The translocation of single-stranded polynucleotides through the pore, which contain secondary structure, can be aided with the use of urea. Future studies may involve probing other conditions that could unfold or prevent secondary structural formation of single-stranded polynucleotides. This can be accomplished by testing other conditions such as pH or types of salt along with different concentrations of salt. Enzymes can also be employed to inhibit intramolecular interactions of ssDNA such as single stranded binding protein (SSB) before attempting to translocate it through the αHL pore [15].

3.5 Materials and Methods

3.5.1 Protein Preparation

The heptamer was prepared in the same manner as discussed in Chapter II. Before the CD and fluorescence experiments were conducted, the buffer of the extracted pre-oligomerized heptamer was exchanged with 20 mM Na phosphate, 150 mM NaCl containing 0.3% (w/v) SDS at pH 8.0 in 0–8.0 M urea by using P6 microcentrifuge columns (732-6221, Bio-Rad) that was spun at 2000 Xg (Eppendorf, 5417R).

3.5.2 CD was conducted in the same manner as described for the alkaline studies on the heptamer in Chapter II.

3.5.3 ITFE Spectroscopy was conducted in the same manner as described for the alkaline studies on the heptamer in Chapter II.

3.5.4 SDS-PAGE was conducted in the same manner as described for the alkaline studies on the heptamer in Chapter II.

3.6 References

1. Henrickson, S., et al. *Driven DNA transport into an asymmetric nanometer-scale pore*. Phys Rev Lett, 2000. **85**: 3057–60.
2. Meller, A., et al. *Rapid nanopore discrimination between single polynucleotide Molecules*. Proc Natl Acad Sci USA, 2000. **97**: 1079–84.
3. Kasianowicz, J., et al. *Simultaneous multi-analyte detection with a nanometer-scale pore*. Anal Chem, 2001. **73**: 2268–72.
4. Butler, T., et al. *Ionic current blockades from DNA and RNA molecules in the α hemolysin nanopore*. Biophys J, 2007. **93**: 3229–40.
5. Berman, H., et al. *The nucleic acid database: a comprehensive relational database of three-dimensional structures of nucleic acids*. Biophys J, 1992. **63**: 751–9.
6. Brown, J., *The Ribonuclease P Database*. Nucleic Acids Res, 1999. **27**: 314.
7. Andersen, E., et al. *The tmRDB and SRPDB resources*. Nucleic Acids Res, 2006. **34**: D163–8.
8. Andronescu, M., *RNA STRAND: the RNA secondary structure and statistical analysis database*. BMC Bioinformatics, 2008. **9**: 340.
9. Levine, L. et al. *The relationship of structure to the effectiveness of denaturing agents for deoxyribonucleic acid*. Biochemistry, 1963. **2**: 168–75.
10. Shelton, V., et al. *Applicability of urea in the thermodynamic analysis of secondary and tertiary RNA folding*. Biochemistry, 1999. **38**: 16831– 9.
11. Koculi, E., et al. *Charge density of divalent metal cations determines RNA stability*. J Am Chem Soc, 2007. **129**: 2676–82.
12. Japrung, D., et al. *Urea facilitates the translocation of single-stranded DNA and RNA through the α-hemolysin nanopore*. Biophysical J, 2010. **98**: 1856 – 63.

13. Kelly, S., et al. *How to study proteins by circular dichroism.* Biochimica et Biophysica Acta, 2005. **1751**: 119–39.

14. Vivian, J., and Callis, P., *Mechanisms of tryptophan fluorescence shifts in proteins.* Biophysical Journal, 2001. **80**: 2093–109.

15. Chan, K., et al. *Single-stranded DNA-binding protein complex for Helicobacter pylori suggests an ssDNA-binding surface*. J Mol Biol, 2009. **388**: 508–519.

Chapter IV: Unfolding and Refolding Studies of Monomeric αHL in Urea

4.1 Introduction

αHL is secreted by *Staphylococcus aureus* in monomeric form, which binds to its target cell membranes. Studies have been conducted on the unfolding of the monomer to determine how it interacts with lipid bilayers and how it oligomerizes into heptamers [1-3], and to determine the Gibbs free energy of unfolding in the presence of increasing urea concentrations at different pH [1]. Studying the unfolding and refolding of proteins has allowed researchers to understand the mechanisms that occur *in vivo* when proteins translocate through cell membranes. Some proteins partially unfold either spontaneously or with the help of enzymes [4, 5]. Protein unfolding studies have been crucial for understanding the accurate folding of newly synthesized peptides or monomers and their assembly into membranes.

Key determinants of thorough unfolding and refolding are the conditions and methods used. An ideal denaturant such as temperature, pH, urea or guanidinium chloride (GdnCl) allows for the renaturation of unfolded proteins via simple methods such as dialysis or dilution. A protein's behavior in one denaturant will not determine its behavior in all others. Additionally, one denaturant's ability to unfold a protein may not be the case for another. Most unfolding and refolding studies in the past have been conducted on soluble proteins, while few have been conducted on membrane proteins successfully such as bacteriorhodopsin [6]. The refolding of proteins is an essential final step in the purification of wild-type (WT) and mutated forms. Site-directed mutagenesis (SDM) is a common method used to construct modified proteins; however, this technique is limited to only natural amino acids. Methods such as native chemical ligation (NCL) and expressed protein ligation (EPL), which utilize synthetic and semi-synthetic methods, have been successfully

used to create variations of proteins such as KcsA and OmpF [7, 8]. These methods can also allow for the incorporation of unnatural amino acids. However, these types of synthesis have many hurdles that must be overcome such as the manipulation of fragments that are difficult to solubilize and purify. The final step of synthesizing proteins is the most crucial and difficult since it involves protein folding from unstructured polypeptides. Therefore, proper solvent conditions must be established to ensure the protein is able to refold. Our work seeks to establish conditions that will make refolding possible after synthetic modification of αHL.

Studying the behavior of the αHL monomer under various denaturing and renaturing conditions can help to determine the conditions necessary to refold a mutated form of the protein. Establishing refolding conditions is essential for the final stages of chemical ligation, a technique that can aid in the construction of novel modified pores that can be used for various applications in sensing, DNA sequencing and drug delivery. In this chapter, the unfolding and refolding of monomeric αHL in urea as well as GdnCl and organic acids was investigated. The conditions tested in our experiments will help in the synthesis of an αHL pore that incorporates unnatural amino acids to further advance the area of single molecule chemistry.

4.2 Results

4.2.1 Structural Studies of Unfolded Monomeric αHL

ITFE spectroscopy was conducted in order to detect structural changes of the αHL monomer due to changes in the microenvironment of its 8 Trp residues. The ITFE spectrum

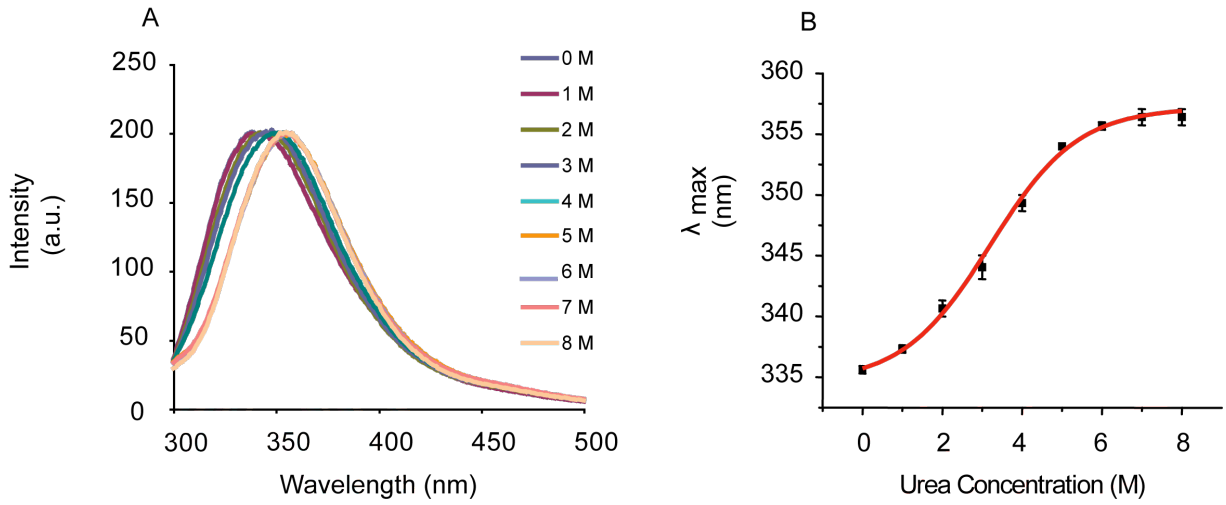


Fig. 1. Effect of urea on the structure of αHL monomers. *(A) Effect of urea on the emission spectra of αHL monomers (λ_{max}^{em}, excitation at 280 nm).). All of the fluorescence emission spectra have been scaled to the same intensity. (B) Changes in λ_{max}^{em} of αHL monomer with increasing urea concentration. The midpoint of the sigmoidal fit is at 3.3 ± 0.1 M urea. The αHL monomers (100 μg mL^{-1}) were incubated for 5 min in 20 mM Na phosphate, 150 mM NaCl at pH 8.0 in urea concentrations that varied from 0 to 8.0 M.*

of native αHL monomer (100 μg mL^{-1}) at pH 8.0 in 20 mM Na phosphate, 150 mM NaCl shows a maximum emission wavelength (λ_{max}^{em} with an excitation of 280 nm) of 334 nm representing buried Trp. The effect of 1.0–8.0 M urea on the structure of αHL monomers was tested. The incubation time at each urea concentration was determined by a time course conducted over a period of 30 min as shown in Fig. 3 and Table 1. The monomer unfolds within 30 s of mixing in 8.0 M urea (20 mM Na phosphate, 150 mM NaCl at pH 8.0) as well as the other urea concentrations. A sigmoidal change is observed in the λ_{max}^{em} of αHL Trp residues from 334 nm at 0 M urea to 356 nm at 8.0 M urea (Fig. 2). The midpoint of the sigmoidal fit is 3.3 ± 0.1 M urea, a concentration at which 50% of the protein is denatured. The λ_{max}^{em} at 8.0 M urea shows that the buried Trp residues may be fully

exposed to the solvent microenvironment since the value is similar to those of N-acetyltryptophanamide and free tryptophan, which are 358 nm and 360 nm, respectively.

The changes observed in the ITFE studies were in agreement with the secondary structural changes detected by CD spectroscopy. Native monomeric αHL in 0 M urea seen in Fig. 2A (20 mM Na phosphate, 150 mM NaCl at pH 8.0) has a prominent β-sheet spectrum at 215 nm [11]. The effect of incubating the αHL monomer (100 μg mL^{-1}) in 1.0–8.0 M urea results in a loss of the protein's β-sheet content in the CD spectra, as the peak gradually disappears at 215 nm (Fig. 2A). Due to the absorption of urea in the far UV region of the spectra [10], data from 210–250 nm are shown for 1.0–8.0 M urea. The CD signal at 215 nm was fitted to a sigmoidal curve. The mean molar residue ellipticity at 215 nm ($[\theta]_{RMME\ 215\ nm}$) changes from –6033 at 0 M urea to –1049 at 8.0 M urea with a midpoint of 3.4 ± 0.1 M urea (Fig. 2B).

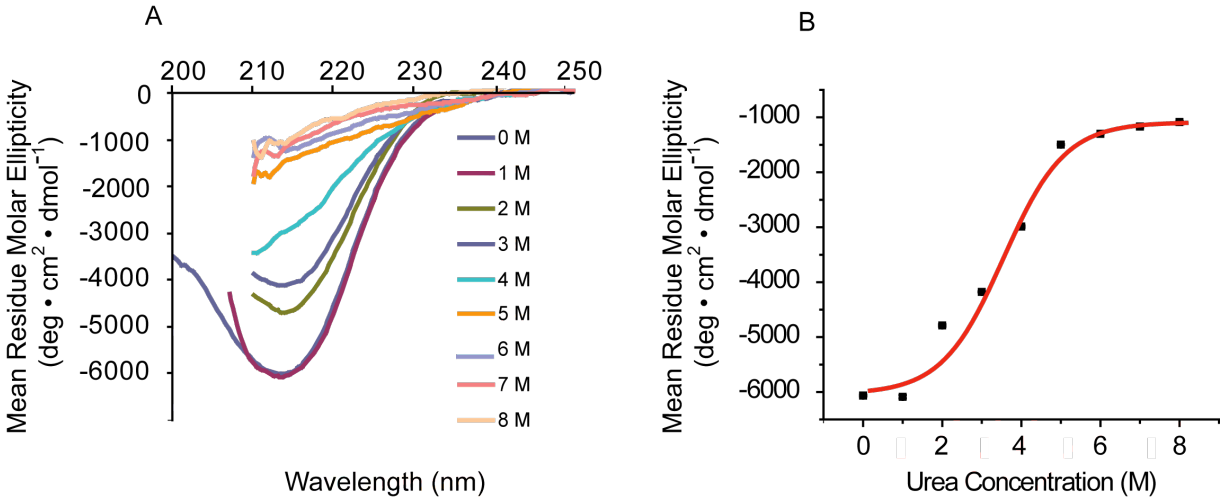


Fig. 2. Effect of urea on the structure of αHL monomers. *(A) Effect of urea on the shape of the CD spectra measured from 200 to 250 nm. (B) Changes in Mean Residue Molar Ellipticity at a wavelength of 215 nm ($[\theta]_{RMME\ 215\ nm}$) as a function of urea. The midpoint of the sigmoidal fit is at 3.4 ± 0.1 M urea. The αHL monomers (100 μg mL^{-1}) were incubated for 5 min in 20 mM Na phosphate, 150 mM NaCl at pH 8.0 in urea concentrations that varied from 0 to 8.0 M.*

4.2.2 Structural Studies of Refolded Monomeric αHL

The refolding of αHL monomers was investigated by diluting a concentrated solution of monomer incubated in 8.0 M urea (in 20 mM Na phosphate, 150 mM NaCl at pH 8.0) resulting in protein solutions with a lower concentration of urea. Monitoring the ITFE, the protein refolds within 4 min to native-like conformations with a λ_{max}^{em} of 334 nm (Fig. 4) after dilution from 8.0 M to 0.8 M urea (Fig. 3B).

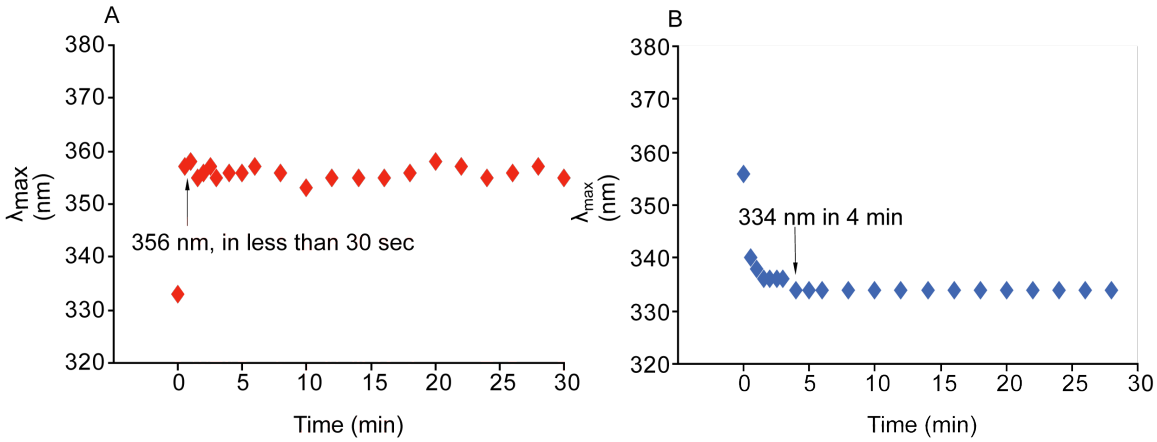


Fig. 3. Time dependence of the unfolding in 8.0 M urea and refolding of the αHL monomer from 8.0 M urea monitored by ITFE. *(A) Monomers (100 μg mL^{-1}) were incubated in 8.0 M urea for 30 min and the unfolding was monitored by measuring the change of the λ_{max}^{em} (ex 280 nm). (B) Unfolded monomers (100 μg mL^{-1}) were diluted to 0.8 M and the refolding was monitored by measuring the change of the λ_{max}^{em} (ex 280 nm). Both experiments were completed at 25 °C, wavelength range of 300–500 nm, with 10 cumulative wavelength scans/h for 1 h, excitation/emission slits of 5 nm with urea buffers made in 20 mM Na phosphate, 150 mM NaCl at pH 8.0.*

Urea Concentration	Unfolding Time Course	Refolding Time Course
8 M	30 sec 334 nm → 356 nm	4 min 356 nm → 334 nm
7 M	30 sec 334 nm → 356 nm	4 min 356 nm → 334 nm
6 M	30 sec 334 nm → 355 nm	4 min 355 nm → 334 nm
5 M	30 sec 334 nm → 355 nm	3 min 355 nm → 334 nm
4 M	30 sec 334 nm → 348 nm	3 min 348 nm → 334 nm
3 M	30 sec 334 nm → 339 nm	1.5 min 339 nm → 334 nm
2 M	30 sec 334 nm → 338 nm	1min 338 nm → 334 nm
1 M	Constant at 334 nm	N/A
0 M	Constant at 334 nm	N/A

Table 1: Time Dependence Studies on the Unfolding and Refolding of the Monomer. *The monomer was incubated in 0–8.0 M urea over a period of 30 min to decipher the time of unfolding in each urea concentration. After the monomer was unfolded at each urea concentration, its refolding time was established after dilution by 10X with 20 mM Na phosphate, 150 mM NaCl at pH 8.0. All experiments were completed at 25 ˚C, wavelength range of 300–500 nm, with 10 cumulative wavelength scans/h for 1 h, excitation 280 nm, excitation/emission slits of 5 nm. Urea buffers were made in 20 mM Na phosphate, 150 mM NaCl at pH 8.*

The monomer was also incubated in 0.8 M urea directly (seen in green Fig. 4A) to confirm the ITFE results of the refolded protein where the urea concentration was diluted to 0.8 M (seen in pink Fig. 4A).

The CD studies reveal that the refolded monomer regains the peak present at 215 nm, comparable to that of the native monomer. The regain in structure is not only evident in the presence of a β-sheet spectrum but also in the $[\theta]_{\text{RMME 215 nm}}$ value that was –5956,

which is in agreement with the value observed for the native monomer. The refolded monomer displays a broader peak in the near UV region between 220 and 250 nm. The difference between the spectra may be due to the protein not completely refolding to its original conformation, differential light scattering as a result of insoluble protein aggregates [10] or a characteristic of the protein at 0.8 M urea. The protein's behavior in 0.8 M urea (seen in green in Fig. 4B) urea is similar to the refolded monomer.

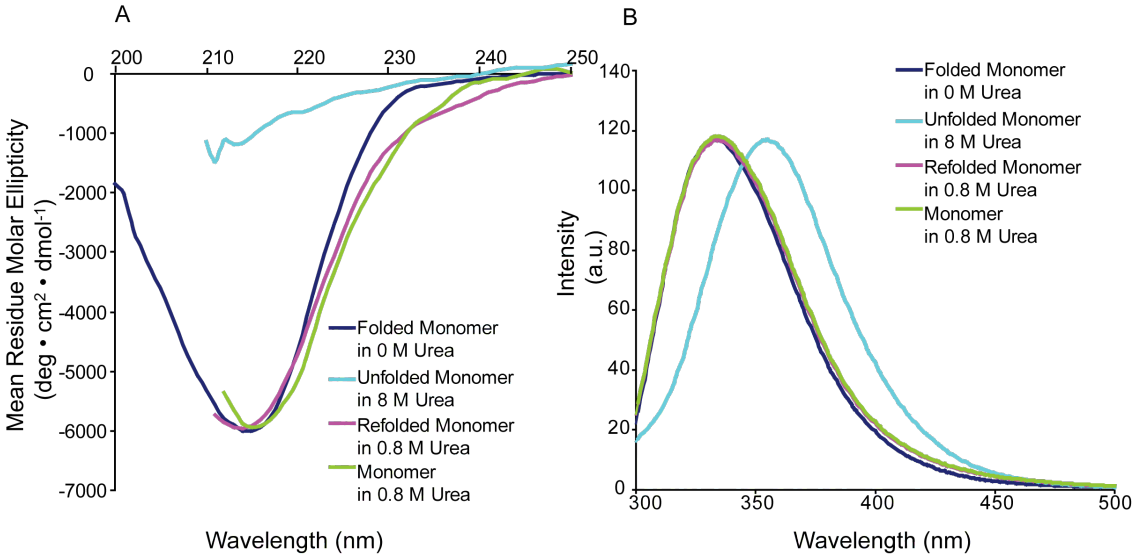


Fig. 4. Spectroscopy evidence of the refolding of αHL. *CD (A) and ITFE (B) spectra of native monomers (dark blue), unfolded monomers in 8.0 M urea (light blue), refolded monomer from 8.0 M urea to 0.8 M urea (pink) and native monomer in 0.8 M urea (green) in 20 mM Na phosphate, 150 mM NaCl at pH 8.0.*

To further compare the structural properties of the monomer and the refolded monomer, two samples of each protein with the same concentration were subjected to proteolysis with 5 μg mL^{-1}, 50 μg mL^{-1}, and 500 μg mL^{-1} of proteinase K (Fig. 5). Proteinase K is a serine protease with broad specificity whose main cleavage site is the

peptide bond near the carboxyl group of aliphatic and aromatic amino acids [11]. It has been used previously to cleave αHL near the C and N terminus [12].

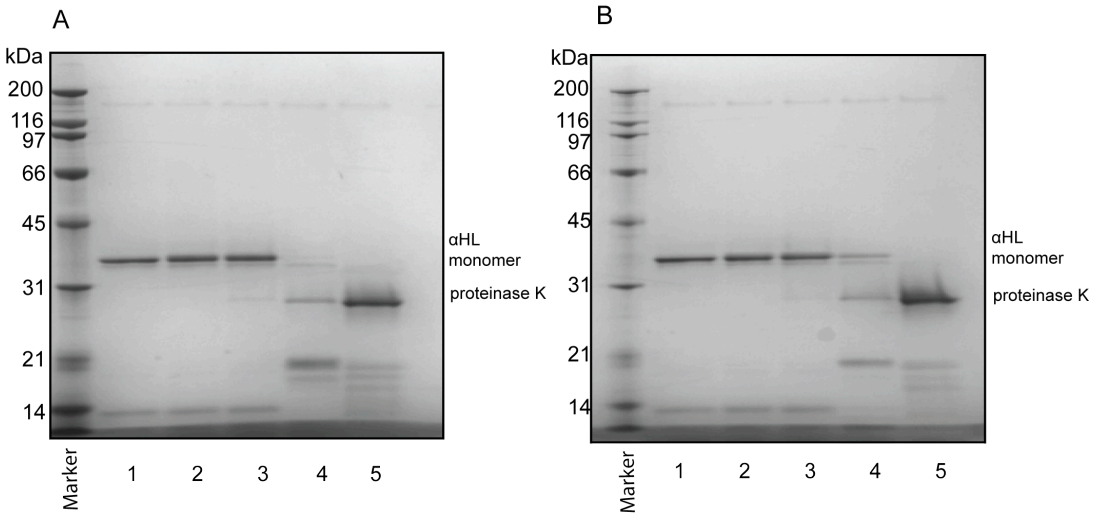


Fig. 5. Proteolysis Studies of the αHL monomer and the refolded monomer. *Both the monomer and refolded monomer were incubated in various concentrations of proteinase K at room temperature and then run on a 12.0% Bis-Tris SDS-PAGE. (A) Monomer incubated with proteinase K Lanes: (1) Protein in 0 M urea buffer (2) Protein in water (3) Protein in 5 $\mu g\ mL^{-1}$ of proteinase K (4) Protein in 50 $\mu g\ mL^{-1}$ of proteinase K (5) Protein in 500 $\mu g\ mL^{-1}$ of proteinase K (B) Refolded monomer incubated with proteinase K Lanes: (1) Protein in 0 M urea buffer (2) Protein in water (3) Protein in 5 $\mu g\ mL^{-1}$ of proteinase K (4) Protein in 50 $\mu g\ mL^{-1}$ of proteinase K (5) Protein in 500 $\mu g\ mL^{-1}$ of proteinase K. The band between 45 and 31 kDa is the monomer (33.2 kDa) and the band below 31 kDa is the proteinase K (28 kDa).*

The major proteinase K cleavage sites in the glycine rich region of αHL are before the Val140 and Ile136 residues while the major N-terminal sites are after the Ile7 and Ile14 residues [13]. The same concentration of native and refolded monomer was incubated in 5 μg mL^{-1}, 50 μg mL^{-1} and 500 μg mL^{-1} of proteinase K for 5 min. The reactions were stopped by the addition of phenylmethanesulfonyl fluoride (PMSF) and then the samples

were run on SDS-PAGE. Both the native monomer and the refolded monomer are cleaved in the same manner in the various concentrations of the protease. This suggests that the native and refolded monomers are folded in the same manner.

4.2.3 Activity Studies of Monomeric αHL

Hemolytic assays were conducted to determine whether the unfolded monomer regains activity upon serial dilution of the denaturant used (Fig. 6A and 6B) or to assess the lytic activity of the protein itself (Fig. 6C). Light scattering hemolytic assays depict the relative change in absorbance at 595 nm over a period of 1 h and 40 min collecting a data point every 30 s. As the amount of cells lysed increases, the apparent absorbance detected from the light scattering hemolytic assay decreases. Active αHL monomers assemble on the lipid bilayer of rabbit red blood cells (rRBCs), and lyse the cell resulting in a sharp sigmoidal decrease in the spectra shown.

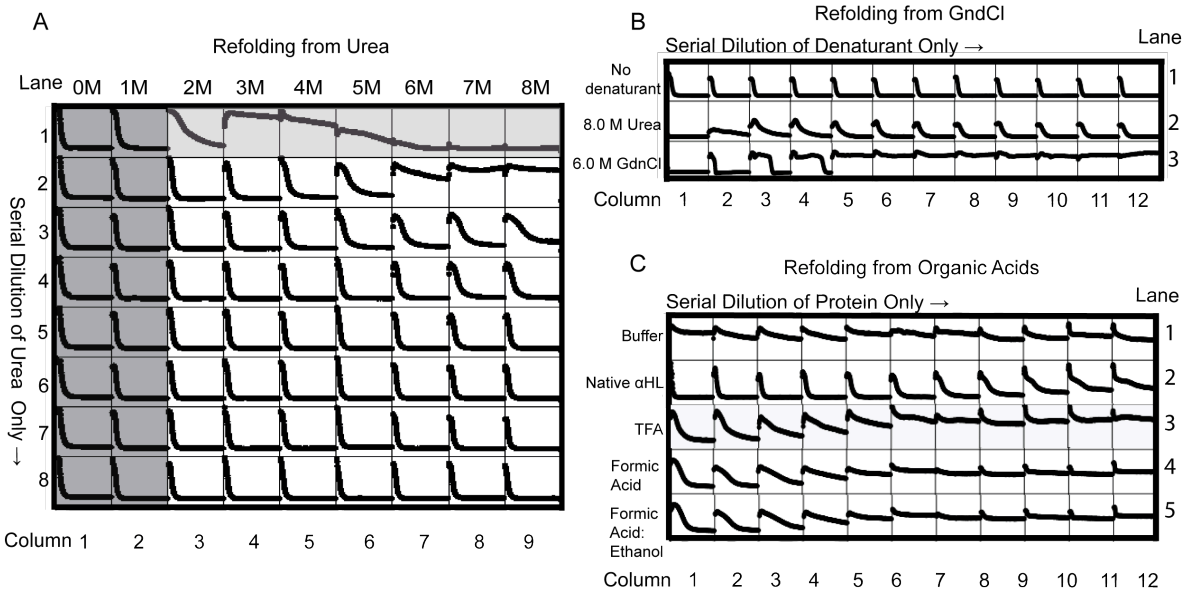


Fig. 6. Refolding of αHL shown by light scattering hemolytic assays. *(A) Refolding from Urea. Lane 1 contained 170 μL of 20 mM Na phosphate, 150 mM NaCl at pH 8.0 buffer containing increasing concentrations of urea from column 1 to 9. Lanes 2 to 7 contained 85 μL of 20 mM Na*

phosphate, 150 mM NaCl at pH 8.0. Each lane was then serially diluted (starting from lane 2 to lane 8) by adding 85 μL from the preceding lane accompanied by mixing. 200 ng (5 μL) of αHL monomers pre-incubated in 0 to 8.0 M urea (columns 1–9) were added to each well and the assay was started by adding 10 μL of rabbit red blood cells (rRBCs) into each well from column 1. The lyses of the rRBCs are shown by the sigmoidal decrease in signal. Dark gray wells show the activity of folded αHL monomers, light gray wells show the activity of unfolded αHL monomers and white wells show the activity of refolded αHL monomers. (B) Refolding from GdnCl. All wells in lane 1 contained 200 ng (5 μL) of αHL monomer, 85 μL of 20 mM Na phosphate, 150 mM NaCl at pH 8.0. The first well (on the left) of lane 2 and 3 contained 170 μL of 8.0 M urea and 6.0 M GdnCl, respectively in 20 mM Na phosphate, 150 mM NaCl at pH 8.0. Each following well of lane 2 and 3 contained 85 μL of buffer 20 mM Na phosphate, 150 mM NaCl at pH 8.0. Each well was then serially diluted from left to right by adding 85 μL from the preceding lane. 200 ng (5 μL) of αHL monomer pre-incubated in 8.0 M urea (lane 2) and 6.0 M GdnCl (lane 3) were added to each well followed by the addition of 10 μL of rRBCs into each well. (C) Refolding from Organic Acids. The first wells of each lane contained 180 μL of MBSA buffer with 200 ng of αHL monomers (except lane 1). The first well of lane 2 contained native αHL monomer, while lanes 3, 4 and 5 contained lyophilized αHL monomers pre-incubated in TFA, formic acid (88.0% v/v) and formic acid: ethanol (30:70 v/v), respectively (see Materials and Methods). Each following well contained 90 μL of MBSA buffer. Each well was then serially diluted from left to right by adding 90 μL from the preceding lane followed by the addition of 10 μL of rRBCs in each well.

The ability to refold the monomer in serially diluted concentrations of urea was tested (Fig. 6A). In lane 1 of columns 1−9 of the hemolytic assay, 170 μL of the corresponding urea buffer from 0–8.0 M urea (columns 1–9) was added. Lanes 2 to 7 were filled with 85

μL of 20mM Na phosphate, 150 mM NaCl in pH 8.0. Each lane, starting at lane 2 was serially diluted from top to bottom with 85 μL from the previous lane. Therefore the concentration of urea was diluted by 50% from one lane to the next lane; for example, in column 9, lane 1 contains 8.0 M urea and after serial dilution to the next well (lane 2), the concentration was reduced to 4.0 M urea. After the serial dilution of the urea buffer, 200 ng (5 μL) of the monomer, which was incubated in the corresponding concentration of urea, was placed into each well, followed by the addition of 10 μL of rRBCs. Therefore, the concentration of the protein was constant in each well. Columns 1 and 2 representing the dilution of 0 and 1.0 M urea show that the protein retains full activity up to 1.0 M urea (seen in dark gray in Fig. 6A). At 2.0 M urea (lane 1, column 3), the protein is less active and regains activity after serial dilution from top to bottom (lane 2, column 3) where the urea concentration is 1.0 M. Columns 4–9 (3.0–8.0 M urea) show that although the αHL monomer is not active at concentrations at or above 3.0 M (lane 1, column 4), urea induces cell lysis at concentrations at or above 5.0 M urea (lane 1, column 6–9). At 3.0 M urea (column 4, lane 1) the protein is not active and the cells are not lysed, which is evident by the high absorbance reading throughout the spectra. After serial dilution to lane 2, the monomer regains activity, suggesting that it has refolded to its native conformation. In 8.0 M urea (lane 1, column 9) the rRBCs are lysed due to the high concentration of urea. Once the urea was serially diluted to 4.0 M urea (lane 2, column 9), the cells are not lysed while the protein remains unfolded, which is represented by the lack of activity. Once the urea concentration was diluted to 1.0 M (lane 4, column 9) the protein regains full activity equivalent to native αHL monomer.

After proving that the unfolding of the monomer is reversible in urea, studies were conducted to study the effect of other denaturants on the monomer. Guanidinium chloride

(GdnCl) is another common denaturant used in substitution for urea. A similar study was conducted on 6.0 M GdnCl as discussed above (Fig. 6B); however, the dilution was conducted from left to right instead of top to bottom. Lane 1 represents the control experiment containing only 200 ng (5 μL) of monomer in each well with 85 μL of 20 mM Na phosphate, 150 mM NaCl at pH 8.0 without denaturant before adding 10 μL of rRBCs. Since each well in the lane contains the same concentration of the monomer and buffer, the results show a consistently active monomer. Lanes 2 and 3 were prepared in the same manner as described for Fig. 6A. Column 1 of lanes 2 and 3 are filled with 8.0 M urea and 6.0 M GdnCl, respectively. All other wells across these two lanes (from left to right) were filled with 85 μL of 20 mM Na phosphate, 150 mM NaCl at pH 8.0. Each succeeding well, from left to right (columns 2–12) in lanes 2 and 3, was serially diluted and mixed with 85 μL from the preceding well; thus, diluting the concentration of denaturant by 50% from one column to the next. Afterwards, 200 ng (5 μL) of protein that had been unfolded in 8.0 M urea or 6.0 M GdnCl (lane 2 and 3, respectively) was added to each well in its corresponding lane followed by the addition of 10 μL of rRBCs. The results indicate that the protein incubated in 8.0 M urea regains activity similar to the native protein after diluting to 1.0 M urea, confirming results seen in Fig 6A. However, in the case of GdnCl, the protein does not regain activity. Columns 1, 2, 3 and 4 of lane 3 show that the cells were lysed due to the disruption of 6.0 M GdnCl on the rRBCs. Observing the succeeding wells (lane 3, columns 5–12); the protein does not refold upon dilution in GdnCl as it does in urea. Furthermore, it seems that unfolding the αHL monomer in 6.0 M GdnCl results in an unstable conformation of the protein preventing it from refolding to its native conformation upon dilution.

Since the unfolding of monomers in 8.0 M urea is reversible, it was used to investigate the refolding of protein that was unfolded by GdnCl. After incubating the protein in 6.0 M GdnCl for 5 min, the GdnCl was diluted to 0.6 M in the presence of various concentrations of urea, 1.0–8.0 M. After the protein was incubated in these new conditions for 5 min, its activity was tested using hemolytic assays (Fig. 7A). The results show that the protein is able to refold to full activity equivalent to native monomer even after a ten-fold dilution in 1.0 M urea (column 2) from 6.0 M GdnCl.

The effect of trifluoroacetic acid (TFA), formic acid (88.0% v/v) and formic acid: ethanol (30: 70 v/v) was also tested since these organic acids have been used to reversibly denature other proteins [6]. These experiments test the efficiency of refolding the monomer after incubation in these organic acids by observing the lytic activity of the protein after its dilution (Fig. 6C). Lanes 1 and 2 are controls testing the effects of the MBSA buffer (lane 1 columns 1–12) and the activity of the monomer after its serial dilution from left to right (lane 2, columns 1–12). After serially diluting the monomer only, a gradual loss of activity is observed. For the experiments conducted with the acids (lanes 3–5), the monomer (100 μg mL^{-1}) was incubated in TFA, formic acid (88.0% v/v) and formic acid: ethanol (30:70 v/v) for 5 min, and was subject to fast freezing before lyophilizing for 20 min. Since the organic acids lyse rRBCs even at low concentrations (results not shown), the samples were lyophilized as a more efficient way to remove the denaturant. The protein was incubated in MBSA buffer containing 500 mM MOPS and 200 ng (2 μL) was then incubated in 178 μL of MBSA buffer (column, lanes 3–5) and serially diluted from column 1 to 12. Lane 3, 4 and 5 contain protein that was lyophilized in TFA, formic acid and formic acid: ethanol, respectively. The results in the first wells (column 1, lanes 3–5) show that the protein regains activity after incubation in TFA, formic acid and formic acid: ethanol after

lyophilization. The protein is 64 times less active than the native protein; however, this value varies depending on factors such as incubation and lyophilization times as well as the refolding solvent's ability to re-solubilize the proteins after lyophilization.

It is likely that after lyophilization the protein may adhere to the sides of its container and the MBSA buffer used may not solubilize all the protein. Since the unfolding studies conducted on the monomer with urea are reversible and it has been used to solubilize proteins [14], it was used to re-solubilize the monomer after unfolding in the organic acids. Columns 1 and 2 in Fig. 7B show the effect of the phosphate buffer and 8.0 M urea buffer on the RBCs while columns 3 and 4 show the effect of native monomer and monomer incubated in 8.0 M urea. These experiments were conducted in the same manner as the experiments described in Fig. 6A. Columns 5−7 are monomers that were first incubated in TFA (column 5), formic acid (column 6) and formic acid: ethanol (column 7), lyophilized and re-solubilized in 8.0 M urea. In all three cases the protein regains activity at the same time as the monomer that was incubated in 8.0 M urea (column 4). This suggests that urea is able to solubilize a larger amount of the monomer than MBSA buffer, allowing the protein to regain complete activity.

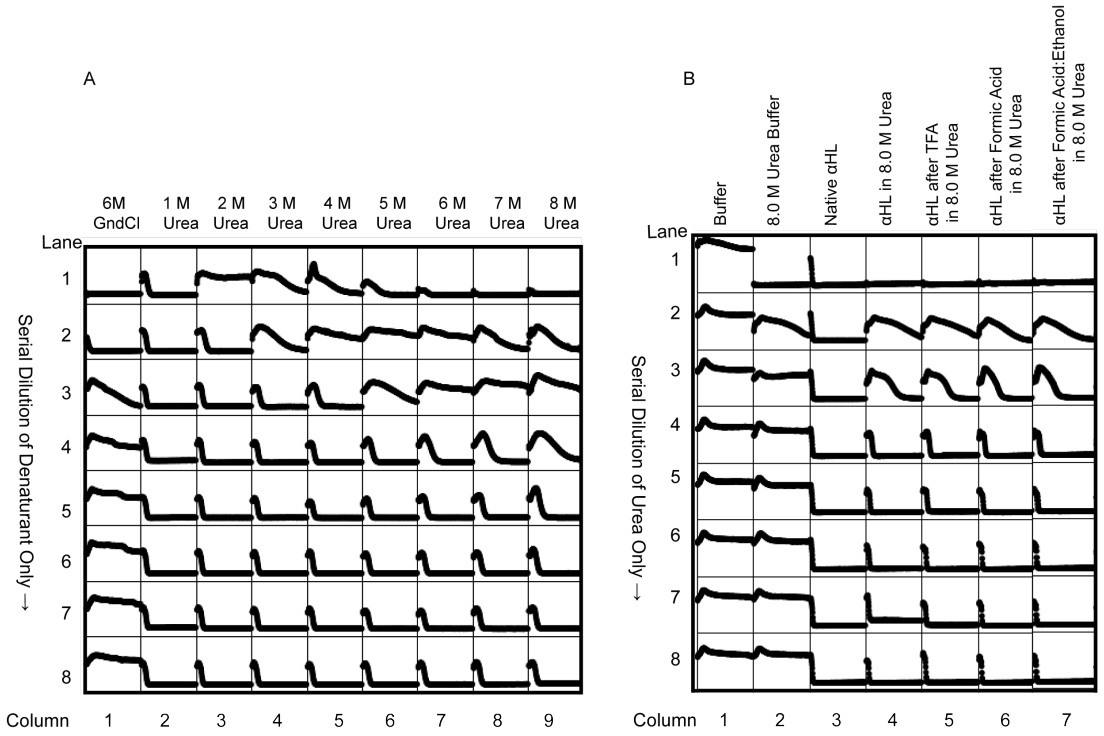


Fig. 7. Effect of urea on αHL monomers shown by light scattering hemolytic assays after incubation in GdnCl (A) and organic acids (B). *(A) Lane 1 contained 170 μL of 20 mM Na phosphate, 150 mM NaCl at pH 8.0 buffer containing 6.0 M GdnCl (column 1) and 1.0– 8.0 M urea (columns 2–9). All other wells (lanes 2–7, columns 1–9) contained 85 μL of 20 mM Na phosphate, 150 mM NaCl at pH 8.0. Each well in each lane was then serially diluted (starting from lane 2 to lane 8) by adding 85 μL from the preceding lane. 200 ng (5 μL) of αHL monomers pre-incubated in 6.0 M GdnCl (column 1) and 6.0 M GdnCl followed by its dilution to 0.6 M GdnCl with 1.0–8.0 M urea (columns 2–9) were added to each well. The assay was started by adding 10 μL of red blood cells (rRBCs) in each well. (B) Columns 1 and 2 are buffer controls depicting the behavior of rRBCs in 20 mM Na phosphate, 150 mM NaCl at pH 8.0 (column 1) and 8.0 M urea made in 20 mM Na phosphate, 150 mM NaCl at pH 8.0 (column 2). Columns 3 is a control that shows the behavior of adding 85 μL of 20 mM Na phosphate, 150 mM NaCl at pH 8.0 with 200 ng (5 μL) of monomer. Lane 1 of columns 4–7 were filled with 170 μL of 20 mM Na phosphate, 150 mM NaCl at pH 8.0 buffer containing 8.0 M urea. All other wells (lanes 2– 8, columns 4–7) were filled with*

85 μL of 20 mM Na phosphate, 150 mM NaCl at pH 8.0. Each well in each lane was then serially diluted (starting from lane 2 to lane 8) by adding 85 μL from the preceding lane. 200 ng (5 μL) of αHL monomers pre-incubated in 8.0 M urea was added to each well in column 4. While 200 ng (5 uL) of αHL monomers pre-incubated in TFA (column 5), formic acid (88.0% v/v) (column 6), and formic acid: ethanol (30:70 v/v) (column 7), that were lyophilized and re-solubilized in 8.0 M urea (in 20 mM Na phosphate, 150 mM NaCl at pH 8.0) were added to each corresponding well. The assay was started when 10 μL of rRBCs were added to all wells.

4.2.4 Single-Channel Recording Studies

Single-channel recording studies were conducted to observe whether the native αHL monomer and refolded αHL monomer were able to oligomerize on lipid bilayers having similar structural properties to pre-oligomerized WT-αHL heptamer purified from *Staphylococcus aureus* (purified in the same manner used in the heptamer experiments in Chapter II and III). The electrophysiology studies were conducted using a chamber separated by a Teflon film with an aperture that was coated with 10% (v/v) hexadecane in pentane. Both the *cis* and *trans* sides of the chamber were filled with 1 mL of 20 mM Na phosphate, 1 M NaCl at pH 8.0. Bilayers were formed by adding 1% (w/v) diphytanoylphosphatidylcholine (DPhPC) in hexadecane to both sides of the chamber while the protein was added to the *cis* side of the chamber. A current-voltage (IV) curve (Fig. 8A) was conducted for the heptamer, native monomer and the refolded monomer revealing that the three have the same rectification pattern from −200 mV to + 200 mV.

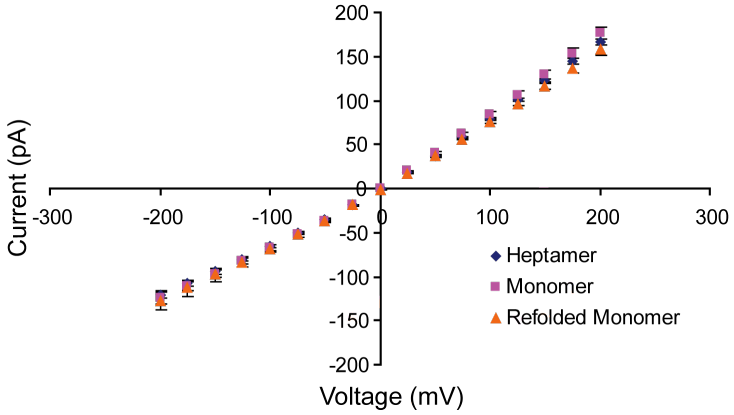


Fig. 8. IV Curves. *Single channel IV curves of the heptamer, native monomer and refolded monomer were conducted from -200 to +200 mV at intervals of 25 mV; heptamer (blue diamonds), native monomer (pink squares) and refolded monomer (orange triangles).*

After confirming that the all three forms of the protein are able to form channels, their ability to bind to a molecular adapter γ-cyclodextrin (γ-CD) was tested. Previous studies conducted [15] revealed that upon adding cyclodextrin to the *trans* side of the pore, it binds to an assembled heptameric pore confirming proper β-barrel formation and reversibly blocking the flow of ions through the pore. The traces in Fig. 9 show that pre-oligomerized heptamers, native monomers and refolded monomers at ± 50 mV are able to form channels and bind to γ-CD.

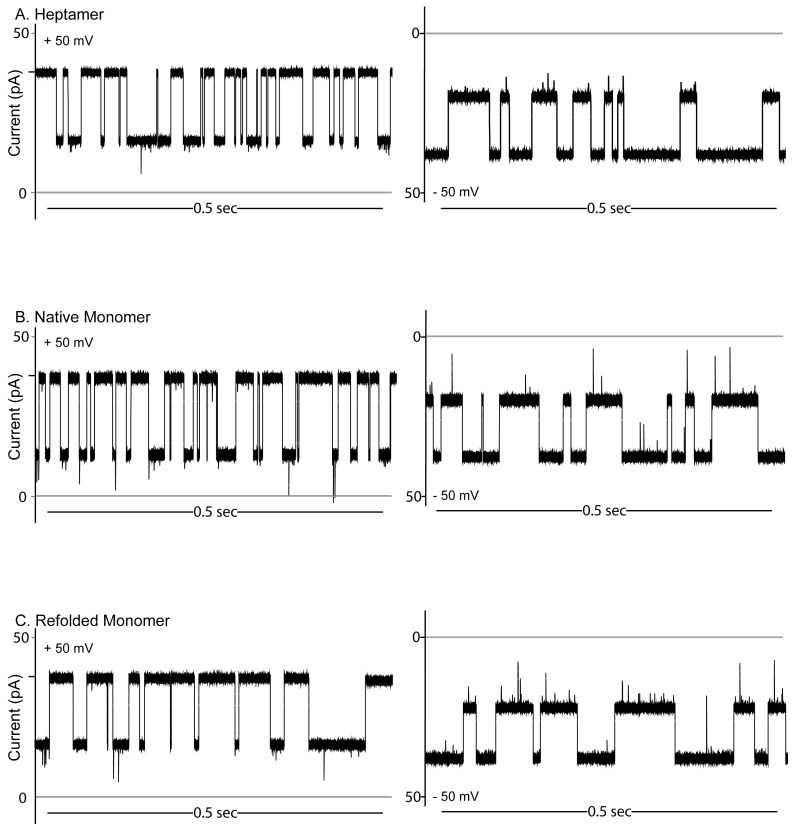


Fig. 9. Binding of γ-cyclodextrin *(from 0.01–0.04 mM) αHL heptamers reconstituted in DPhPC planar lipid bilayers from (A) pre-oligomerized heptamers, (B) native monomer and (C) refolded monomers at ± 50 mV. The buffer used in these experiments was 20 mM Na phosphate, 1 M NaCl at pH 8.0.*

Observing binding events in the electrophysiology traces in Table 2, the average percentage block between the heptamer, monomer and refolded monomer at ± 50 mV and ± 100 mV is the same. At + 50 mV and + 100 mV the percent block is approximately 62%, which is in agreement with past literature values [15]. At −50 mV and −100 mV it is slightly lower with values at 46% and 51%, respectively. The association rate constant (k_{on}) and the dissociation rate constant (k_{off}) for the heptamer, monomer and refolded monomer are similar at ± 50 mV and ± 100 mV (Table 2).

Protein	Voltage	k_{on} (s^{-1} mM^{-1})	k_{off} (s^{-1})	Percentage Block
Pre-oligomerized heptamer	+ 50 mV	60.6 ± 3.48	5.82 ± 0. 110	61.3 %
Native Monomer	+ 50 mV	61.1 ± 6.30	5.41 ± 0.384	62.3 %
Refolded Monomer	+ 50 mV	63.7 ± 4.87	5.41 ± 0.901	62.4 %
Pre-oligomerized heptamer	− 50 mV	47.7 ± 1.909	2.97 ± 0.119	45.3 %
Native Monomer	−50 mV	41.8 ± 4.33	3.20 ± 0.492	47.2 %
Refolded Monomer	− 50 mV	43.5 ± 3.12	2.61 ± 0.205	47.0 %
Pre-oligomerized heptamer	+ 100 mV	50.8 ± 2.69	10.6 ± 0.474	62.3 %
Native Monomer	+ 100 mV	65.9 ± 5.58	11.1 ± 0.530	62.3 %
Refolded Monomer	+ 100 mV	57.1 ± 2.59	10.5 ± 2.15	61.7 %
Pre-oligomerized heptamer	− 100 mV	37.4 ± 3.96	2.26 ± 0.221	52.0 %
Native Monomer	−100 mV	43.4 ± 0.812	1.32 ± 0.0270	51.3 %
Refolded Monomer	− 100 mV	35.5 ± 1.46	1.71 ± 0.127	50.5 %

Table 2. Binding of γ-cyclodextrin (γ-CD) to αHL heptamers. *Heptamers reconstituted in DPhPC planar lipid bilayers from pre-oligomerized heptamers, native monomers and refolded monomers at ± 50 mV and ± 100 mV. The table displays the association rate constant (k_{on}), the dissociation rate constant (k_{off}) and percentage block of γ-CD in 20 mM Na phosphate, 1 M NaCl at pH 8.0.*

In addition to testing the formation of pores from native monomers and refolded monomers directly, they were allowed to assemble into heptamers by oligomerizing them on deoxycholic acid (DOC). The pre-formed heptamers from the native monomer and refolded monomer were gel extracted and single-channel recording studies were conducted to

determine whether γ-CD binding channels formed. Table 3 shows that the pre-formed heptamers from native monomer and refolded monomers had similar k_{on} and k_{off} values to the pre-oligomerized heptamers.

Protein	Voltage	k_{on} (s^{-1} mM^{-1})	k_{off} (s^{-1})
Pre-oligomerized heptamer	+ 50 mV	60.6 ± 3.48	5.82 ± 0. 110
Pre-formed heptamers from native monomer	+ 50 mV	64.8 ± 3.57	6.03 ± .772
Pre-formed heptamers from refolded monomer	+ 50 mV	64.0 ± 3.18	6.20 ± 0.67
Pre-oligomerized heptamer	− 50 mV	47.7 ± 1.91	2.97 ± 0.119
Pre-formed heptamers from native monomer	−50 mV	50.9 ± 4.43	3.29 ± 0.154
Pre-formed heptamers from refolded monomer	− 50 mV	48.9 ± 3.29	2.67 ± 0.5
Pre-oligomerized heptamer	+ 100 mV	50.8 ± 2.69	10.6 ± 0.474
Pre-formed heptamers from native monomer	+ 100 mV	51.0 ± 5.49	12.4 ± 1.24
Pre-formed heptamers from refolded monomer	+ 100 mV	47.7 ± 1.45	9.63 ± 1.43
Pre-oligomerized heptamer	− 100 mV	37.4 ± 3.96	2.26 ± 0.221
Pre-formed heptamers from native monomer	−100 mV	35.7 ± 3.64	1.53 ± 0.34
Pre-formed heptamers from refolded monomer	− 100 mV	36.5 ± 0.896	2.30 ± 0.423

Table 3. Binding of γ-cyclodextrin (γ-CD) to pre-formed αHL heptamers. *Heptamers reconstituted in DPhPC planar lipid bilayers from pre-oligomerized heptamers, pre-formed heptamers from native monomers and pre-formed heptamers from refolded monomers at ± 50 mV*

and ± 100 mV. The table displays the association rate constant (k_{on}), the dissociation rate constant (k_{off}) and percentage block of γ-CD in 20 mM Na phosphate, 1 M NaCl at pH 8.0.

4.3 Discussion:

The purpose of this work was to explore the unfolding and refolding capabilities of the αHL monomer (MW 33.2 kDa), a soluble protein that oligomerizes into the αHL heptamer on lipid bilayers. The conditions explored will provide insight to more efficient ways of purifying αHL that will allow for the incorporation of unnatural amino acids using methods such as native chemical ligation (NCL) and expressed protein ligation (EPL). The conditions investigated in this body of work can be applied to the final folding steps of NCL and EPL, which utilize synthetic and semi-synthetic ways to create proteins that are difficult to obtain by recombinant means [7, 8, 16, 17].

These studies show that the αHL monomer unfolds reversibly in urea. Investigating the monomer's structural changes using ITFE and CD (Fig. 1 and 2) provided insight to the behavior of the protein since its is composed of 8 buried tryptophan residues in the cap domain (Trp80, Trp167, Trp265, Trp286, Trp179, Trp187, Trp260 and Trp274) and 16 β-sheet strands, which comprise 52.9% of its secondary structure. In 0 to 8.0 M urea there was a sigmoidal change of the monomer's λ_{max}^{em} and the $[\theta]_{RMME\ 215\ nm.}$ These results confirm the notion that two populations, the folded and unfolded forms of the protein, exist in solution. Therefore as the concentration of denaturant increases, the fraction of unfolded protein present in solution also increases. The midpoint of the sigmoidal fit, which represents the point at which 50% of the protein is denatured, of the ITFE and CD data are the same within experimental error with values of 3.3 ± 0.1 M and 3.4 ± 0.1 M, respectively. This suggests that the αHL monomer cooperatively unfolds in the presence of

urea. These values are also in correlation with previous studies conducted by Bortoleto *et al.* [1], in which the unfolding of the αHL monomer in the presence of urea with changing pH was investigated. The studies revealed that the midpoint of the ITFE and CD unfolding curve increases as the pH increases. The monomer seems completely unfolded by 5.0 M urea, suggesting that it is not as stable as the heptamer, which remains intact even at 8.0 M urea [18].

Upon confirming the unfolding ability of the monomer in urea, its ability to refold was tested in order to implement the conditions in future protein synthetic techniques. The ITFE and CD studies revealed that upon diluting the protein ten-fold, from 8.0 M urea to 0.8 M urea the αHL monomer was able to regain a λ_{max}^{em} at 334 nm and a $[\theta]_{RMME\ 215\ nm}$ of −5956, which is comparable to the native conformation of the protein (Fig. 4). Inspecting the CD spectra of the refolded monomer more closely, a shoulder is present from 220–250 nm, which may be a result of the protein not refolding to its native conformation or dynamic light scattering due to protein aggregates or insoluble urea particles. After incubating the monomer in 0.8 M urea directly, it seems the shoulder is still present. Therefore, the difference in spectra between the native and refolded monomer may be a result of the protein in that particular urea concentration. Studies conducted using hemolytic assays confirm that the protein is able to regain activity after diluting the urea concentration to concentrations ≤ 1.0 M urea, suggesting that it is refolded into its native conformation. The structure of the protein is further confirmed with the visual comparison of the native and refolded protein on SDS-PAGE after incubation in proteinase K where both proteins are cleaved at the C and N terminus (Fig. 5).

The single channel recording studies confirm that denaturing the protein in the presence of urea does not affect its ability to form pores on planar lipid bilayers with

rectification patterns similar to native monomer and pre-oligomerized heptamer (Fig. 8). The reversible binding of a noncovalent molecular adaptor such as γ-cyclodextrin confirms that the refolded monomer's β-barrel is formed properly (Fig. 9). The cyclodextrin contains primary hydroxyl groups on its narrower rim, and secondary and tertiary hydroxyl groups on its wider rim. When these groups interact with the binding site accessible on the *trans* side of the pore, it is known to alter the unitary conductance by 33–43%, a value that varies depending on the transmembrane potential applied and the pH of the buffer used [15]. Studies conducted with β-cyclodextrin concluded that it may be retained by a ring of 7 leucine residues (Leu135) that are found half-way through the transmembrane domain. Its passage through the pore is restrained by the restriction near the *cis* entrance containing Met113, Lys 147 and Glu111 [15]. The law of mass action is often used to explain the binding between a receptor, in this case αHL, and a ligand, in this case cyclodextrin, assuming that binding is reversible:

$$\alpha\text{HL} + \text{cyclodextrin} \underset{k_{off}}{\overset{k_{on}}{\rightleftharpoons}} \alpha\text{HL} \bullet \text{cyclodextrin}$$

The k_{on} value represents the association rate constant that is dependent upon the concentration of cyclodextrin added while the k_{off} value represents the dissociation rate constant. The percentage block, k_{off} and k_{on} of the heptamer, native monomer and refolded monomer as well as pre-formed heptamers from native and refolded monomer at (± 50 mV or ± 100 mV were similar in value (Table 2 and 3).

After the reversible denaturation of the αHL monomer in urea, its refolding capabilities were tested in GdnCl. The guanidinium ion is very weakly hydrated and can also associate with hydrophobic residues [4]. Previous studies conducted on soluble proteins and enzymes after incubation in 6.0 M GdnCl proved reversible after dilution and were

confirmed after a regain in activity [19]. In 6.0 M GdnCl, the unfolding of the monomer was not reversible as it is in 8.0 M urea via dilution (Figure 6B). Trace amounts of GdnCl even after a thousand-fold dilution; seem to prevent the protein from refolding and regaining activity. The second, third and fourth wells in the GdnCl experiment (Fig. 6B, lane 3, columns 2–4) show a sigmoidal change in the relative absorbance; however, this is not a result of the cells being lysed but of their aggregation. Certain barriers such as the protein misfolding into kinetic traps or aggregation of the unfolded state after dilution of the denaturant could be preventing the monomer from folding to its native active conformation [4]. These competing reactions increase the folding barrier, reduce the folding rate constant and decrease the folding efficiency. The folding free energy change could be unfavorable or small under these conditions. It seems that after incubation in 6.0 M GdnCl the monomer has an unstable conformation preventing it from renaturing via dilution. Unlike urea, GdnCl does not seem to help solubilize the monomer in a conformation that allows it to refold. It may appear that GdnCl's interaction with the protein is negative because the kinetics are too slow for refolding to occur on the experimental time scale used for urea. Studies conducted on other proteins in 6.0 M GdnCl exhibit the properties of a random coil; however, this is not true for all cases [4]. There is now evidence suggesting that even in 6.0 M GdnCl, proteins can have large amounts of internal structure [19]. This compactness is a result of hydrophobic intramolecular interactions that are stronger than the intermolecular interactions between the protein and solvent that result in clustering and leads to complex secondary structures [4, 20 and 21]. Once urea is added to the αHL monomer solution that was incubated in 6.0 M GdnCl, it competes with the intermolecular interactions that GdnCl has established with the protein as well as any intramolecular protein interactions (Fig 7A). The urea succeeds in interfering with the bonding between GdnCl and the protein forming

stronger interactions with the protein. Since urea is incorporated into the solution the monomer is able to refold to its original conformation after diluting the urea buffer ≤ 1.0 M. The protein regains activity even after diluting the protein in 1.0 M urea suggesting that at low concentrations of urea, the protein is being solubilized and its folded state must be stabilized. At higher concentrations of urea, the protein is brought to an unfolded state.

Urea and GdnCl are the two most common denaturants used; however, others such as temperature, SDS, various salt conditions and acids have also been used to denature proteins. TFA, formic acid (88.0% v/v) formic acid: ethanol (30:70 v/v) have been used to denature integral membrane proteins in the past [6]. Therefore, their interaction with the αHL monomer was also investigated. Conducting the experiment via dilution did not result in the monomer refolding and regaining activity equivalent to that of the urea studies (data not shown) since the pH of the solution was interfering with the stability of rRBCs. In order to completely eliminate the effect of the organic acids on the protein and the cells, the samples were lyophilized first and refolding was attempted by the addition of MBSA buffer. Hemolytic assays conducted on the protein after incubation in these acids show that the protein is 64-times less active than the native αHL monomer (Fig. 6C). This may have been due to the fact that residual organic acid was present even after lyophilization or that the MBSA buffer was not able to resolubilize the protein, since it may adhere to the sides of its container. Using urea to solubilize the protein after lyophilization; however, the hemolytic assays revealed that the protein was able to regain activity equivalent to the native protein (Fig. 7B). Therefore, organic acids as well as other denaturants can be used in protein synthetic reactions such as NCL or EPL. However, urea's incorporation in the solubilizing and final refolding stages may be crucial in implementing these conditions in chemical synthetic methods. These techniques will be beneficial in constructing modified

αHL heptameric pores that can be used for various applications in sensing, DNA sequencing and drug delivery.

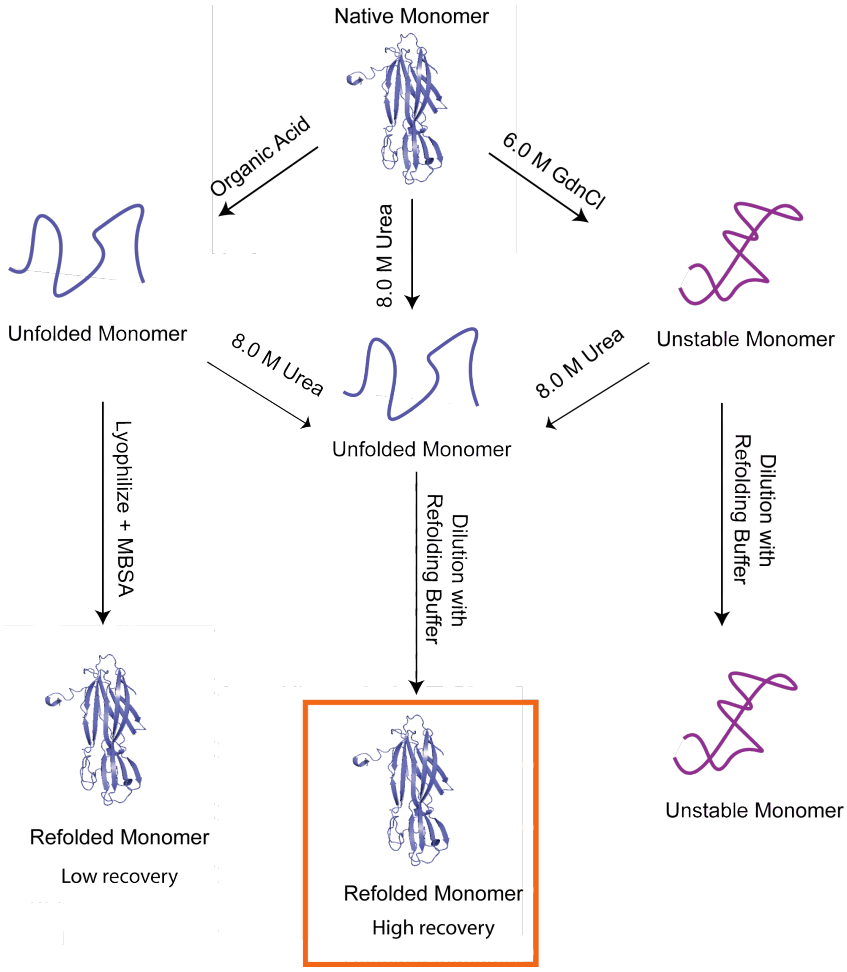


Fig. 10. Scheme of the Refolding Behavior of αHL monomer in various denaturants. *The native αHL monomer (A) was denatured using urea, GdnCl and organic acids. After incubation in 8.0 M urea, the protein unfolds (B.2) and then refolds upon dilution with Na phosphate buffer to its native confirmation (C.2). After incubating the monomer in organic acids such as TFA, formic acid and formic acid: ethanol the protein unfolds (B1). Then after lyophilization and addition of MBSA, the protein refolds and regains activity (C.1) but not equivalent to the native monomer. Upon adding 8.0 M urea instead of MBSA buffer after lyophilizing, the monomer regains complete activity equivalent to its native conformation (C.2). The monomer was also incubated in 6.0 M GdnCl, leaving the protein in an unstable conformation (B.3), which does not allow its refolding by dilution*

with Na phosphate buffer (C.3). However, adding 8.0 M urea after incubation with 6.0 M GdnCl, results in the protein regaining activity equivalent to the native monomer (C.2).

Furthermore, urea allows for a facile way of refolding the αHL monomer via dilution. It can be considered a suitable solvent since it seems to interact favorably with the monomer as opposed to GdnCl. These studies support the idea that urea acts as a surfactant with αHL monomer by solubilizing the side chains in water and preventing the aggregation of hydrophobic groups [22]. Urea allows for the stability of the folded state at low concentrations (≤ 1.0 M urea) while stabilizing the unfolded state at high concentrations of urea (≥ 5.0 M urea).

4.4 Conclusions

The behavior of monomeric αHL was investigated in various concentrations of urea (0–8.0 M) using ITFE and CD spectroscopy. These studies revealed that the monomer unfolds with increasing urea concentration and completely unfolds at 5.0 M urea. Then its ability to refold was investigated after incubation in 8.0 M urea via dilution to 0.8 M urea. Stability and activity of the refolded monomer was elucidated via ITFE, CD, proteolysis assay with proteinase K on SDS-PAGE and light scattering hemolytic assays. The structure and activity of the monomer was regained completely in concentrations ≤ 1.0 M urea. The refolded monomer's ability to oligomerize into stable pores was confirmed in single-channel recording experiments, which were compared to native monomer and pre-oligomerized WT-αHL heptamer. The ability of the monomer to refold after incubation in other denaturants such as GdnCl, TFA, and formic acid: ethanol (30:70 v/v) and formic acid (88% v/v) were also studied through light scattering hemolytic assays. GdnCl was not an appropriate solvent to use for the reversible denaturation of the αHL monomer.

However, attempting to refold the monomer with urea after incubation in GdnCl resulted in a regain of structure and function. After incubation in the organic acids, the monomer was able to regain activity but not comparable to the native monomer until urea was added to solubilize the protein after lyophilization. In conclusion, urea is the best solvent to use for reversible renaturation of the αHL monomer via dilution after incubation in conditions that could be used in synthetic studies. Future studies will involve implementing native chemical ligation and expressed chemical ligation to incorporate unnatural amino acids into αHL. This will allow us to explore the pore's ability to conduct single molecule chemistry. Urea can be implemented in the final stages of the synthesis, which will result in a folded protein that has structure and function similar to that of the wild type protein.

4.5. Materials and Methods

4.5.1 Protein Preparation

The αHL monomer was expressed and purified from Wood 46 strain of *Staphylococcus aureus* by Qiuhong Li (See Appendix). Monomers (500 μg mL^{-1}) used in the circular dichroism (CD) and intrinsic tryptophan fluorescence emission spectroscopy (ITFE) experiments were unfolded by using P6 microcentrifuge columns (732-6221, Bio-Rad) pre-incubated with 20 mM Na phosphate, 150 mM NaCl at pH 8.0 containing different urea concentrations, 0–8.0 M urea. Monomers were refolded by diluting the monomers that were unfolded in 8.0 M urea (500 μg mL^{-1}) in 20 mM Na phosphate, 150 mM NaCl at pH 8.0. The final concentration of protein and urea was 50 μg mL^{-1} and 0.8 M urea respectively.

Pre-formed heptamers from native monomers and refolded monomers were obtained by incubating 200 μg mL^{-1} of both native and refolded monomers in 6.25 mM deoxycholic acid (DOC). DOC was added gradually ever 10 min and the reaction was

allowed to continue over night with constant stirring. The samples were then diluted 1:1 with Lamilie sample and run on a 8% SDS-PAGE at 70 V for 18 h. The Precision Plus Protein Marker (161-0374, Bio-Rad) was used to decipher the position of the heptamer. After running the gel using 1x TGS buffer (Bio-Rad), the lane containing the marker and the neighboring protein lane was cut out and stained using instant blue buffer (Expedeon Protein Solutions). This portion of the gel was stained for 10 min and washed thoroughly with water before placed it next to the entire gel to prevent contamination. Using the stained marker lane as a guide, the heptamer band present in each well was cut out and placed in a 1.5 ul eppendorf tube. The gel samples were crushed using a pestle (Cat. 1980-41015, Bellco Glass) in the presence of 500µl of buffer (20 mM Na Phosphate, 150 mM NaCl, 0.3% (w/v) SDS, pH 8.0). The crushed gel was transferred into a QIAshredder Mini Spin Column (13176027, QIAGEN) and spun at a speed of 200 rpm for 10 min.

The pre-formed heptamers were then tested in electrophysiology.

4.5.2 CD

CD data were collected after the monomer was incubated in 0–8.0 M urea. Each of the samples was placed in a 0.1 cm path length CD cuvette (Hellma UK, Essex, UK) and the signal was measured between 250 to 200 nm (Chirascan, Applied Photophysics Limited, Leatherhead, UK). The data were collected at 0.5 nm intervals for 1 s per point at 25 °C. At least 10 spectra were collected for each sample incubated in 0–8.0 M urea. The urea measurements began with the protein solution that had been incubated at 0 M urea and ended with the solution at 8.0 M. The spectra were averaged and smoothed with the Chirascan Pro Data Viewer program. The signal in millidegrees was converted to mean residue molar ellipticity at a wavelength of 215 nm $[\theta]_{\text{RMME 215 nm}}$ with the same software. This procedure was done three separate times. The signal at 215 nm, corresponding to the

minimum in the β-sheet signal from each of the three experiments was plotted versus the values for urea concentration. The same procedure was conducted for the refolding experiments of the monomer after unfolding in 8.0 M urea. The native monomer was compared to the unfolded monomer in 8.0 M urea, the refolded monomer and the monomer incubated in 0.8 M urea.

4.5.3 ITFE

ITFE spectroscopy studies were conducted for the monomer after incubation in 0–8.0 M urea. Time dependent studies were conducted for the unfolding and refolding of the monomer at various urea concentrations (0–8.0 M urea) over a period of 30 min. After the appropriate incubation time was determined, the protein was placed in a fluorescence cuvette of 1.0 cm path length (Hellma, UK) and the fluorescence emission was measured every 0.2 nm from 300 to 500 nm with excitation at 280 nm and 5 nm slit width with a Cary Eclipse fluorescence spectrophotometer (Varian Inc, Palo Alto, CA, USA) at 25 °C. At least 10 spectra were collected, averaged and smoothed before determining the λ_{max}^{em} value. Three separate experiments were repeated in this manner for each urea condition. The same procedure was conducted for the refolding experiments of the monomer after unfolding in 8.0 M urea as described above. The native monomer was compared to the unfolded monomer in 8.0 M urea, the refolded monomer and the monomer incubated in 0.8 M urea.

4.5.4 Light Scattering Hemolytic Assays

Hemolytic assays were conducted on the monomer (100 μg mL^{-1}) just after incubation in 0–8.0 M urea (Fig. 6A). A 96 well plate was used. Each initial well (lane 1, columns 1–9) was filled with 170 μL of urea buffer that ranged from 0–8.0 M. Stock solutions were made to account for the eventual addition of rabbit red blood cells (rRBCs), which would

change the concentration of urea. All other wells (in lanes 2–8, columns 1–9) were filled with 85 μL of 20 mM Na phosphate, 150 mM NaCl at pH 8.0. The first wells (lane 1, columns 2–9) which were filled with 1.0–8.0 M urea, were serially diluted from top to bottom by transferring 85 μL to each consecutive well. Afterwards, 200 ng (5 μL) of protein, which was incubated in 1.0–8.0 M urea was added to each well in its corresponding column (1–9). Then 10 μL of RBCs were added resulting in a total volume of 100 μL in each well before placing the plate in a microplate spectrophotometer (Benchmark Plus, Bio-Rad) to detect the apparent absorbance change at 595 nm every 30 s after vigorous mixing over a total period of 1 h and 40 min. The lower absorbance limit was 0 while the upper absorbance limit was 0.8, which was later adjusted to 0.3 for analysis. Studies were also conducted in a similar manner without the addition of protein to see the effect of urea on the rRBCs. Similar experiments were conducted after the protein (50 μg mL^{-1}) was buffer exchanged into 6.0 M GdnCl and incubated for 5 min (Fig. 6B). The same experiment was conducted to test the effect of unfolding the protein from 6.0 M GdnCl into 8.0 M urea. The protein (500 μg mL^{-1}) was buffer exchanged into 6.0 M GdnCl and then diluted to 0.6 M GdnCl with 1.0–8.0 M urea (Fig. 7).

A separate experiment was carried out in order to test the refolding capabilities of the monomer after being incubated in acidic denaturants: trifluoroacetic acid (TFA), formic acid (88.0% v/v) and formic acid: ethanol (30: 70 (v/v)) as seen in Fig. 6C. The experiment involved incubating 2 μL of the protein (1 mg mL^{-1}) in 8 μL of the denaturant for 5 min accompanied by fast freezing. The samples were lyophilized for 20 min and then incubated for 10 min in 10 μL of MBSA buffer containing 500 mM MOPS, 0.1% BSA (w/v), 150 mM NaCl at pH 7.4. The 96 well-plates were prepared by placing 178 μL of MSBA buffer containing 10 mM MOPS, 0.1% BSA (w/v), 150 mM NaCl at pH 7.4 in column 1 of lanes

3−5. Then 2 μL of the protein that was once incubated in TFA (lane 3), formic acid (lane 4) and formic acid: ethanol (lane 5) was added resulting in 180 μL of solution in column 1. Then 90 μL of MBSA buffer was added to each succeeding well (lanes 1−5, columns 2−12). The activity of the protein was tested by serially diluting from left to right with 90 μL from the preceding well. The activity of the protein was detected using the microplate reader. This experiment was repeated by using the 8.0 M urea instead of MBSA buffer to solubilize the protein. Afterwards, the assay was conducted in order to study the effect of refolding the protein in serially diluted concentrations of 8.0 M urea (as described in the first paragraph).

4.5.5 Proteolysis Studies

Further studies were conducted to compare the structure of native monomer with refolded monomer by observing its interaction with proteinase K, an enzyme involved in protein cleavage. The native monomer and the refolded monomer were incubated in 5 μg mL^{-1}, 50 μg mL^{-1} and 500 μg mL^{-1} of proteinase K for 5 min. The reaction was stopped with 200 mM of phenylmethanesulphonylfluoride (PMSF) in isopropanol. After 2 min of incubation, the samples were diluted 1:2 at room temperature with loading buffer (XT sample buffer, Bio-Rad Laboratories Ltd, Hertfordshire, UK) and loaded onto Criterion XT Bis-Tris 12.0% gel (Bio-Rad Laboratories). The Precision Plus Protein Marker (161-0374, Bio-Rad) was used to determine the position of the monomer after electrophoresis. The SDS-PAGE was run at 200 V for 55 min with 1X MOPS as running buffer. The gels were stained with Instant Blue buffer (no. ISB01L, Expedeon Protein Solutions) overnight and washed thoroughly with water.

4.5.6 Single-Channel Recording

Single channel recording experiments were conducted on the WT-αHL pre-oligomerized heptamer, which was purified by previously published methods [32], native monomer and refolded monomer. αHL proteins were incorporated onto planar phospholipid bilayers comprising of 1, 2-diphytanoyl-*sn*-glycero-3-phosphocholine (DPhPC) in hexadecane (1.0% w/v) (Avanti Polar Lipids). A 25 μm-thick Teflon film with a 100 μm-diameter orifice separated the *cis* and *trans* chamber. The orifice was pre-treated with hexadecane in pentane (10.0% v/v). Ag/AgCl electrodes were used while 1 mL of 20 mM Na phosphate, 1 M NaCl at pH 8.0 to each side of the chamber. The heptamer, native monomer and refolded monomer were added in individual experiments to the *cis* chamber. A positive potential of 50 mV was applied and the solution was stirred until a channel inserted. An IV curve from ± 200 mV was collected for all three reconstituted channels to ensure that the ionic current asymmetry was comparable to the heptamer and that the protein was inserted in the proper orientation. Ten IV curves were collected, averaged and plotted for all three protein samples. After a single channel was obtained for all three cases, its ability to bind γ-cyclodextrin (γ-CD) was elucidated after adding 1–4 μL of 10 mM γ-CD (0.01–0.04 mM) to the *trans* side of the chamber and applying voltages of ± 50 mV and ± 100 mV.

The ionic current was filtered at a bandwidth of 50 kHz with a low-pass Bessel filter and sampled at 250 kHz with a computer equipped with a Digidata 1440 A digitizer (Molecular Devices). Analysis of the γ-CD binding events was observed by calculating their corresponding, percentage block, association rate constant (k_{on}) and dissociation rate constant (k_{off}) using Clampfit 10.0 (Axon Instruments).

4.6 References

1. Bortoleto, R. and Ward, R., *A stability transition at mildly acidic pH in the alpha-hemolysin (alpha-toxin) from Staphylococcus aureus.* FEBS Letters, 1999. **459**: 438–42.
2. Vecsey-Semjen, B., et al. *Conformational changes due to membrane binding and channel formation by Staphylococcal alpha–toxin*. J Biol Chem, 1997. **272**: 5709–17.
3. Vecsey-Semjen, B., et al. *Partial C-terminal unfolding is required for channel formation by staphylococcal alpha-toxin.* J Biol Chem, 1996. **271**: 8655–60.
4. Dill, K. and Shortle, D., *Denatured states of proteins.* Annu Rev Biochem, 1991. **60**: 795 –825.
5. Makhatadze, G., et al. *Energetics of protein structure.* Adv Protein Chem, 1995. **47**: 307– 425.
6. Huang, K., et al. *Refolding of an integral membrane protein*. J Biol Chem, 1981. **256**: 3802–9.
7. Valiyaveetil, F., et al. *Semisynthesis and folding of the potassium channel KcsA*. J Am Chem Soc, 2002. **124**: 9113–20.
8. Reitz, S., et al. *On the Function and structure of synthetically modified porins*. Angew Chem Int Ed, 2009. **48**: 4853–7.
9. Giraldo, R., *Defined DNA sequences promote the assembly of a bacterial protein into distinct amyloid nanostructures.* Prot Nat Aca Sci, 2007. **104**: 17388–93.
10. Kelly, S., et al. *How to study proteins by circular dichroism.* Biochimica et Biophysica Acta, 2005. **1751**: 119–39.

11. Ebeling, W., et al. *Proteinase K from Tritirachium album Linder.* Eur. J. Biochem, 1974. **47:** 91–7.

12. Cheley, S., et al. *Spontaneous oligomerization of a staphylococcal a-hemolysin conformationally constrained by removal of residues that form the transmembrane b-barrel*. Protein Engineering, 1997. **10**:1433–43.

13. Walker, B., et al. *Assembly of the oligomeric membrane pore formed by Staphylococcal alpha-hemolysin examined by truncation mutagenesis*. J Biol Chem, 1992. **267**: 21782–6.

14. Bennion, B., and Daggett, V. *The molecular basis for the chemical denaturation of proteins by urea.* Prot Nat Aca Sci, 2003. **100**: 5142–7.

15. Gu, L. and Bayley, H., *Interaction of the noncovalent molecular adapter, β-cyclodextrin, with the staphylococcal α-hemolysin pore.* Biophys J, 2000. **79**:1967 – 75.

16. Severinov, K. and Muir, T., *Expressed protein ligation, a novel method for studying protein-protein interactions in transcription*. J Biol Chem, 1998. **273**: 1605–9.

17. Muir, T., et al. *Expressed protein ligation: a general method for protein engineering.* Prot Nat Aca Sci, 1998. **95**: 6705–10.

18. Japrung, D., et al. *Urea facilitates the translocation of single-stranded DNA and RNA through the α-hemolysin nanopore*. Biophysical J, 2010. **98**: 1856 – 1863.

19. Akhtar, M., *Divalent cation induced changes in structural properties of the dimeric enzyme glucose oxidase: dual effect of dimer stabilization and dissociation with loss of cooperative interactions in enzyme monomer.* Biochemistry, 2002**. 41**: 7142 – 9.

20. Flory, P.J. Principles of Polymers Chemistry. 1953. Ithaca, New York: Cornell Univ.

21. Tandon, S., and Horowtiz, P., *Detergent-assisted refolding of guanidinium chloride-denatured rhodanese.* J Bio Chem, 1986. **261**: 15615 – 18.

22. Hua, L., et al. *Urea denaturation by stringer dispersion interactions with proteins than water implies a 2-stage unfolding.* Prot Nat Aca Sci, 2008. **105**: 16928–33.

Chapter V: Appendix

5.1 Materials and Methods Supplementary

5.1.1 Protein Preparation: αHL Heptamer (Taken from Maglia et al. 2009)

αHL used in the structural studies for CD and fluorescence was produced via large-scale purification of pre-oligomerized αHL WT homoheptamer from *Staphylococcus aureus*. The Wood46 strain (American type Culture Collection) of *Staphylococcus aureus* was streaked onto a Tryptic Soy Broth (TSB) plate and incubated at 37˚ C. A single colony was picked and placed in 200 ml of TSB and grown overnight at 37˚ C while shaking at a speed of 200 rpm. This culture was used as inoculum (10 mL was added to each 1 L of TSB in a 2 L flask) to grow a 20 L culture for 16–18 hours at 37˚ C while shaking at a speed of 200 rpm. Afterwards all steps were carried out at 4˚ C unless specified. The culture was centrifuged and cultured at a speed of 8000 rpm (Avanti J-25 rotor; Beckman Coulter, USA) for 30 minutes. The supernatant containing water soluble αHL monomer was recovered and concentrated overnight with the addition of 500 g ammonium sulphate $(NH_4)_2SO_4$ per 1 L culture of supernatant obtained in the pervious step (ammonium sulphate was added in 5 equal portions at 30–60 min intervals). This will produce a concentrated solution of monomer as well as pre-oligomerized heptamer. Then the ammonium sulphate-saturated supernatant was centrifuged at a speed of 8000 rpm (Avanti J-25 rotor; Beckman Coulter, USA) for 30 minutes. The pellet was recovered and resuspended in 200 mL of Buffer A (10 mM NaAc, 1 mM EDTA at pH 5.2) with 0.5 mM phenylmethanesulfonyl fluoride (made in DMSO) and 1 tablet of Protease inhibitor cocktail from Roche. The 2X 100 mL re-suspended pellet solution was dialyzed in 2X 10 L of Buffer A overnight. The buffer was exchanged twice during this period. The suspension was centrifuged at a speed of 8000 rpm for 30 min and the clear supernatant was loaded

onto a 300 mL S-Sepharose FF Cation exchanger, which was pre-equilibrated with Buffer A. After loading the protein, the column was washed with Buffer A. The monomer and pre-oligomerized heptamer were eluted with a linear gradient of 0–500 mM NaCl, using Buffer B (10 mM NaAc, 0.5 M NaCl, 1 mM EDTA at pH 5.2). The fractions collected were tested via SDS-PAGE, 10% Bis-Tris gel (Bio-Rad, UK). The peak fractions corresponding to the αHL heptamer were collected and dialyzed against Buffer A overnight to remove salt. Afterwards, a second cation exchange was conducted using a 40 mL S-Sepharose FF Cation exchanger. The fractions were tested again via SDS-PAGE 10% Bis-Tris gel. The peak fractions of the homoheptamer were collected and concentrated via ultracel using 50 kDa MW cut off (Amicon) to approximately 10 mg mL^{-1}. The homoheptamer was purified further via gel filtration using the Superdex 200, HiLoad gel filtration column, which was first equilibrated with Buffer C (10 mM Tris, 150 mM NaCl, 0.2% (w/v) SDS at pH 8.0) with a flow rate of 1 mL min^{-1}. The peak fractions were analyzed again using SDS-PAGE 10% Bis-Tris gel.

The purified fractions were collected and loaded onto an 8% Polyacrylamide gel using a gel preparation set (Z375047, Sigma). Approximately 100–150 ul of the fractions were diluted 1:1 with Lamilie sample buffer onto 12 wells. The Precision Plus Protein Marker (161-0374, Bio-Rad) was used to decipher the position of the heptamer. After running the gel using 1x TGS buffer (Bio-Rad) at a voltage of 70 V for 18 h, the lane containing the marker and the neighboring protein lane was cut out and stained using instant blue buffer (Expedeon Protein Solutions). This portion of the gel was stained for 10 min and washed thoroughly with water before placed it next to the entire gel to prevent contamination. Using the stained marker lane as a guide, the heptamer band present in each well was cut out and placed in a 1.5 μL eppendorf tube. The gel samples were crushed

using a pestle (Cat. 1980-41015, Bellco Glass) in the presence of 500 µl of buffer (20mM Sodium Phosphate, 150 mM NaCl, 0.2% (w/v) SDS, pH8). The crushed gel was transferred into a QIAshredder Mini Spin Column (13176027, QIAGEN) and spun at a speed of 200 rpm for 10 min. The flow-through was collected and filtered using a microfilterfuge tubes (0.2 µm cellulose acetate filter, 7016-024, RAININ) column to remove traces of polyacrylamide via centrifuging at a speed of 25,000 rpm for 1–2 h. The flow-through was concentrated to approximately 2 mg mL^{-1} using ultracel 50 kDa (Amicon) membranes.

Before the CD and fluorescence experiments were conducted, the buffer was exchanged with 10 mM Na phosphate, 10 mM Tris-HCl, 10 mM CAPS, 150 mM NaCl with 0.3% (w/v) SDS using P6 microcentrifuge columns (732-6221, Bio-Rad). Their purity and concentration were tested using SDS-PAGE 10% Bis-Tris gel and Absorption Spectroscopy using the Nanodrop with an extinction coefficient of 1.95 M^{-1} cm^{-1}.

5.1.2 Protein Preparation: αHL Monomer

Monomeric αHL was produced via large-scale purification from *Staphylococcus aureus*. The Wood 46 strain (American type Culture Collection, ATCC) of *Staphylococcus aureus* was streaked onto a Tryptic Soy Broth (TSB) plate and incubated at 37˚ C. A single colony was picked and placed in 100 mL of TSB and grown overnight at 37˚ C while shaking at a speed of 200 rpm. This culture was used as inoculum (10 mL was added to each 1 L of TSB in a 2 L flask) and grown for 16–18 h at 37˚ C while shaking at a speed of 200 rpm. Afterwards all steps were carried out at 4˚ C unless specified. The culture was centrifuged and cultured at a speed of 7741 Xg (Avanti J-25 rotor; Beckman Coulter, USA) for 30 min. The supernatant containing water soluble αHL monomer was recovered and concentrated overnight with the addition of 500 g ammonium sulphate $(NH_4)_2SO_4$ per 1 L culture of supernatant obtained in the pervious step (ammonium sulphate was added in 5

equal portions at 30–60 min intervals) producing a concentrated solution of monomer. Then the ammonium sulphate-saturated supernatant was centrifuged at a speed of 7741 Xg (Avanti J-25 rotor; Beckman Coulter, USA) for 30 min. The pellet was recovered and re-suspended in 10 to 20 mL of buffer A (10 mM NaAc, 1 mM EDTA at pH 5.2) with 0.5 mM phenylmethanesulfonyl fluoride (from a 1000X stock in DMSO). The re-suspended pellet was dialyzed in 1 L of Buffer A during the day for 5 to 7 h and then the buffer was exchanged and dialyzed overnight. The clear supernatant was filtered using 0.2 μm pore sized filter units (Millipore) before conducting FPLC purification. The filtered supernatant was loaded into the 300 mL S-Sephrose FF (Cat. 17072901, GE Healthcare) cation exchanger (Model XK50), which was first equilibrated with Buffer A. After loading, the column was washed with Buffer A. The bound protein was eluted with linear gradient of 0–500 mM NaCl, using Buffer B (10 mM NaAC, 0.5 M NaCl, 1 mM EDTA at pH 5.2). Approximately 15–30 μL portions of each 1 mL fraction, was analyzed via SDS-PAGE using a 10% Bis-Tris gel (Cat. 3450112, Bio-Rad, UK) at 200 V for 55 min using 1X XT-MOPS 9Cat. 1610788, Bio-Rad) with a running buffer and XT-sample buffer (Cat. 1610791) as the loading buffer. All peak fractions were collected and dialyzed in Buffer A overnight to remove salt before conducting the second cation exchange. Afterwards, the peak fractions were collected and concentrated via ultra filtration using 1- kDa MW cut off (Cat. Amicon) to approximately 10 mg mL^{-1} at 2906 Xg (Centrifuge 5810R, eppendorf) to approximately 3 mg mL^{-1}. The protein was then purified via gel filtration. Approximately 2 mL of the concentrated peak fractions were loaded to the superdex 200, HiLoad gel filtration column (Cat. 17107101, GE Healthcare), which was first equilibrated with Buffer C (10 mM Tris, 150 mM NaCl at ph 8.0). A flow rate of 1 mL min^{-1} was applied to elute the protein. The peak fractions that contained αHL monomer were collected and quantified

by measuring the absorbance at 280 nm (OD 280 of 1.0 mg mL^{-1} solution = 1.95). The peak fractions were concentrated by using Ultracel 10 kDa MW (Centrifuge 5810R, Eppendorf).

5.1.3 Rabbit Red Blood Cell Preparation

rRBCs (Harlan) were pre-treated before conducting the hemolytic assays by taking 450 μL of the blood and placing it in 900 μL of MBSA (10 mM MOPS, 0.1% Bovin Serum Albumin from Sigma, 150 mM NaCl at pH 7.4). This solution was mixed and then spun for 2 min at 100 Xg. The supernatant was removed and another 900 μL of MBSA was added. This procedure was repeated three times, until the supernatant was completely clear. Then the rRBCs were diluted to 1.0% with MBSA.

5.1.4 Hemolytic Assays: Urea Buffer Controls

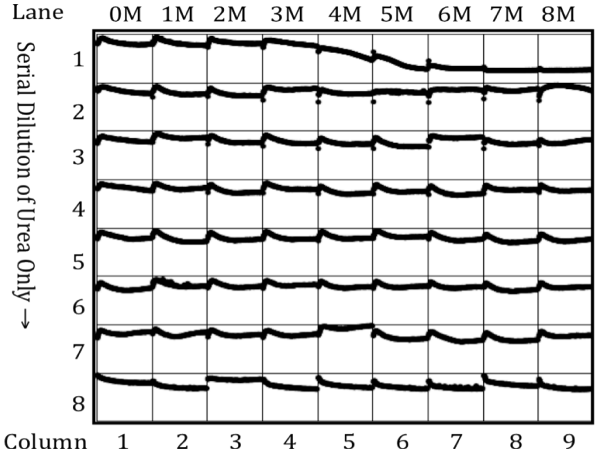


Fig. 1. Light scattering hemolytic assay depicting the effects of 0–8 M urea buffers.

In order to observe the effects of 0-8 M urea on rRBCs, a hemolytic assay was conducted. Each initial well of the 96 well plate was filled with 180 μL of urea buffer that ranged from 0-8 M. Stock solutions were made to account for the eventual addition of rabbit red blood cells, which would change the concentration of urea. Therefore the urea concentrations added were 8.89, 7.78, 6.67, 5.56, 4.44, 3.33, 2.22 and 1.11 M urea. All

other wells in all columns except the last column were filled with and 90 μL of 20 mM Na phosphate, 150 mM NaCl at pH 8. Then a serial dilution of the urea buffers was conducted. Finally, 10 μL of 1.0 % rabbit red blood cells (RBCs) was added to the wells before placing the plate in a microplate spectrophotometer (Benchmark Plus, Bio-Rad) to detect the absorbance change after 1 h 40 min.

The assay in Fig. 1 shows that the rRBCs do not rupture in 0–3 M urea, since the apparent absorbance is high. Wells containing 4–8 M urea (columns 5–9, lane 1) have a much lower absorbance, showing that these urea concentrations affect the osmotic pressure of RBCs. After the first serial dilution; however, the RBCs are more stable and resistant to lysing.

5.1.5 Curve Fitting

All fluorescence and CD curves were fitted to a sigmoid curve using OriginPro 8 using the Boltzmann function with the equation: $y = [(A_1\text{-}A_2)/1 + e^{(x - x_0)/dx}] + A_2$.